CAPITAL UNIVERSITY OF SCIENCE AND TECHNOLOGY, ISLAMABAD

Comparative Anticancer Analysis of *Zygophyllum arabicum* and *Mentha longifolia* var. *asiatica* for Novel Drug Discovery Against Breast Cancer

by

Iqra Bashir

A dissertation submitted in partial fulfillment for the degree of Doctor of Philosophy

in the

Faculty of Health and Life Sciences
Department of Bioinformatics and Biosciences

2025

Comparative Anticancer Analysis of *Zygophyllum arabicum* and *Mentha longifolia* var. *asiatica* for Novel Drug Discovery Against Breast Cancer

By

Iqra Bashir

(DBS203002)

Dr. Behcet Inal, Associate Professor

Siirt University, Siirt, Türkiye

(Foreign Evaluator 1)

Dr. Ming Zhou Qin, Professor

Henan University, Kaifeng, Henan,China

(Foreign Evaluator 2)

Dr. Erum Dilshad

(Research Supervisor)

Dr. Syeda Marriam Bakhtiar

(Head, Department of Bioinformatics and Biosciences)

Dr. Sahar Fazal

(Dean, Faculty of Health and Life Sciences)

DEPARTMENT OF BIOINFORMATICS AND BIOSCIENCES

CAPITAL UNIVERSITY OF SCIENCE AND TECHNOLOGY

ISLAMABAD

2025

I dedicate this dissertation to my family, Specially to my father (Late) and mother whose unconditional love, unwavering support, and endless encouragement have been my pillars of strength throughout this challenging journey. Their belief in me and sacrifices made have been the driving force behind my success. I am grateful for their patience, understanding, and constant motivation. This achievement is a testament to their unwavering faith in my abilities. I dedicate this work to them as a token of my deepest appreciation and love.

CAPITAL UNIVERSITY OF SCIENCE & TECHNOLOGY ISLAMABAD

Expressway, Kahuta Road, Zone-V, Islamabad
Phone:+92-51-111-555-666 Fax: +92-51-4486705
Email: info@cust.edu.pk Website: https://www.cust.edu.pk

CERTIFICATE OF APPROVAL

This is to certify that the research work presented in the dissertation, entitled "**Comparative Anticancer Analysis of *Zygophyllum arabicum* and *Mentha longifolia* var. *asiatica* for Novel Drug Discovery Against Breast Cancer**" was conducted under the supervision of **Dr. Erum Dilshad**. No part of this dissertation has been submitted anywhere else for any other degree. This dissertation is submitted to the **Department of Bioinformatics & Biosciences, Capital University of Science and Technology** in partial fulfillment of the requirements for the degree of Doctor of Philosophy in the field of **Biosciences**. The open defence of the dissertation was conducted on **February 14, 2025.**

Student Name : Iqra Bashir (DBS203002) IBashir

The Examination Committee unanimously agrees to award PhD degree in the mentioned field.

Examination Committee :

(a) External Examiner 1: Dr. Maria Shabbir
Associate Professor
ASAB, NUST, Islamabad

(b) External Examiner 2: Dr. Nosheen Akhtar
Associate Professor
NUMS, Islamabad

(c) Internal Examiner : Dr. Sohail Ahmed Jan
Associate Professor
CUST, Islamabad

Supervisor Name : Dr. Erum Dilshad
Associate Professor
CUST, Islamabad

Name of HoD : Syeda Marriam Bakhtiar
Associate Professor
CUST, Islamabad

Name of Dean : Dr. Sahar Fazal
Professor
CUST, Islamabad

AUTHOR'S DECLARATION

I, **Iqra Bashir** (Registration No. **DBS203002)**, hereby state that my dissertation titled, '**Comparative Anticancer Analysis of *Zygophyllum arabicum* and *Mentha longifolia* var. *asiatica* for Novel Drug Discovery Against Breast Cancer**' is my own work and has not been submitted previously by me for taking any degree from Capital University of Science and Technology, Islamabad or anywhere else in the country/ world.

At any time, if my statement is found to be incorrect even after my graduation, the University has the right to withdraw my PhD Degree.

I Bashir

(**Iqra Bashir**)

Dated: 14th February, 2025

Registration No: DBS203002

PLAGIARISM UNDERTAKING

I solemnly declare that research work presented in the dissertation titled "**Comparative Anticancer Analysis of *Zygophyllum arabicum* and *Mentha longifolia* var. *asiatica* for Novel Drug Discovery Against Breast Cancer**" is solely my research work with no significant contribution from any other person. Small contribution/ help wherever taken has been duly acknowledged and that complete dissertation has been written by me.

I understand the zero-tolerance policy of the HEC and Capital University of Science and Technology towards plagiarism. Therefore, I as an author of the above titled dissertation declare that no portion of my dissertation has been plagiarized and any material used as reference is properly referred/ cited.

I undertake that if I am found guilty of any formal plagiarism in the above titled dissertation even after award of PhD Degree, the University reserves the right to withdraw/ revoke my PhD degree and that HEC and the University have the right to publish my name on the HEC/ University Website on which names of students are placed who submitted plagiarized dissertation.

IBashir

(Iqra Bashir)

Dated: 14th February, 2025

Registration No: DBS203002

List of Publications

It is certified that following publication(s) have been made out of the research work that has been carried out for this dissertation:-

1. Iqra Bashir and Erum Dilshad (2025). A comparative study of *Zygophyllum arabicum* var. *asiatica* and *M. longifolia* ZnO nanoparticles against breast cancer targeting Rab22A gene. PLOS One 19(8):e0308982.

(Iqra Bashir)
Registration No: DBS203002

Acknowledgement

To start with the greatest name of Almighty Allah. Most gracious and merciful, whose bounties are unbounded, whose benevolence is everlasting, whose blessings are uncountable, whose being is eternal, whose mercy is unlimited, whose provisions are un-ending, whose Love is our life, whose worship is our faith. First and foremost, all attributes to Almighty ALLAH, The Gracious and The Merciful, who blessed me with the perfect circumstances throughout my life, and bestowed me with the potential, ability and an optimal environment to accomplish my PhD project. I owe my deep gratitude to the teachings of Holy Prophet Hazrat Muhammad (SAW), which are a source of inspiration for every aspect of life, for the entire creation. First and foremost, I am extremely grateful to my supervisor, Dr. Erum Dilshad Associate Professor Department of Bioinformatics and Biosciences, CUST for her invaluable advice, motivation, continuous support and peservance during my PhD study. Her immense knowledge and plentiful experience have encouraged me in all the time of my academic research and daily life. I am indebted to her sheer guidance and unwavering support during my research. I could not have imagined having a better advisor and mentor for my PhD thesis. I cannot thank her for her unconditional support.

I would like to express my sincere gratitude to Dr. Sahar Fazal Dean Faculty of Health and Life Sciences, CUST for her kind and affectionate behavior and guidance throughout my PhD journey. She is indeed a kind hearted soul. I owe a deep sense of gratitude to Dr. Syeda Marriam Bakhtiar HOD Faculty of Health and Life Sciences, CUST and respected faculty members for their insightful encouragement, motivation and extraordinary kindness throughout my studies. Additionally, I would like to express gratitude to Dr. Naeem Ashraf for his treasured support which was really influential in shaping my experiment methods and critiquing my results. I am indebted to his assistance at every stage of my research project. I would extend my gratitude to Arsalan Hamid for helping me to analyze the computational results. I would like to thank my friends Ms. Sajida Tayyaba, lab mates Amna Naheed Khan and Rukhsana Tabassum and research team for a

cherished time spent together in the lab and in social setting. My appreciation also goes out to my colleagues for always being there for me to pray and support whenever I need them.

Atlast but not the least, I express my profound gratitude to my mother for her utter support and massive belief on me that allowed me to chase my dreams. Her untiring efforts made us to become good human beings and excel in our lives. I would like to appreciate my family especially my brothers, sister (Beenish Anna), nieces (Huda, Bareera and Udaina) and nephews (Mairaj and Hassan). This accomplishment have not been possible without their prayers.

(Iqra Bashir)

Abstract

Breast cancer is the most common health concern all around the world. It is frequently diagnosed cancer type in females followed by lung cancer. The incidence of breast cancer is highest among the Pakistani population in South Asia. According to the latest data, one out of every four deaths is attributed to breast cancer. Moreover, one out of every nine females has this malignancy in Pakistan. The incidence of breast cancer has increased by 300% in the last 3 decades. The currently employed methods for treating breast cancer such as chemotherapeutic drugs have contributed to drug resistance, relapse of cancer and various side effects. Due to these problems, plentiful research is ongoing on using natural products for cancer treatment. The current studies aimed to assess the role of plant-based synthesized nanoparticles in treating breast cancer. It serves as a novel way to determine prognostic markers for breast cancer diagnosis and treatment. Rab22A belongs to the Rab5 superfamily. This small GTPase protein is a cargo protein involved in the intracellular uptake of nutrients and transportation of substances within different cellular networks. This protein is a part of the endocytic pathway. Aberrant endocytosis is the hallmark of various cancer types, particularly breast cancer. The current study was aimed to target the Rab22A gene and its role as a prognostic marker for the treatment of breast cancer.

For the current study, two pharmacologically novel plants *Zygophyllum arabicum* and *Mentha longifolia* var. *asiatica* were selected for comparative anticancer study. Both plants have been used to treat different ailments for centuries. These plants were obtained from different geographical regions and later on verified from QAU herbarium, Islamabad. Zinc oxide nanoparticles were prepared from both plants and they were characterized by UV-VIS, SEM, FTIR, EDS and XRD analysis. UV-Vis spectroscopy showed characteristic peaks at 295nm for *Z. arabicum* ZnO nanoparticles and 345nm for *Mentha longifolia* var. *asiatica* ZnO nanoparticles. SEM analysis was done to determine the size and shape of the nanoparticles. SEM analysis revealed *Z. arabicum* mediated ZnO NPs to be spherical having a size of 25±4nm whereas *M. longifolia* var. *asiatica* nanoparticles were hexagonal

and their size was 35±6nm. FTIR analysis was done to determine the presence of various bioactive compounds. FTIR spectra of *Z. arabicum* ZnO NPs showed major bands at 2970, 2888, 2832, 2370, 2318, 1379 and 1067 cm-1 and minor bands were observed at 2160, 1561, 1375, 873, 600 and 594 cm-1. These bands indicated the presence of alcohols, aldehydes and polyols. *M. longifolia* var. *asiatica* ZnO NPs showed major bands at 3649, 2989, 2969, 2900, 2365, 2025 and 1383 cm-1 and minor bands at 1558, 1570, 1370, 1261 and 852 cm^{-1}. These bands corresponded to the presence of proteins, alkanes and hydroxyl flavones. EDX analysis was carried out to determine the elemental composition of nanoparticles. The results indicated the presence of zinc as a major component in the EDS spectra of both samples. The crystalline nature of ZnO nanoparticles was determined by XRD analysis. The XRD peaks for both samples were following standard ICSD No. 98-018-08.

The anticancer potential of ZnO nanoparticles was tested on MCF-7 breast cancer cell lines. For this purpose, a cell viability assay was performed for both nanoparticles and plant extracts. Different concentrations i.e. 20, 40, 60, 80 and 100 μM of ZnO nanoparticles of both plants and their extracts showed cytotoxicity. The cell viability of *Z. arabicum* extract was 60.3'% whereas *M. longifolia* var. *asiatica* was 69.4 % at maximum concentration i.e. 100 μM. The cell viability for *Z. arabicum* ZnO NPs was 32.8% in comparison to *M. longifolia* var. *asiatica* ZnO NPs which was 43.2 % at the same concentration.

The IC50 value of nanoparticles and plant extracts was also determined. *Z. arabicum* extract and nanoparticles showed higher cytotoxicity (IC50 64.01 μM and 51.68 μM respectively) as compared to *M. longifolia* var. *asiatica* extract and respective nanoparticles (IC50 107.9 μM and 88.02 μM respectively). The expression of various apoptotic genes and our target Rab22A gene was done by real-time qPCR. The results showed that the expression of bax, caspase 3, caspase 8 and caspase 9 genes was increased in the cells which were treated with ZnO nanoparticles as compared to control cells. The expression of the Rab22A gene was less for *Z. arabicum* plant extract and ZnO nanoparticles as compared to *M. longifolia* var. *asiatica* extract and nanoparticles which suggests that *Z. arabicum* plant extract

and nanoparticles are more effective in downregulating the expression of Rab22A gene. The expression of bax, caspase 3, caspase 8 and caspase 9 was upregulated in the cells treated with *Z. arabicum* plant extract and nanoparticles as compared to the cells treated with *M. longifolia* var. *asiatica* extract and ZnO NPs. The protein analysis of Rab22A and apoptotic genes was also done by ELISA. The results indicated that both ZnO NPs of selected plants showed promising results. The expression of Rab22A protein was downregulated in the cells treated with extract of *Z. arabicum* and ZnO nanoparticles as compared to the cells treated with *M. longifolia* var. *asiatica* extract and ZnO NPs. The level of bax proteins was high in the cells treated with *Z. arabicum* extract and nanoparticles. In the same way, the level of apoptotic proteins (caspase 3, caspase 8 and caspase 9) was also upregulated in the cells treated with *Z. arabicum* extract and nanoparticles when compared to the cells treated with *M. longifolia* var. *asiatica* extract and ZnO NPs.

The phytochemical screening of both selected plants was done by the HPLC/DAD system to identify bioactive compounds. The methanolic extracts of *Z. arabicum* and longifolia var. *asiatica* were subjected to HPLC. The results showed the presence of eight compounds i.e. chlorogenic acid, gallic acid, coumaric acid, salicylic acid, quercetin, benzoic acid and rutin in *Z. arabicum* whereas nine compounds i.e. chlorogenic acid, gallic acid, kaempferol, sinapic acid, salicylic acid, coumarin, quercetin, 3-Hydroxy butyric (HB) acid and rutin in the extract of *M. longifolia* var. *asiatica* extract. These compounds were then studied for CADD to discover the potential role of these compounds as drug candidates against breast cancer. Molecular docking was used to assess the binding of all the selected compounds with the target Rab22A protein. Different software was used for the cleaning of protein and to visualize protein-ligand interactions such as PYMOL and LIGPLOT+. One lead compound was identified from each selected plant based on vina score and other parameters. Chlorogenic acid was selected from *Z. arabicum* whereas 3-hydroxybutyric acid was selected from *M. longifolia* var. *asiatica*. These lead compounds were studied in comparison with the reference drug palbociclib. The lead compounds and the drug were subjected to Lipinski RO5, molecular

dynamic simulation and drug likeliness study by ADMET properties. All lead compounds followed Lipinski's RO5. Multiple parameters such as RMSD, RMSF, Hydrogen bond analysis, SASA analysis and radius of gyration of lead compounds and the drug showed that chlorogenic acid is far better than 3-hydroxybutyric acid and palbociclib drug. The ADMET properties also showed that chlorogenic acid is a far better drug choice as compared to other lead compound and drug. Based upon all the above studied characterization results and computational results it was concluded that *Z. arabicum* has more anticancer potential than *M. longifolia* var. *asiatica*. The computational study also revealed chlorogenic acid a novel drug target against breast cancer. Thus, it can be explored further as a novel drug candidate against novel drug target Rab22A gene for treatment of breast cancer.

Keywords: Breast cancer, Rab22A gene, *Zygophyllum arabicum, Mentha longifoli*a var. *asiatica*, Endocytic pathway, Molecular docking, Computer aided drug designing, Molecular dynamics simulation

Contents

Author's Declaration vi

Plagiarism Undertaking vii

List of Publications viii

Acknowledgement ix

Abstract xi

List of Figures xx

List of Tables xxiii

Abbreviations xxiv

1 Introduction 1

1.1 Background of the Study 1

1.2 Gap Analysis 6

1.2.1 Absence of Prior Studies on the Synthesis and Anticancer Studies of ZnO Nanoparticles from *Zygophyllum arabicum* . 6

1.2.1.1 Gap 6

1.2.1.2 Implication 6

1.2.2 Absence of Comparative Analysis of *Mentha longifolia* var. *asiatica* and *Zygophyllum arabicum* Mediated ZnO Nanoparticles and their Potential Role in Breast Cancer Treatment In vitro 6

1.2.2.1 Gap 6

1.2.2.2 Implication 7

1.2.3 Restricted Knowledge about the Plant-Mediated ZnO Nanoparticles Targeting Rab22A Gene in the Breast Cancer Prognosis and Treatment 7

1.2.3.1 Gap 7

1.2.3.2 Implication 7

1.3 Problem Statement 8

1.4 Research Questions . . . 8
1.5 Research Objectives . . . 9
1.6 Scope and Significance . . . 10

2 Literature Review **11**
2.1 Cancer . . . 11
2.2 Human Breast Cancer . . . 13
2.2.1 Types of Breast Cancer . . . 15
2.2.2 Stages of Breast Cancer . . . 16
2.2.3 Metastasis in Breast Cancer . . . 16
2.2.4 Detachment of Breast Cancer Cells & Local Invasion . . . 17
2.2.4.1 Penetration in the Circulatory System . . . 17
2.2.4.2 Circulation . . . 17
2.2.4.3 Cell Cycle Arrest and Extravasation . . . 17
2.2.4.4 Development of Tumour . . . 17
2.3 Risk Factors . . . 18
2.3.1 Demographic Factors . . . 18
2.3.1.1 Gender . . . 18
2.3.1.2 Age . . . 18
2.3.1.3 Blood Group . . . 18
2.3.1.4 Reproductive Factors . . . 19
2.3.1.5 Age of Menarche . . . 19
2.3.1.6 Age of Menopause . . . 19
2.3.1.7 Full-Term Pregnancy . . . 19
2.3.1.8 Abortion . . . 19
2.3.2 Hormonal Factors . . . 20
2.3.2.1 Contraceptive Methods . . . 20
2.3.2.2 Ovulation Stimulating Drugs . . . 20
2.3.2.3 Postmenopausal Hormone Therapy . . . 20
2.3.2.4 Family History of Breast Cancer . . . 20
2.3.3 Breast-Related Factors . . . 20
2.3.3.1 Lactation . . . 20
2.3.3.2 Breast Density . . . 21
2.3.3.3 Benign Breast Disorders . . . 21
2.3.4 Lifestyle Factors . . . 21
2.3.4.1 Obesity . . . 21
2.3.4.2 Alcohol Consumption . . . 21
2.3.4.3 Smoking . . . 21
2.3.4.4 Physical Activity . . . 22
2.3.4.5 Diabetes . . . 22
2.3.4.6 Radiation . . . 22
2.4 Diagnosis . . . 22
2.4.1 History and Physical Examination . . . 22
2.4.2 Diagnostic Imaging . . . 23

2.4.3 Mammography . . . 23
2.4.4 MRI . . . 23
2.4.5 Ultrasound . . . 23
2.5 Current Treatment Regimens for Different Subtypes of Breast Cancer 24
2.5.1 Luminal BC (HR+ BC) . . . 24
2.5.2 CDK4/6 Inhibitors . . . 24
2.5.3 HER2+ BC . . . 24
2.5.4 Inhibitors Targeting HER-Family Receptors . . . 25
2.5.5 Triple Negative Breast Cancer . . . 25
2.6 Rab22A Gene in Breast Cancer . . . 25
2.7 Chemotherapeutic Nanoparticles . . . 28
2.8 Role of Secondary Metabolites . . . 29
2.8.1 Genus Zygophyllum . . . 30
2.8.2 Taxonomic Classification . . . 31
2.8.3 Medicinal Importance . . . 31
2.8.4 Genus Mentha . . . 33
2.8.5 Taxonomic Classification . . . 33
2.8.6 *Mentha longifolia* var. *asiatica* . . . 34
2.8.7 Medicinal Importance . . . 35
2.9 Role of Nanotechnology in Research . . . 36
2.9.1 Synthesis of Nanoparticles . . . 38
2.9.1.1 Physical Methods . . . 38
2.9.1.2 Chemical Method . . . 39
2.9.1.2.1 Chemical Reduction . . . 39
2.9.1.2.2 Microemulsion Techniques . . . 39
2.9.1.2.3 Microwave Assisted Synthesis . . . 39
2.9.2 Biological Methods . . . 39
2.9.2.0.1 Synthesis of Nanoparticles by Bacteria . . . 40
2.9.2.0.2 Synthesis of Nanoparticles by Fungi . . . 40
2.9.2.0.3 Synthesis of Nanoparticles by Algae . . . 41
2.9.2.0.4 Synthesis of Nanoparticles by Plants . . . 41
2.10 Computer-aided Drug Designing . . . 42
2.10.1 Molecular Docking . . . 43

3 Material and Methods 45
3.1 Synthesis of Nanoparticles . . . 46
3.1.1 Preparation of Plant Extract of *Z. arabicum* . . . 47
3.1.2 Preparation of Zinc Acetate Salt Solution . . . 47
3.1.3 Synthesis of Nanoparticles of *Z. arabicum* . . . 48
3.1.4 Preparation of the Plant Extract of *M. longifolia* var. *asiatica* 49
3.1.5 Synthesis of Nanoparticles of *M. longifolia* var. *asiatica* . . . 50
3.2 Characterization of Synthesized Nanoparticles . . . 50

3.2.1 UV-Vis Spectroscopy . . . 50
3.2.2 FTIR Analysis . . . 51
3.2.3 X-ray Diffraction (XRD) Pattern Analysis . . . 52
3.2.4 Scanning Electron Microscopy (SEM) . . . 53
3.2.5 EDX Analysis . . . 54
3.3 Cell viability (MTT) Assay . . . 55
3.3.1 Statistical Analysis . . . 56
3.4 Gene Expression Studies by Real-Time qPCR . . . 56
3.4.1 Statistical Analysis . . . 59
3.5 Determination of Protein Expression by ELISA . . . 59
3.5.1 Statistical Analysis . . . 60
3.6 Phytochemical Screening by HPLC . . . 60
3.7 Preparation of Plant Extract . . . 61
3.8 Preparation of Standards . . . 61
3.9 Instrumentation Conditions for HPLC . . . 61
3.10 HPLC/DAD Analysis . . . 62
3.11 In silico Analysis of Detected Flavonoids Against Target Protein Rab22A . . . 63
3.11.1 Preparation of Ligands for Molecular Docking . . . 63
3.11.2 Retrieval and Analysis of Protein Structure . . . 64
3.11.3 Molecular Docking by CB Dock and Analysis of Docked Complex . . . 64
3.12 Molecular Dynamics (MD) Simulation . . . 65
3.12.1 System Preparation, Energy Minimization and Equilibration . . . 65
3.13 Production MD Simulation . . . 66
3.14 Analysis of MD Simulation Results . . . 66
3.15 Toxicity Prediction by ADMET Properties . . . 67

4 Results **68**
4.1 Synthesis of ZnO Nanoparticles . . . 69
4.2 Characterization of ZnO Nanoparticles . . . 69
4.2.1 UV-Vis Analysis . . . 69
4.2.2 Scanning Electron Microscopic (SEM) Analysis . . . 70
4.2.3 FTIR Analysis . . . 71
4.2.4 EDX Analysis . . . 73
4.2.5 XRD Analysis . . . 74
4.3 Cell viability (MTT) Assay . . . 75
4.4 Gene Expression Studies . . . 77
4.5 Protein Analysis by ELISA . . . 78
4.6 Determination of Bioactive Compounds by HPLC . . . 79
4.7 Computational Study . . . 82
4.7.1 Ligands preparation . . . 82
4.7.2 Protein's Primary Sequence Retrieval . . . 83

4.7.3 Physiochemical Properties Analysis . . . 84
4.7.4 Identification of Functional Domains and 3D Structure of Protein . . . 84
4.7.5 Refining of Protein Structure . . . 85
4.7.6 Molecular Docking . . . 85
4.7.7 Analysis of Ligands and Target Protein Interaction through Lig-Plot+ . . . 90
4.8 Molecular Dynamics Simulation . . . 91
4.8.1 Root Mean Square Deviation (RMSD) . . . 94
4.8.2 Root Mean Square Fluctuation (RMSF) . . . 96
4.8.3 Hydrogen Bonds Analysis . . . 98
4.8.4 Radius of Gyration (Rg) . . . 100
4.8.5 Solvent Accessible Surface Area (SASA) . . . 102
4.9 ADMET Properties of Ligands . . . 103
4.9.1 Lead Compound and Synthetic Drug Comparison . . . 109

5 Discussion 110
5.1 Synthesis and Characterization of Nanoparticles . . . 111
5.2 Cytotoxic Analysis of ZnO Nanoparticles . . . 116
5.3 Gene Expression Analysis of Rab22A, Bax and Caspases . . . 118
5.4 Protein Expression Analysis of Rab22A, Bax and Caspases . . . 120
5.5 Phytochemical Analysis of *Mentha longifolia* var. *asiatica* and Zygophyllum arabicum . . . 123
5.6 Computational Analysis . . . 126

6 Conclusion and Future Work 132
6.1 Future Recommendations . . . 134

List of Figures

2.1 Stages of tumour development [42]. 12
2.2 Combinatorial therapy used in the treatment of cancer [46]. 13
2.3 Global mortality rate of breast cancer (courtesy of IARC 2018) [48]. 14
2.4 Stages of breast cancer development [57]. 16
2.5 Action of drugs against triple-negative breast cancer (TNBC) [103]. 26
2.6 Activation of PI3K/AKT/mTOR signaling pathway [116]. 28
2.7 *Zygophullum arabicum* 31
2.8 Medical attributes of Mentha sp. [139]. 34
2.9 *Mentha longifolia* var. *asiatica* [142]. 35
2.10 Essential oils present in Mentha species [144]. 36
2.11 Approaches of nanoparticle synthesis [151]. 37
2.12 Applications of nanotechnology in multiple fields [154]. 38
2.13 Types of CAAD [178]. 43

3.1 An Overview of Methodology 45

4.1 Synthesized ZnO NPs of (A)*Zygophullum arabicum* and (B) *Mentha longifolia* var. *asiatica* 69
4.2 UV-vis spectroscopy of ZnO nanoparticles from *Z. arabicum* and *M. longifolia* var. *asiatica* 70
4.3 SEM analysis of *Z. arabicum* ZnO nanoparticles 71
4.4 SEM analysis of *M. longifolia* var. *asiatica* ZnO nanoparticles . . . 71
4.5 FTIR analysis of *Z. arabicum* ZnO nanoparticles 72
4.6 FTIR analysis of *M. longifolia* var. *asiatica* ZnO nanoparticles . . 73
4.7 EDS spectra of *Z. arabicum* ZnO nanoparticles 73
4.8 EDS spectra of *M. longifolia* var. *asiatica* ZnO nanoparticles . . . 74
4.9 The XRD pattern of *Z. arabicum* and *M. longifolia* var. *asiatica* ZnO nanoparticles 74
4.10 AGraphical representation of% cell viability of plant extract and ZnO NPS of *Z. arabicum* and *M. longifolia* var. *asiatica* 75

4.11 Decreased cell viability of MCF-7 cell line treated with plant extract and ZnONPS of *Z. arabicum* and *M. longifolia* var. *asiatica* in a dose-dependent manner. Error bars indicate the standard error (SE) of three means, asterisk represents the significant difference in data compared with control at *P < 0.05, **P < 0.01 and ***P< 0.001. ZA=*Zygophullum arabicum*, ML= *Mentha longifolia* var. *asiatica* 76
4.12 Gene expression studies: level of Rab22A, bax and caspase 3, caspase 8 and caspase 9 genes determined by real time q-PCR. Error bars indicate the standard error (SE) of three means, asterisk represents the significant difference in data compared with control at *P < 0.05, **P < 0.01 and ***P< 0.001. ZA=*Zygophullum arabicum*, ML= *Mentha longifolia* var. *asiatica* 78
4.13 Determination of protein levels: Rab22A, bax and caspases protein levels determined by ELISA. Error bars indicate the standard error (S.E.) of three means, asterisk represents the significant difference in data compared with control at *P < 0.05, **P < 0.01 and ***P< 0.001. ZA=*Zygophullum arabicum*, ML= *Mentha longifolia* var. *asiatica* 79
4.14 Preparation of methanolic extract of Z.arabicum and *M. longifolia* var. *asiatica* ZnONPs for HPLC analysis 80
4.15 HPLC profile of *Z. arabicum* methanolic extract 80
4.16 Graphical representation of HPLC results of *Z. arabicum* methanolic extract 81
4.17 HPLC results of *Mentha longifolia* var. *asiatica* methanolic extract 81
4.18 Graphical representation of HPLC profile of *Mentha longifolia* var. *asiatica* methanolic extract 81
4.19 Identification of functional domains of Rab22A by Interpro 85
4.20 3D structure of Rab22A protein obtained from Protein Data Bank . 86
4.21 Refined 3D structure of Rab22A protein by Pymol software 86
4.22 Best docking pose of 3-hydroxybutyric acid 87
4.23 Best docking pose of chlorogenic acid 88
4.24 Best docking pose of palbociclib drug 88
4.25 Best docked pose of chlorogenic acid and Rab22A complex by Chimera 92
4.26 Electrostatic interactions of the best-docked pose of chlorogenic acid and Rab22A complex viewed via GROMACS 2022.1 92
4.27 Best docked pose of 3-hydroxybutyric acid and Rab22A complex by Chimera 92
4.28 Electrostatic interactions of the best-docked pose of 3-hydroxybutyric acid and Rab22A complex viewed via GROMACS 2022.1 93
4.29 Best docked pose of palbociclib and Rab22A complex by Chimera . 93
4.30 Electrostatic interactions of the best-docked pose of palbociclib and Rab22A complex viewed via GROMACS 2022.1 93
4.31 RMSD plot of chlorogenic acid 94
4.32 RMSD plot of 3-hydroxybutyric acid 94

4.33 RMSD plot of palbociclib 95
4.34 Comparative RMSD plot of chlorogenic acid, 3-hydroxybutyric acid and palbociclib 95
4.35 RMSF analysis of the chlorogenic acid-Rab22A complex 96
4.36 RMSF analysis of the 3-hydroxybutyric acid-Rab22A complex . . . 97
4.37 RMSF analysis of the palbociclib-Rab22A complex 97
4.38 Comparative RMSF analysis of chlorogenic acid, 3-hydroxybutyric acid and palbociclib-Rab22A complexes 97
4.39 Hydrogen bond analysis of chlorogenic acid 98
4.40 Hydrogen bond analysis of 3-hydroxybutyric acid 99
4.41 Hydrogen bond analysis of palbociclib 99
4.42 Comparative hydrogen bond analysis of ligands and drug 99
4.43 Radius of gyration plot of chlorogenic acid 100
4.44 Radius of gyration plot of 3-hydroxybutyric acid 101
4.45 Radius of gyration plot of palbociclib 101
4.46 Comparative analysis of radius of gyration plot of ligands and reference drug 101
4.47 Solvent accessible surface area (SASA) analysis of chlorogenic acid . 102
4.48 Solvent accessible surface area (SASA) analysis of 3-hydroxybutyric acid 103
4.49 Solvent accessible surface area (SASA) analysis of palbociclib 103
4.50 Comparative analysis of solvent accessible surface area (SASA) of ligands and reference drug 104

List of Tables

2.1 Subtypes of Breast Cancer 15
2.2 Types of nanoparticles synthesized by bacteria 40

3.1 List of materials used for nanoparticles synthesis 46
3.2 Materials used for the preparation of *Z. arabicum* extract 47
3.3 Materials used for the preparation of zinc acetate salt solution . . . 48
3.4 Materials used in ZnO NPs synthesis 48
3.5 Detailed experimental conditions for the synthesis of ZnO NPs using the green synthesis method 49
3.6 Materials used in *M. longifolia* var. *asiatica* extract preparation . . 49
3.7 Reagents used in cell viability assay (MTT assay) 55
3.8 Specific primer sequences used for real-time PCR 58
3.9 Cycling conditions for real-time-qPCR 59

4.1 Analysis of variance for factors affecting the viability of MCF-7 Cells 77
4.2 Ligands of *Zygophullum arabicum* & *Mentha longifolia* var. *asiatica* 82
4.3 Physiochemical properties of Rab22A 84
4.4 Docking results of selected ligands of *Mentha longifolia* var. *asiatica* and standard drug against Rab22A protein 88
4.5 Docking results of selected ligands of *Mentha longifolia* var. *asiatica* and standard drug against Rab22A protein 89
4.6 Docking results of selected ligands of *Zygophyllum arabicum* and standard drug against Rab22A protein 89
4.7 Docking results of selected ligands of *Zygophyllum arabicum* and standard drug against Rab22A protein 90
4.8 Findings of interaction between ligands and standard drug molecule with target protein 90
4.9 Findings of interaction between ligands and standard drug molecule with target protein 91
4.10 ADMET properties of selected ligands 104

Abbreviations

kV	kilo Volt
mg	milligram
mL	milli Litre
mM	milli Molar
mm	millimeter
nm	nanometer
ps	picosecond
rpm	round per minute
µg	microgram
µL	micro Litre
µm	micrometer
µM	micro Molar

Chapter 1

Introduction

1.1 Background of the Study

Cancer is classified into a group of diverse diseases which is distinguished by dysregulation in multiple gene expressions that control normal cellular proliferation and differentiation leading to an imbalance in apoptosis and replication. These events result in the emergence of a population of cells that can invade surrounding tissues, localize to zonal lymph nodes and metastasize to faraway sites within the body [1]. Compromised immunity, genetic predisposition, inflammation, nutrient deficiencies, and several other factors contribute to malignancy which proves lethal for the host [2]. The incidence of cancer is growing manyfold worldwide. It is thought to be the major reason of death and the utmost barrier against increasing expectancy of life in the 21st century. According to WHO statistics, there were approximately 9.6 million deaths attributed to cancer.

As of 2021, breast cancer is now the most common cause of cancer incidence worldwide surpassing lung cancer in women. It accounts for over 2.3 million cases annually (12%) [3]. Chemotherapy is often initially effective in treating malignancies but later on resistance develops [4]. Because the chemotherapeutic and chemo-preventive drugs available in the market have unfavourable side effects, it

is essential to find a biocompatible and affordable cancer therapy strategy. Numerous factors including tumour size, grade, invasion status to lymph nodes, and human epidermal growth factor receptor 2 (HER2) among others can cause delayed diagnosis and ultimately treatment [5]. Due to the undesirable effects of present medications and the absence of specific cytotoxicity to tumours, the therapeutic index is decreased which results in a higher proportion of patients receiving suboptimal drug doses [6].

High interstitial fluid pressure (IFP) in solid tumours serves as a hurdle to the medication's ability to pass through capillaries. Sometimes drug efflux proteins amplify and this amplification makes tumour cells resistant to the treatment and results in treatment failure[7]. Additionally, some chemotherapy medications have very short half-life which makes it difficult for the substances to effectively infiltrate tumour tissue [8]. As a result, research into new methods to fight breast cancer is urgently needed due to the significant global mortality of the disease and the financial toll it takes on contemporary society [9].

The incidence of breast cancer in Asian countries has alarmingly increased particularly among the Pakistani population. In Pakistani women, breast cancer accounts for 34.6%. The Asian population is more prone than Jews to have breast cancer. This significant increase accounts for 2.5 times higher than that of Iran and India. The population of Pakistan lacks knowledge about the epidemiology and etiology of breast cancer. The efforts carried out by various research groups have considered consanguinity as a significant mutational risk factor. These findings also provide insight into the genetic basis of BC among various ethnic groups in Pakistan [10]. The majority of breast cancer susceptibility is polygenic. In Pakistani populations of different races, there are several genes with moderate to low penetrance as well as high penetrance genes (BRCA1 and BRCA2). High morbidity and susceptibility to breast cancer have also been linked to single nucleotide polymorphisms in numerous genes [11]. The use of nanotechnology in the fight against cancer generated a new domain called "Cancer Nanotechnology," which is defined as the enactment of nanotechnology in the detection, diagnosis, imaging and cancer treatment [12].

In comparison to free pharmaceuticals, nanoscale-based medications offer several advantages, including enhanced selectivity which lowers systemic toxicity and improves drug penetration into the targeted tissue while delaying the onset of early degradation in the compounds [13]. Metallic nanoparticles (MNPs) have a lot of potential for medicinal applications like cancer treatment. MNPs can be made using a simple and basic method using several physicochemical techniques which makes them potential candidates for anticancer medications [14].

Over 150 different small GTPases, that are members of distinct families, make up the Ras superfamily. The Ras family (36 members), Rho family (20 members), and Rab family (more than 60 members) are the subfamilies of small GTPases superfamily [15]. These proteins take part in vital cellular signalling networks which control gene expression, cytoskeletal structure, protein and vesicle transport inside cells and cell proliferation [16]. The Ras superfamily member Rab22A coding gene is found at chromosome 20q13.32. According to the literature, Rab22A participates in the endocytic pathway at several levels [17]. Additionally, endocytic recycling and uptake control the makeup of the plasma membrane receptors. In literature, it is reported that Rab22A also mediates the trans-Golgi network and early endosome trafficking [18].

In a particular study, the aberrant expression of the Rab22A gene in vitro caused early endosomes to expand. According to the literature, short interfering RNAs limit the activity of Rab22A by preventing the recycling of the transferrin receptor and the major histocompatibility complex-I (MHC-I). According to numerous reports, endocytosis dysregulation is a common feature of many malignancies. Therefore, aberrant Rab GTPase expression may contribute to the development of tumours [19]. Another study discovered that Rab22A knockdown prevents BC metastasis in vivo [20].

In another study, it is reported that in triple-negative breast cancer metastasis is inhibited by changing the expression of miR-203/Rab22A resulting in the development and synthesis of O(2)-3-Aminopropyl diazeniumdiolates 3a-f in vivo as well as in vitro [21]. The non-nutrient chemical components of plants are known as

phytochemicals or secondary plant metabolites. Vegetables, fruits, cereals, drinks, and medicinal plants are sources of phytochemicals [22]. Numerous polyphenols, carotenoids, organo-sulfur compounds, and alkaloids are examples of bioactive phytochemicals [23]. Herbs are used in traditional Chinese medicine (TCM) to both inhibit and treat ailments. Whether it could prevent, treat, or improve traditional anticancer therapy is currently being researched [24]. Although Sumerian written records of plants used for medicine stretch back 5000 years, archaeological research has revealed evidence of their use 60,000 years ago in Iraq. Even though its long history of usage and frequent efficacy, the use of herbal treatment decreased as modern or conventional Western medicine advanced because there were no independent scientific studies to back it up [25].

Phytochemicals have a range of biological effects which include antioxidant, antimicrobial, anti-inflammatory and anticancer properties. They can also be found in entire plant diets alone or mixture form. Additionally, phytochemicals are frequently readily available, inexpensive and may only have minor negative effects [26]. Preclinical research has demonstrated the enormous potential of phytochemicals to treat or prevent breast cancer [27]. According to the literature, the utilization of plants secondary metabolites and prevention of tumour formation by modification of several cell signalling pathways are directly related [28]. Numerous phytochemicals found in functional foods control apoptosis, proliferation, angiogenesis, inflammation, invasiveness and metastasis events linked to malignant transformation. Numerous studies revealed that phytochemicals have a major role in controlling epigenetic alterations and metabolic reprogramming is two crucial processes for the initiation, development and advancement of cancer [29].

Zygophyllaceae is a diverse plant family having around 27 genera of which genus *Zygophyllum* has 80 species [30]. *Zygophyllum arabicum* (L.) Christenh. & Byng is one of the species of this genus. The plants of the genus *Zygophyllum* have been used to treat different ailments including diabetes, hypertension, rheumatism, and microbial infections. Moreover, several reports confirm the diverse pharmacological activities of these plants. They are important for their anti-inflammatory activities and are used as Ayurvedic medicine in the Indian subcontinent.

Different phytochemicals found in the plant including flavonoids saponins and essential oils help cure stomach problems, skin diseases and cancer. The genus Mentha is another important genus and holds a very important position in the family Lamiaceae. This genus typically comprises 25–30 species and they are widely found in various regions of the world. They are found abundantly in the South Africa, Australia and temperate regions of Eurasia [31]. *Mentha longifolia* var. *asiatica* known as Asian mint is a member of the family Lamiaceae. Various kinds of bioactive compounds and essential oils have been isolated from this species which show cytotoxic activity [32].

In addition to this, Mentha spp. has long been used as a folk remedy for different ailments such as ulcers, nausea, flatulence, bronchitis, liver complaints and colitis due to the presence of phytochemicals [33].

This conventional use can be attributed to the fact that there are two types of secondary metabolites found in mint. These are essential oils and various structural compounds. Mint also contains phenolic acids such as rosmarinic acid [34].

The essential oils are used in a variety of food, perfume and pharmaceutical industries. These compounds are significant medically since some flavonoids, including thymonin, caffeic acid, rosmaric acid and limonene are present. They improve blood flow and relieve pain, menstrual cramps and flu symptoms [35].

Synthesis of nanoparticles from biological organisms (plants, bacteria, algae, fungi) proved to be very cost-effective and environmentally stable. This is known as green synthesis of nanoparticles. Plants contain different types of active compounds and secondary metabolites which aid in the synthesis process. Plants are reportedly used to remove heavy metal pollutants which are very toxic even in small amounts [36].

The biological route of metallic nanoparticle synthesis is a simple and cost-effective method with fewer adverse side effects. Silver, iron oxide and zinc oxide nanoparticles can be used in the treatment of cancer as they help design anticancer drugs [37].

1.2 Gap Analysis

1.2.1 Absence of Prior Studies on the Synthesis and Anticancer Studies of ZnO Nanoparticles from *Zygophyllum arabicum*

1.2.1.1 Gap

The plant-mediated ZnO nanoparticles synthesis from *Zygophyllum arabicum* and its role in breast cancer diagnosis and treatment by targeting the Rab gene family has not been investigated.

1.2.1.2 Implication

This gap necessitates the potential research of biological synthesis of ZnO nanoparticles from this plant and then the study of these nanoparticles on breast cancer cell lines to know about the therapeutic potential of the *Zygophyllum arabicum* species. These efforts will also be helpful in our understanding of the function of secondary metabolites in finding new biomarkers for the treatment of breast cancer.

1.2.2 Absence of Comparative Analysis of *Mentha longifolia* var. *asiatica* and *Zygophyllum arabicum* Mediated ZnO Nanoparticles and their Potential Role in Breast Cancer Treatment In vitro

1.2.2.1 Gap

The comparative analysis of *Mentha longifolia* var. *asiatica* and *Zygophyllum arabicum* ZnO nanoparticles has not been carried out. This underscores the need

that there must be a comparative study to understand which particular species has more active bioactive compounds in the treatment of breast cancer.

1.2.2.2 Implication

There is very little literature available about which of these two plant species has more medicinal efficacy.

1.2.3 Restricted Knowledge about the Plant-Mediated ZnO Nanoparticles Targeting Rab22A Gene in the Breast Cancer Prognosis and Treatment

1.2.3.1 Gap

Rab22A belongs to Rab5 super family of RabGTPase. Rab22A is a novel prognostic marker which can be used in the treatment of breast cancer as it is involved in the endocytic pathway. However, there is no information available about how metallic nanoparticles can target this particular gene and later be involved in prognosis and treatment.

1.2.3.2 Implication

Our knowledge about how plant-based nanoparticles can target the Rab22A gene is lacking as there is only information about the role of micro RNAs in targeting this particular gene. There is information available about other members of Rab family such as Rab23, Rab25. However, very little information is available about the role of Rab22A particularly in the prognosis of breast cancer.It has been reported in various studies that mutation in Rab22A is responsible for the lung adenocarcinoma and liver cancer. The role of Rab22A in breast cancer studies is poorly understood. Moreover, this gene is responsible for the endocytic recycling and membrane transport. These two crucial functions are necessary for the

survival of a cell and for maintaining the integrity of cell membrane. Metallic nanoparticles have the ability to reach to the biological systems efficiently because they have large surface area to volume ratio which enable them excellent drug candidates. In this context, it is necessary to do further research on how plant-based nanoparticles can be used in regulating the expression of the Rab22A gene. Moreover, studies may also be carried out to study the role of Rab22A in comparison with apoptotic pathway genes and proteins.

1.3 Problem Statement

The prevalence of breast cancer has increased 2 folds in the last three decades. There are many risk factors associated with the BC. The prevalence has mostly increased due to the modifiable risk factors and current treatment regimes. Moreover, the currently employed treatment methods against breast cancer are very expensive and also have various side effects.

1.4 Research Questions

This study will answer the questions mentioned below:

Research Question 1:

How much are the extracts of *Zygophyllum arabicum* and *M. longifolia* var. *asiatica* useful against breast cancer?

Research Question 2:

How plant-based synthesis of ZnO nanoparticles be carried *M. longifolia* out using *Zygophyllum arabicum* and *M. longifolia* var. *asiatica* and a comparative analysis of their characterization and cytotoxicity be done against breast cancer?

Research Question 3:

What is the role of ZnO nanoparticles and respective plant extracts in targeting the Rab22A gene apart from the apoptotic pathway genes and proteins?

Research Question 4:

Does the downregulation of Rab22A is linked with the upregulation of apoptotic pathway genes and proteins?

Research Question 5:

Which metabolites of *Zygophyllum arabicum* and *M. longifolia* var. *asiatica* are effective in targeting Rab22A protein when checked computationally?

1.5 Research Objectives

The study has the following objectives:

Research Objective 1:

To identify the anti-proliferative role of *Zygophyllum arabicum* and *M. longifolia* var. *asiatica* plant extract and their metallic (ZnO) nanoparticles against breast cancer cell lines.

Research objective 2: To study the impact of ZnO nanoparticles of both selected plants on the expression of breast cancer target gene (Rab22A) and its protein along with apoptotic pathway genes and protein.

Research Objective 3:

Characterization of extracts of *Zygophyllum arabicum* and *M. longifolia* var. *asiatica* plants for identification of bioactive compounds.

Research Objective 4:

To analyze the role of identified bioactive compounds of *Zygophyllum arabicum* and *M. longifolia* var. *asiatica* against breast cancer-targeted gene (Rab22A) by computational approaches.

1.6 Scope and Significance

It is imperative to develop new medications or agents that are far more potent, long-lasting and low in negative effects. Phytochemicals are important bioactive compounds which have strong pharmacological potential with much less adverse effect. There is a need to study extracts of *Zygophyllum arabicum* and *M. longifolia* var. *asiatica* and their metallic nanoparticles to discover authentic agents for therapeutic usage and check their therapeutic potential on breast cancer cell lines. The current study would serve the purpose of detecting the inhibitory compounds against receptor-associated protein (Rab22A) that could be useful in drug development and improvements to fight the challenges of breast cancer.

Chapter 2

Literature Review

2.1 Cancer

Cancer is the main cause of mortality all around the globe. It is reported that one out of every 6 deaths globally is due to cancer. Cancer is the slow transformation of normal cells into malignant ones which ultimately leads to the formation of tumours. Although cancer arises due to genetic mutations, it is accelerated by different biological, chemical and physical carcinogens. Lifestyle and diet play a significant contribution in the development of tumours [38]. It has been proved through research that the incidence of cancer increases many folds with increasing age because repairing mechanisms within the body become ineffective with age. Moreover, smoking, unhealthy diet, no physical activity and excessive alcohol usage are also major risk factors for chronic types of cancer [39].

The process of tumour initiation begins with 5 or 6 mutations because a single mutation is not enough to initiate disease progression (Figure 2.1). It is also found that mutation does not take place in differentiated cells because they can be eliminated rapidly and there can only be a single mutation. Oncogenic mutations mostly take place in stem cells. It has also been observed that microenvironment in which inflammation is present enhances the rate of mutation. Also, inflammatory microenvironments speed up the proliferation of mutated cells [40, 41].

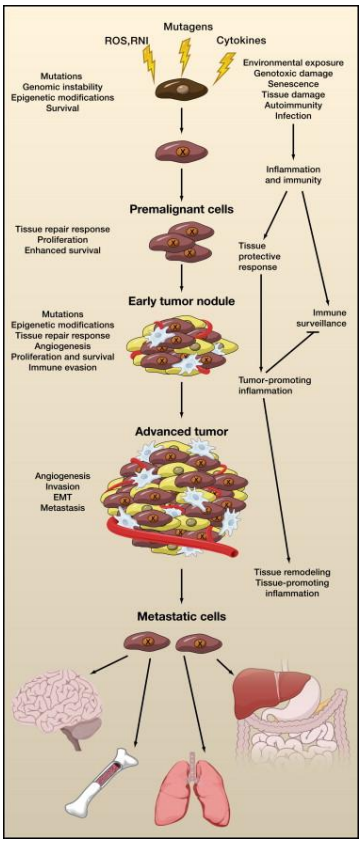

FIGURE 2.1: Stages of tumour development [42].

Every year, more than 6 million individuals worldwide die due to cancer. Positive population-wide improvements can significantly lower the burden of cancer because there is strong evidence that factors such as lifestyle have an impact as a cancer risk factor. Current epidemiologic research has connected behavioural factors to frequent malignancies identified including lung, colorectal, prostate, and breast cancer [43]. It is reported in the literature that 50% of cancers can be intercepted because of the strong risk-modifying effects of modifiable factors. Moreover, lifestyle factors should also be modified to lower the incidence rates of cancer [44].

It has been also reported that working on a single drug does not produce effective results due to different limitations such as the solubility of the drug and resistance offered by cancer cells to a certain drug. Combination therapy of photo dynamic therapy (PDT) and CBD has proven very fruitful in the treatment of cancer (Figure 2.2). In photodynamic therapy drug is delivered to the tumor site with the aid of a sensitizer and light of a suitable wavelength is given which results in the production of ROS and causes oxidative damage to the tumor site. Cancer cells

possess the ability to adapt to a new environment quickly and this type of non-invasive drug delivery system directly affects the tumor cells. This combinational therapy increases the survival rate of the patient by eradicating maximum cancer cells by necrosis and apoptosis [45].

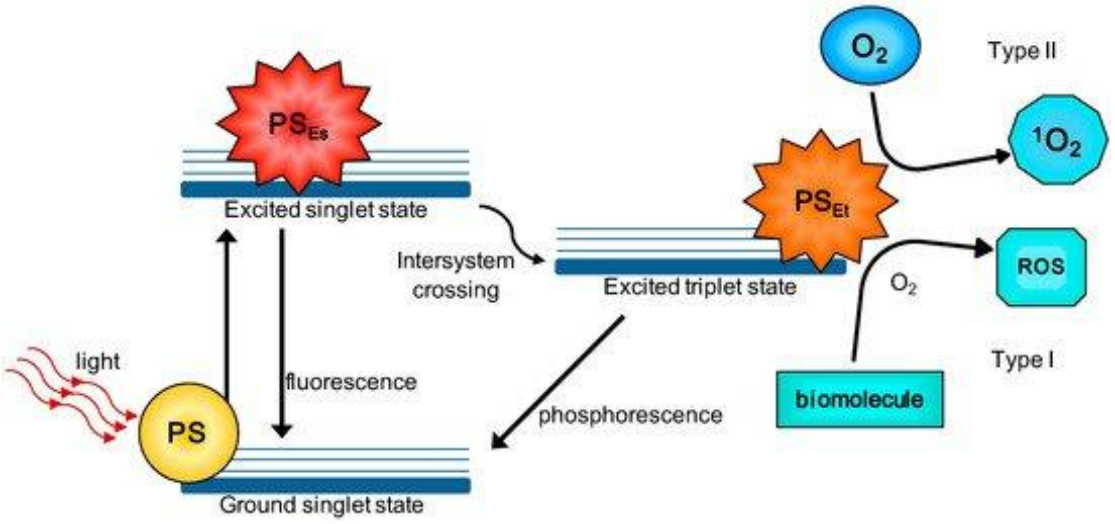

FIGURE 2.2: Combinatorial therapy used in the treatment of cancer [46].

2.2 Human Breast Cancer

There are over 2.2 million new cases of breast cancer globally as per reports of a study conducted in 2020. According to statistical data from WHO, there has been a rise of 24.5 % in all cancer cases and about 685,000 deaths (Figure 2.3). The majority (59.5 %) of the world's population lives in Asian countries, where there are 45.4 % of new cases and 50 % of fatalities from breast cancer. Despite making up only 8 % of the world's population, North America and Oceania have 13.6% of new cases of breast cancer and an eight % mortality rate. It is the prevalent malignancy in women globally with roughly about 1.2 million women diagnosed annually. According to the Shaukat Khanum's cancer registry report from the year 2004 to 2014 breast cancer prevalence trend among females is 13882 and among males 110. As stated by SEER data in 2004, there were a total of 519,000 deaths reported of breast cancer as compared to 627,000 deaths in 2018. Among Asian countries, breast cancer is most prevalent in Pakistan with 34.6 % of all female

cancers. In the year 2014, the breast cancer prevalence rate in Pakistan was 25.8 % with 1425 cases out of 5521 total malignancies [47].

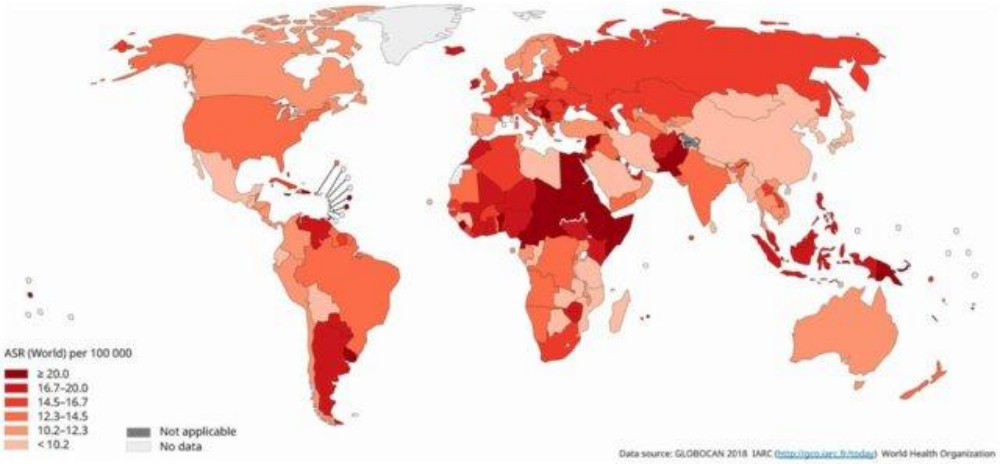

FIGURE 2.3: Global mortality rate of breast cancer (courtesy of IARC 2018) [48].

By 2030, the World Health Organization (WHO) predicts that over 11 million new cases of cancer will be reported in underdeveloped countries, which is an increase of 80 % from 2008. Cancer is anticipated to be the biggest barrier to increasing human life expectancy by the end of the 21st century, according to extrapolation. Women are at greater risk than men to be diagnosed with breast cancer. Above 7 % of breast cancer diagnoses are made in under-40-year-old women and less than 4 % are made in under-35-year-old women [49]. Breast cancer is rare in young women. Due to the disease's variability, there are numerous subtypes of breast cancer that differ in terms of progesterone receptor, estrogen receptor, and HER-2/neu receptor expression [50, 51].

Breast cancer metastatic growth and development are significantly influenced by BC stem cells. These stem cells have the potential to undergo self-renewal and when they divide simultaneously they produce daughter cells, which give rise to tumour cells with the capacity to multiply themselves in large numbers [52]. Most tumours include very few breast cancer stem cells, but in some, like melanoma, they make up over 25 % of the total mass. Breast cancer is classified into four stages using the TNM (tumour nodes metastasized) classification, depending on the size of the tumour, progression of the tumour to the lymph nodes and metastasis [53]

2.2.1 Types of Breast Cancer

It is heterogenous disease which is divided into four subtypes based upon their genetic profiles. These include Luminal A, Luminal B, and epidermal growth factor receptor HER2 (Table 2.1) [54].

Table 2.1: Subtypes of Breast Cancer

Subtype	**Immunohistochemistry and Incidence**
Luminal A	Estrogen and Progesterone receptor-positive HER-2 negative. It is most common. They grow very steadily and are less aggressive as compared to other subtypes.
Luminal B	Estrogen and Progesterone receptor-positive HER-2 negative/positive The incidence rate is greater than Luminal A and they have poor survival rate as well.
HER-2 positive	Estrogen and Progesterone receptor-negative HER-2 positive Anti-HER-2 monoclonal antibodies do not work on all tumour types. They tend to grow very slowly but they spread aggressively.
HER2-negative (basal)	Estrogen and Progesterone receptor-negative HER-2 negative Occurrence is common among black women. They are also common in premenopausal women [56].

The pathophysiology of breast cancer is poorly understood due to its complex nature. There are various risk factors which are primarily linked with breast cancer which include increasing age, female sex, hormone therapy, greater body mass index (BMI), late menopause and family history [56]. In addition to this,

it is also reported that women who undergo hormone therapy after menopause, white women and those women who have a chest radiation history are at high risk of developing cancer [55].

2.2.2 Stages of Breast Cancer

There are multiple stages of breast cancer described as follows (Figure 2.4) [57].

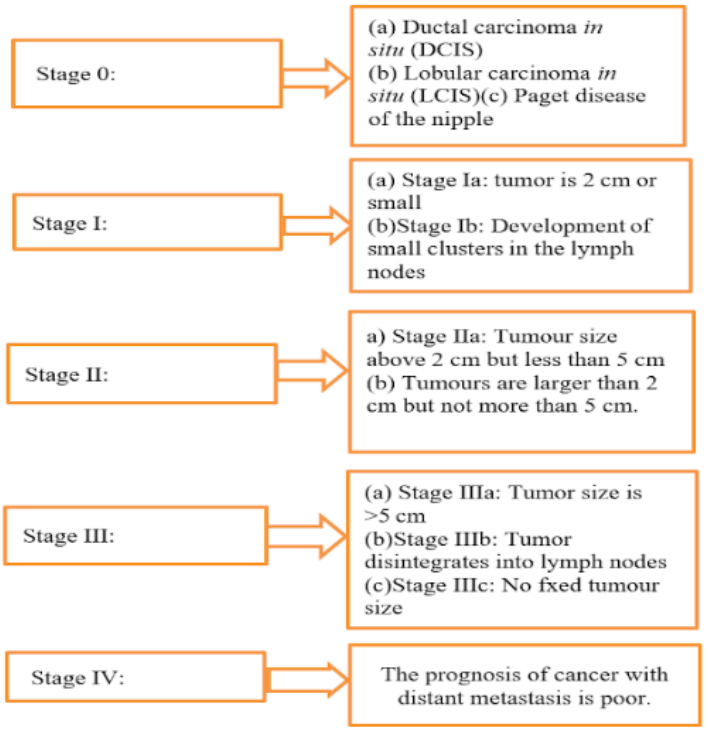

FIGURE 2.4: Stages of breast cancer development [57].

2.2.3 Metastasis in Breast Cancer

Metastasis causes 90 % of cancer deaths. "Metastasis" describes cancer cells migration from primary tumour to neighbouring tissues or other organs. Hence, it has been widely acknowledged how important it is to comprehend the mechanism of the metastatic process, the factors which accelerate metastasis, as well as the pathways that are engaged in the process. The majority of patients die from metastasizing tumours, not the primary tumour, making breast cancer the second most lethal disease in the United States. Within 3 years of the main tumour

growing, 10-15% of breast cancer patients have severe illness that causes tumour to spread to other organs [58]. Breast cancer is a diverse disease which means that its metastasis takes different forms making it challenging to treat. Initial BC cells typically migrate to distant organs such as the lungs, liver, and bones through blood vessels. In many solid tumours, the common metastasis process includes the following steps which may lead to the dispersion of breast cancer cells [59].

2.2.4 Detachment of Breast Cancer Cells & Local Invasion

2.2.4.1 Penetration in the Circulatory System

Cancer cells attach themselves to the endothelium wall of lymphatic or blood vessels, penetrate, and spread there [60].

2.2.4.2 Circulation

The lymphatic or blood circulation allows the tumour cells to travel to other organs. For the cells to continue to survive in a way that is independent of anchoring, they must develop anoikis resistance [61].

2.2.4.3 Cell Cycle Arrest and Extravasation

Cell-cycle arrest occurs in cancer cells before their extravasation into the metastatic site. Then, they adhere to the target organs' capillary walls [62].

2.2.4.4 Development of Tumour

Cancer cells that have the potential to become tumours start to grow and form miniature tumours. Metastasis is a challenging, multi-step process that requires a variety of characteristics for metastatic cells to overcome the barriers. Above all, they must be able to proliferate new tumours, infiltrate other areas and endure in

detached environments. Cancer does not spread when any of these pathways are disrupted. However, for cancer cells to survive, they must avoid apoptotic signals and the immune response that would ordinarily destroy them. If the tumour cells can compete these steps, secondary metastasis will result [63].

2.3 Risk Factors

2.3.1 Demographic Factors

2.3.1.1 Gender

Breast cancer, which often only affects women, accounts for less than 1% of all cancer incidences in men [64]. The development of breast cancer in older adult men is associated with radiation exposure, hormone imbalance and a higher risk of familial history. The mutation in the BRCA2 gene is the most prominent risk factor in men [65].

2.3.1.2 Age

Age is the second most significant risk factor after gender. When women reach menopausal age, breast cancer incidence rates peak and then progressively decline or remain steady [66]. Breast cancer incidence was connected to age above 50 years in a case-control study. Younger women's breast cancers have positive lymph nodes and a worse prognosis, even though they tend to be larger at advanced stages [67].

2.3.1.3 Blood Group

Women who are Rh+ and have blood group A have more chances of having breast cancer when compared with Rh- persons having blood group AB. Several studies that looked for a connection between blood type and breast cancer did not find a link [68].

2.3.1.4 Reproductive Factors

The number of pregnancies and their final decline following menopause, as well as the action of ovarian hormones which become active around puberty age, are linked to the association between reproductive factors and breast cancer [69].

2.3.1.5 Age of Menarche

According to a case study, menarche happening at a puberty age doubles the risk of breast cancer. Numerous researches have supported this finding. The incidence of breast cancer is higher among younger and menarche-aged women in China, according to cohort research involving a large population of 11,889 women [70].

2.3.1.6 Age of Menopause

Menopause that occurs beyond age 50 is correlated with an elevated chance of breast cancer. The relationship between advanced menopausal age and breast cancer incidence was confirmed by case-control research [71].

2.3.1.7 Full-Term Pregnancy

Women who are parous experience a decreased risk of breast cancer. The time of first pregnancy is an important risk factor. It was reported in a study that the greater the age at first pregnancy, the chances of cancer become sixfold [72].

2.3.1.8 Abortion

In a particular study, it has been reported that a higher risk of breast cancer was linked to a higher number of abortions [73].

2.3.2 Hormonal Factors

2.3.2.1 Contraceptive Methods

It is reported in the literature that birth control pills may have lethal effects and can contribute towards cancer development. In a particular study, it was revealed that using an oral contraceptive pill doubles your breast cancer risk [74, 75].

2.3.2.2 Ovulation Stimulating Drugs

According to the literature, the consumption of hormonal stimulating drugs for more than six months can exacerbate your chances of cancer [76].

2.3.2.3 Postmenopausal Hormone Therapy

According to data collected from 51 epidemiological studies, it is found that hormonal replacement therapy is linked to higher cancer lethality [77].

2.3.2.4 Family History of Breast Cancer

Women with any past family history of breast cancer are more prone to developing the disease according to published research. It is also reported that women without BRCA mutations but having a family breast cancer history are prone to the disease [78].

2.3.3 Breast-Related Factors

2.3.3.1 Lactation

Many studies have proved that lactation helps in the prevention of breast cancer. Multiple studies have found a connection between breastfeeding duration and BC. Longer nursing periods increase the lactation protective effect [79].

2.3.3.2 Breast Density

Breast density is also a major risk factor. It is reported in the literature that there is an enormous increase in the density of breasts after the onset of estrogen and progesterone therapy. It is reported that with an increase of 1 % in breast density, the chances of developing cancer rose to 3.4% [80].

2.3.3.3 Benign Breast Disorders

According to the findings of a study, an increased chance of both ER+ and ER- invasive breast cancer is associated with benign breast diseases, and the rate of this increase varies with age [81].

2.3.4 Lifestyle Factors

2.3.4.1 Obesity

In literature, it's reported that there is a sound relationship between obesity and breast. It's a fact that inside adipose tissue there is aromatization of different androgen precursors into estrogen. This fuels up the metastatic process [82, 83].

2.3.4.2 Alcohol Consumption

Alcohol is a mixture of toxic carcinogens which may be a potent factor for breast cancer as reported in several studies. In a case-control study, alcohol intake resulted in a 4.2-fold escalation in the growth of breast tumours, second only to elderly age at the time of the first childbirth [84].

2.3.4.3 Smoking

It is reported in a study that chances of cancer development in women after their menopause phase who are prone to prenatal smoking (HR, 1.18; 95% CI, 1.10-1.27)

and active smoking (HR, 1.16; 95% CI, 1.00-1.34) are elevated for every increment of 20 pack/years [85].

2.3.4.4 Physical Activity

According to the findings of a cohort research involving 74, 171 women between the ages of 50 and 79, postmenopausal women who exercise more frequently have a lower risk of acquiring BC [86].

2.3.4.5 Diabetes

By interfering with biological processes or by having an impact on screening and therapy, diabetes can accelerate breast cancer incidence. According to the recent findings, postmenopausal women with greater BMI and diabetes have more chances of developing breast cancer [87]. According to research conducted by meta-analysis, women suffering from type II diabetes have a 20 % higher risk of cancer development [88].

2.3.4.6 Radiation

It is reported in the literature that women who have any previous radiation history of cancer treatment are at a two to three-fold higher risk of breast cancer, screening for tuberculosis or monitoring for pneumonia [89].

2.4 Diagnosis

2.4.1 History and Physical Examination

The Clinical history is used to evaluate the risk of cancer and to ascertain if any symptoms suggestive of breast cancer are present or missing. Menstrual history, menopausal status, previous pregnancies, oral contraceptive use, and post

menopausal hormone replacement treatment should be taken into account for diagnosis [90].

2.4.2 Diagnostic Imaging

Using diagnostic imaging and image-guided needle biopsies, patients with breast cancer are identified, diagnosed, and staged [91].

2.4.3 Mammography

Women who have a palpable tumour or another symptom of breast illness, or breast cancer history within the last five years are all candidates for diagnostic mammograms. Special views on diagnostic mammography may involve magnification pictures of a certain area of the breast tissue [92].

2.4.4 MRI

Even though mammography is the standard procedure of breast screening or imaging, magnetic resonance imaging (MRI) has also gained a lot of appraisals and become an important tool in the diagnosis, assessment, staging, and therapy of breast cancer in a subgroup of patients. For women with a higher risk of cancer, MRI screening is more sensitive but less specific for cancer diagnosis. When compared to mammography, which has a sensitivity range of 0.33 to 0.39, MRI is more sensitive [93].

2.4.5 Ultrasound

Supplementary screening ultrasound in high-risk individuals with thick breast tissue is supported by different studies, it does come with a significant but recognized number of false positives. The physician may be able to examine for breast cancers not detected by standard mammography using whole breast ultrasonography,

particularly in breasts of high density where the sensitivity of mammography is lower [94].

2.5 Current Treatment Regimens for Different Subtypes of Breast Cancer

2.5.1 Luminal BC (HR+ BC)

Luminal BC also known as hormone receptor-positive (HR+) accounts for 60–80% of occurrences of BC in industrialized countries and is becoming more common in premenopausal women [95]. The foundation of treatment for HR+ BC is endocrine therapy, which prevents the effects of hormones or lowers hormone levels. The medications currently available in the market include tamoxifen, aromatase inhibitors and luteinizing hormone-releasing drugs which prevent the production of hormones in the ovary. Since endocrine medicines have different modes of action, they are frequently taken in combination for enhanced anticancer effects [96].

2.5.2 CDK4/6 Inhibitors

Cell cycle progression is governed by cyclin D1 and CDK4/6's reversible interaction. In one study, amplification of CDK4 and Cyclin D1 was observed in around 29% and 14% of individuals with HR+/HER2 BC, respectively [97]. For advanced cancer that is HR+/HER2, the FDA has approved the use of palbociclib and ribociclib in combination with aromatase inhibitors. This primarily serves as the first-line treatment. It was demonstrated that they dramatically increased median PFS by 10 months [98].

2.5.3 HER2+ BC

Many molecularly targeted medications are authorized for treating HER2+ BC,

either isolated or in combination with conventional chemotherapy. The current recommended treatment for early-stage HER2-positive BC is neoadjuvant chemotherapy combined with anti-HER2 targeted therapy. After that, there will be another course of HER2-targeted therapy, surgery, and radiotherapy for one year. Based on tumour analysis, endocrine adjuvant therapy might be fruitful too [99].

2.5.4 Inhibitors Targeting HER-Family Receptors

Trastuzumab's anticancer activities are known to be blocked by growth factor ligands for HER-family receptors [100]. The HER2/HER3 heterodimers show overexpression due to which they are more active than other HER family dimers. It is linked to trastuzumab resistance [101].

2.5.5 Triple Negative Breast Cancer

TNBC is very challenging to treat. Standard chemotherapy is still used for the treatment of TNBC. It's interesting to note that TNBC has the BC subtype that responds to chemotherapy the most completely (22%) compared to those with non-TNBC malignancies, their rates of recurrence and metastasis are higher [102, 103]. The unavailability of ER, PR, and HER2 expression prohibits the use of targeted treatments in advanced TNBC. Chemotherapy, which is typically taxanes, anthracyclines, and platinum drugs, is the only systemic therapeutic option that has been approved (Figure 2.5).

2.6 Rab22A Gene in Breast Cancer

Rab22A is a GTPase protein which is mostly found in endosomes and Golgi bodies. It is a member of the RAB protein family, the RAB5 subfamily [104]. Exosome production and vesicular flow are regulated by RAB proteins [105]. According to research, the RAB5 subfamily, which consists of RAB5, RAB21, RAB22A and

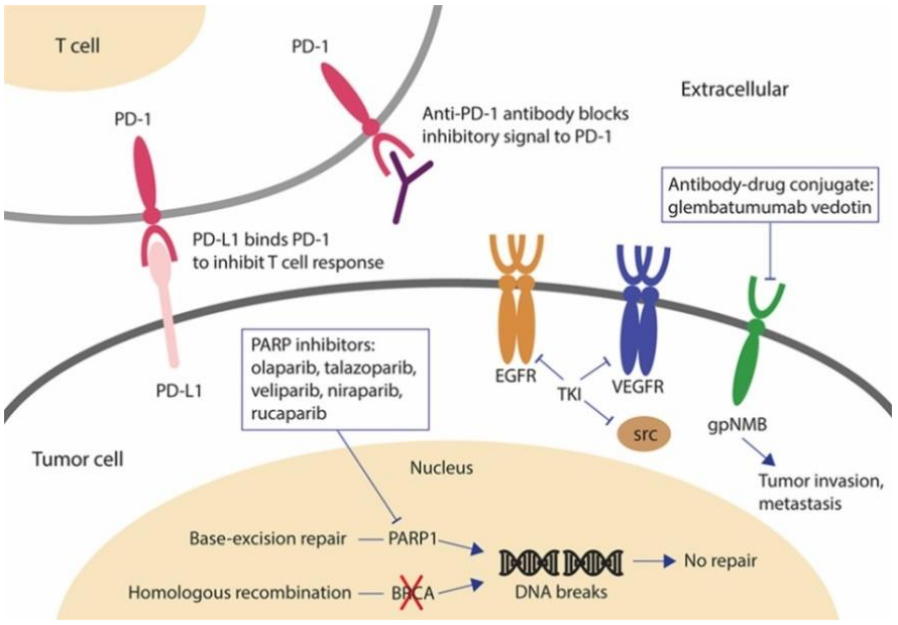

FIGURE 2.5: Action of drugs against triple-negative breast cancer (TNBC) [103].

RAB22B. All these members are predominantly responsible for the endocytosis and metabolism of growth factor receptors which ultimately leads to the development of cancer [106].

The accepted theory holds that Rab GTPases shift between their GTP and GDP-bound states. It is reported that when they are in the GTP state, they attract a variety of downstream effector proteins to membranes [107]. Rab-effector complexes have a variety of roles, including protein phosphorylation, anchoring of vesicles at their target membranes and microtubule-dependent organelle motility [108]. Rab5 is exclusively involved in the transport of materials across EE compartments which is mediated by clathrin-coated vesicles. Rab4 and Rab11 are thought to govern the recycling processes known as early "sorting" endosomes, while Rab11 is thought to be participating in the trafficking of cargo via the perinuclear recycling endosomes [109].

Rab22A is a protein that is linked with endosomes and in the development of exocrine vehicles in several cell types [110]. Data on DNA copy numbers and gene expression together show that Rab22A functions as an oncogene and causes

high-level amplifications [107]. It has been demonstrated that this protein has up-regulative activities in hepatocellular carcinoma [111]. Rab22A has demonstrated positive expression in malignant melanoma utilizing the human HG-U133A gene chip. Moreover, it has been demonstrated that Rab22A co-localizes with autophagic vacuoles and is linked to early and late endosomes [112].

In MDA-MB-231 cells, Rab22A behave as a microvesicle component at the plasma membrane. The potential of BC cells to intercalate other cells and the development of exocrine vehicles caused by hypoxia are both reduced when the Rab22A gene is knocked down [113]. Rab22A is more abundant in tumour tissue, however its function in breast cancer is still unknown. Rab22A is expressed in multiple cancers with growing aggressiveness and a bad prognosis. For instance, a research study showed that the overexpression of Rab22A facilitated the development of melanoma cells. Gastric and colorectal cancer cells can exhibit proliferative effects by suppressing the expression of miR-204-5p, which also targets Rab22A [114].

Another study reported that the relationship between clinical information and Rab22A in >700 breast cancer cases has discovered a high level of Rab22A mRNA expression connected to a reduced overall survival time. Also, they discovered that in hypoxic environments, extracellular vesicles which are coated with Rab22A increased the migration of cancerous cells [115]. Recent research has demonstrated that Rab22A is overexpressed and plays an oncogenic function in several malignant tumours, including ovarian cancer, osteosarcoma, nasopharyngeal carcinoma and melanoma. It has been demonstrated in a study that Rab22A increased CD147 expression at the cell surface and encouraged CD147 recycling, which directly inhibited CD147 degradation and accelerated the malignant development of lung cancer. It is also reported that Rab22A increases epithelial-mesenchymal transition (EMT), ultimately enhancing the malignant phenotype of lung cancer [17].

Transfection with Rab22A dramatically increased cell proliferation and invasion in the lung cancer cell lines A549 and H1299, whereas inhibition with Rab22A-specific siRNA considerably decreased the aforementioned abilities. PI3K/Akt/mTOR pathway key effector protein phosphorylation levels were also increased upon

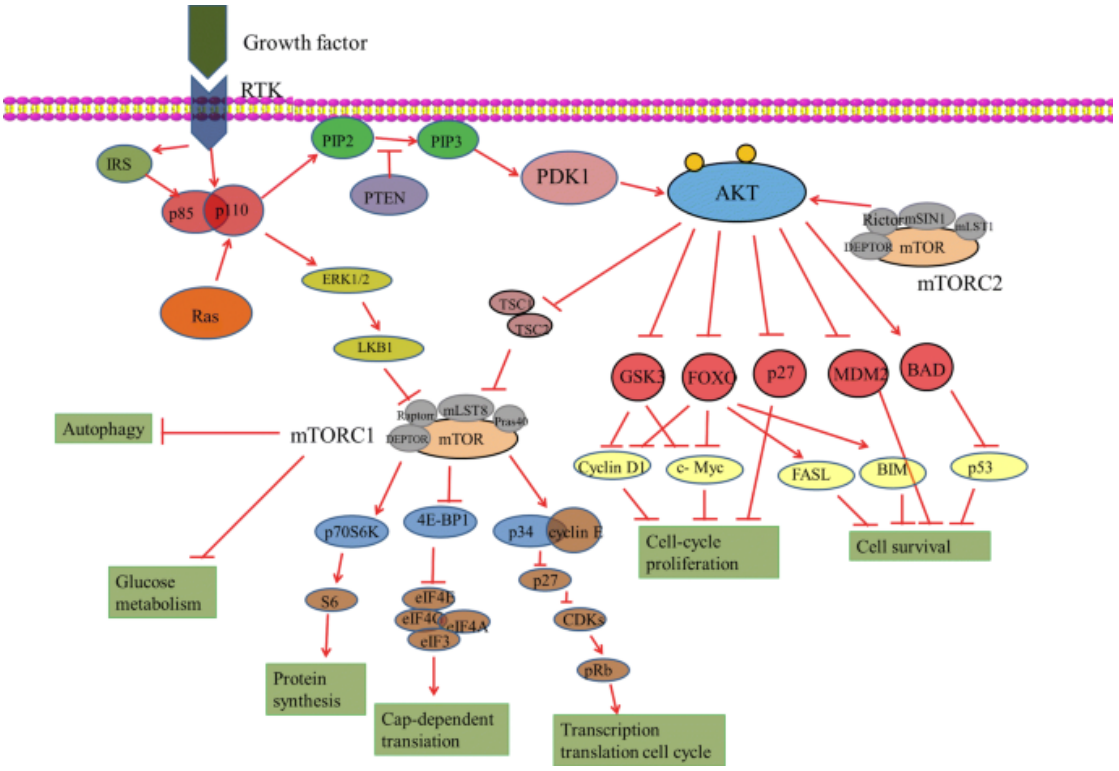

FIGURE 2.6: Activation of PI3K/AKT/mTOR signaling pathway [116].

Rab22A transfection. The association of Rab22A and PI3Kp85, which is considered to be the primary key subunit of PI3K, was further validated by the Co-IP test. Administration of the mTOR inhibitor rapamycin dramatically decreased the ability of lung adenocarcinoma cells which are transfected with Rab22A to proliferate, migrate and invade. All such findings suggest that Rab22A acts as a potential target for anti-tumour therapy by upregulating the PI3K/Akt/mTOR signalling pathway, which can increase the malignant phenotype of lung adenocarcinoma (Figure 2.6) [116].

2.7 Chemotherapeutic Nanoparticles

Chemotherapeutic medications are "cytotoxic," or cell-killing by nature. Women with hormone-insensitive breast cancer require cytotoxic chemotherapy which is delivered into the body while considering treatment goals including pain alleviation, disease progression, symptom relief, patient longevity and improvement of mood disturbances into account [117]. It can be injected intravenously or given

orally. It functions systemically by eliminating both cancerous and healthy cells throughout the body, which has numerous short and long-term negative effects. Chemotherapy is typically used to treat recently developed breast cancer as well as in its early stages. Targeting may be accomplished and harmful side effects may be decreased by using nanoparticles as the carrier. Even the most sophisticated chemotherapy drugs are ineffective at distinguishing between healthy cells and malignant cells, which results in nonspecific drug distribution in the body, systemic toxicity, and unpleasant consequences [118].

The maximum permitted drug dose is restricted so to have the anticipated therapeutic impact in tumour tissue, a substantial amount of the drug must be provided which is not cost-effective and may also have negative side effects. Systemic or cell toxicity can be prevented by using nanoparticles as the tailored delivery mechanism for chemotherapeutic drugs by using both active and passive targeting [119]. Chemotherapy, immunotherapy, radiation, surgery and a combination of different strategies are prominent therapeutic options for cancer treatment but they are not productive specifically when cancer cells develop drug resistance [120]. There are frequently negative side effects associated with the usage of anti-cancer medications. The initial tumour may also be effectively treated, but it may have already spread to other body organs [121]. Inhibiting or reversing carcinogenesis earlier at the premalignant phase by chemoprevention, which primarily utilizes different pharmacological agents and phytochemicals is thus a technique for treating breast cancer in women [122]. Due to their alleged anti-diabetic, laxative, hepatoprotective, antipyretic and anti-microbial effects, these phytochemicals are widely used by practitioners of traditional medicine for a variety of diseases in some South Asian Nations [123].

2.8 Role of Secondary Metabolites

Secondary metabolites (SMs) are compounds that are obtained from plants and are utilized as flavouring agents, additives, agrochemicals and in the synthesis of

medicines. Although primary metabolites are present in large amounts in plants their medical efficacy depends upon the presence of secondary metabolites [124]. There are various plants on this earth which have medicinal importance and indeed they are a blessing from nature. In most regions of the world, phytotherapy is very common for the treatment of various ailments. Every year two-thirds of novel chemicals are identified from higher plants [125]. According to numerous studies, it is a fact that secondary metabolites of plants have antioxidant, anti-inflammatory, antifungal, antibacterial, antiviral and insecticidal actions. The SMs are also used in various industries such as agro-industries, cosmetic, fragrance and food preservation industries [124].

2.8.1 Genus Zygophyllum

Zygophyllaceae is a diverse plant family having around 27 genera of which genus Zygophyllum also known as Fagonia has 80 species [13]. *Zygophullum arabicum* (L.) Christenh. & Byng is one of the species of this genus (Figure 2.7). The plants of the genus Zygophyllum have been used to treat different ailments including diabetes, hypertension, rheumatism, and microbial infections. Moreover, several reports confirm the diverse pharmacological activities of these plants. They are important for their anti-inflammatory activities and are used as Ayurvedic medicine in the Indian subcontinent. Different phytochemicals found in the plant including flavonoids saponins and essential oils help cure stomach problems, skin diseases and cancer [14, 15].

As per reports, species of this genus were used by Bedouins and Native Africans for treating different ailments. Plants of this genus can be found in wadis in the desert as well as sandy plains and calcareous coastal ridges. In Egypt, it can be found along the Mediterranean coast, in the Sinai Peninsula's entire area of desert and in the western desert's oasis. This species is frequently employed as a natural therapy. It is reported that extracts (aqueous and alcoholic) are medically significant and utilized to treat ailments like diabetes, fever, asthma and renal issues [126]. All species of this genus are shrubs, shrublets, or herbs rarely growing higher than

(60 to 100 cm), and they can reach a width of up to 100 cm. It features pink or purple petals, spine-scented or pointed stipules and an obconical, sometimes hairy, loculicidal capsule. It is well known that Zygophyllum species circumscription is notoriously challenging [127].

2.8.2 Taxonomic Classification

- Class Dicotyledon
- Order Zygophyllalles
- Family: Zygophyllaceae
- Genus: Fagonia
- Specie: *Zygophullum arabicum*

FIGURE 2.7: *Zygophullum arabicum*

2.8.3 Medicinal Importance

Zygophullum arabicum is utilized as a blood purifier in its whole and children with anemia are fed plant ash. Ascorbic acid is abundant in this plant's fruit. As teeth

brushes and for treating scabies, twigs are frequently used. Additionally, it has been utilized to treat dropsy. To treat sore mouth and stomatitis, its leaves, twigs and juice are used as a decoction or infusion to gargle. A medicinal bath made from the plant's decoction can help people with extreme itching and irritation of the skin [128].

Indicacin and fagonicin, two novel substances were found in the methanolic extract of *Zygophullum arabicum*. These substances were used for treatment against the human colorectal cancer cell line H-29. Fagonicin showed 40% cytotoxicity at the aforementioned level, but the cytotoxicity of indicacin was 51.40% at 6.25 mM/mL [129]. It is also reported that *Fagonia cretica* aqueous extract may inhibit breast cancer cell growth before inducing the expression of FOXO3a and p53 in reaction to DNA damage by combining with several anti-cancer drugs or alone[130].

Zygophullum arabicum was shown to have a significant cytotoxic effect against brine shrimps at LD50 of 118.89 ppm, and antitumor tests revealed that the extract caused tumours to grow on potato discs. Overall findings show this herb has potent anti-cancer properties [131]. In another study, an IC50 of 8.72 and 9.80 g/ml, respectively, was reported in prior research on *Fagonia taeckholmiana*, which showed that the aerial portions have cytotoxic action against MCF7 human breast tumour cells in-vitro [132].

The antibacterial properties of ethanol extracts from *F. arabica* leaves were evaluated against strains of both Gram-positive and Gram-negative bacteria. In comparison, ethanol extract significantly inhibited Bacillus cereus and had a minimal effect on *P. aeruginosa* [126]. In another study, rat tail flick method was used to study the analgesic effects of *Fagonia indica* extracts (200 and 400 mg/kg). According to the statistical analysis of the data using the regression approach, the ethanol extract has a major inhibitory and a lesser inhibitory effect in response to *B. cereus* and a lesser *P. aeruginosa* respectively. Both extracts (ethanol and aqueous) in this experiment showed considerable (p 0.05) analgesic efficacy. In another report, an extract of *F. indica* was tested in rats and showed inflammatory properties in them [133].

The effects of *F. indica* methanolic extract on CCl4-induced hepatotoxicity in albino rats were investigated. These findings revealed that MEFI has considerable hepatoprotective action. This may be due to the presence of flavonoids and tannins found in this plant [134]. In another study, it was reported that the aerial portions (leaves and twigs) of the plant *Fagonia cretica* include a methanolic extract that possesses anti-haemorrhagic potential. This extract was tested on black snake poison and further evaluation of results was done. Based on scientific evidence, the extract has been shown to be a hemorrhagic inhibitor against snakes and can be used to treat snake bites [135].

2.8.4 Genus Mentha

Genus Mentha is an important genus and holds a very important position in the family Lamiaceae. This genus typically comprises 42 species and they are widely found in various regions of the world. They are found abundantly in the South Africa, Australia and temperate regions of Eurasia [136]. This taxon is very predominant because of its commercial importance as well as therapeutically. It has been known from pre-historic times that plants and their parts are used in the preparation of herbal medicines, teas as well as spice mixtures. Due to these phytochemicals, plants offer aroma and give flavour to foods [137]. In addition to this, Mentha spp. has long been used as a folk remedy for different ailments such as ulcers, nausea, flatulence, bronchitis, liver complaints and colitis due to the presence of phytochemicals (Figure 2.8) [138].

2.8.5 Taxonomic Classification

- Class: Dicotyledon
- Order: Lamiales
- Family: Lamiaceae
- Genus: Mentha

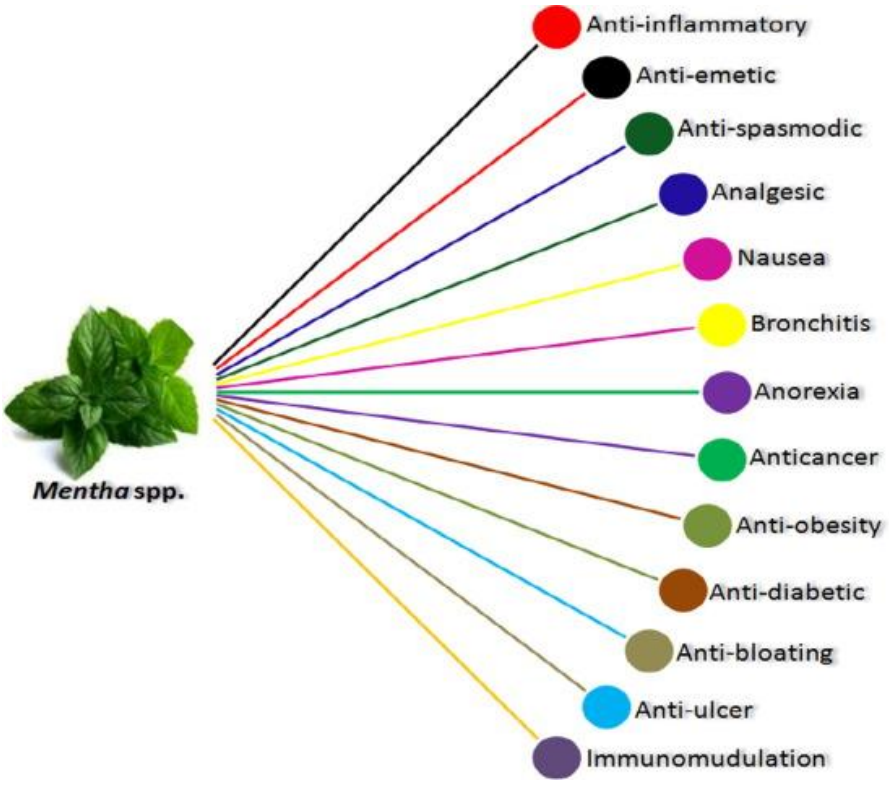

FIGURE 2.8: Medical attributes of Mentha sp. [139].

- Specie: *Mentha longifolia* var. *asiatica*

2.8.6 *Mentha longifolia* var. *asiatica*

Mint (*Mentha longifolia* var. *asiatica*) is a member of the family Lamiaceae (Figure 2.9). It is an aromatic herb normally it grows from May to October. It is a shade-loving plant. It contains various secondary metabolites such as volatile oils (2-3.5 % essential oil), flavonoids and vitamins. The volatile oils found in all members of the genus Mentha are used in the perfumery industry. Peppermint oil obtained from *Mentha longifolia* var. *asiatica* is used in the medicine industry as well as a flavouring agent [140]. The use of mint in teas and food goes back to the pre-historic era as it improves blood circulation, warms the body and also helps to fight against any disease and its cure. The tincture of mint can be used to treat nausea. It is used to reduce the intake of sodium. Mint contains rosmarinic acid as it is an anti-allergen and can be used to treat various seasonal allergies (Figure

2.9). *Mentha longifolia* var. *asiatica* also contains tannins which are helpful in curing stomach disorders such as constipation [141].

FIGURE 2.9: *Mentha longifolia* var. *asiatica* [142].

2.8.7 Medicinal Importance

Phytotherapy has been growing and gaining much attention nowadays all around the world. Most of the plants have become natural medicines. According to WHO 80 % people all around the world are using phytotherapy methods and 3.3 billion people are using medicinal plants for medical purposes. This growing trend is because of the low toxicity and side effects of plants [143]. Various bioactive compounds present in Mentha species are essential oils which are pharmacologically active compounds (Figure 2.9) [144].

Essential oils present in leaves shows antiseptic properties in minute quantities and show toxicity in large doses (Figure 2.10). In addition to this, Mentha spp. has been known for centuries in treatments of various lethal diseases such as ulcers, liver infections, nausea, malaise and colitis due to its carminative, diaphoretic anti-inflammatory and anti-catarrhal activities [145]. Various kind of flavonoids have been isolated from *Mentha longifolia* var. *asiatica* species and these flavonoids show cytotoxic activity. The essential oils also show significant antibiotic activity against various bacteria, fungi and yeasts [146].

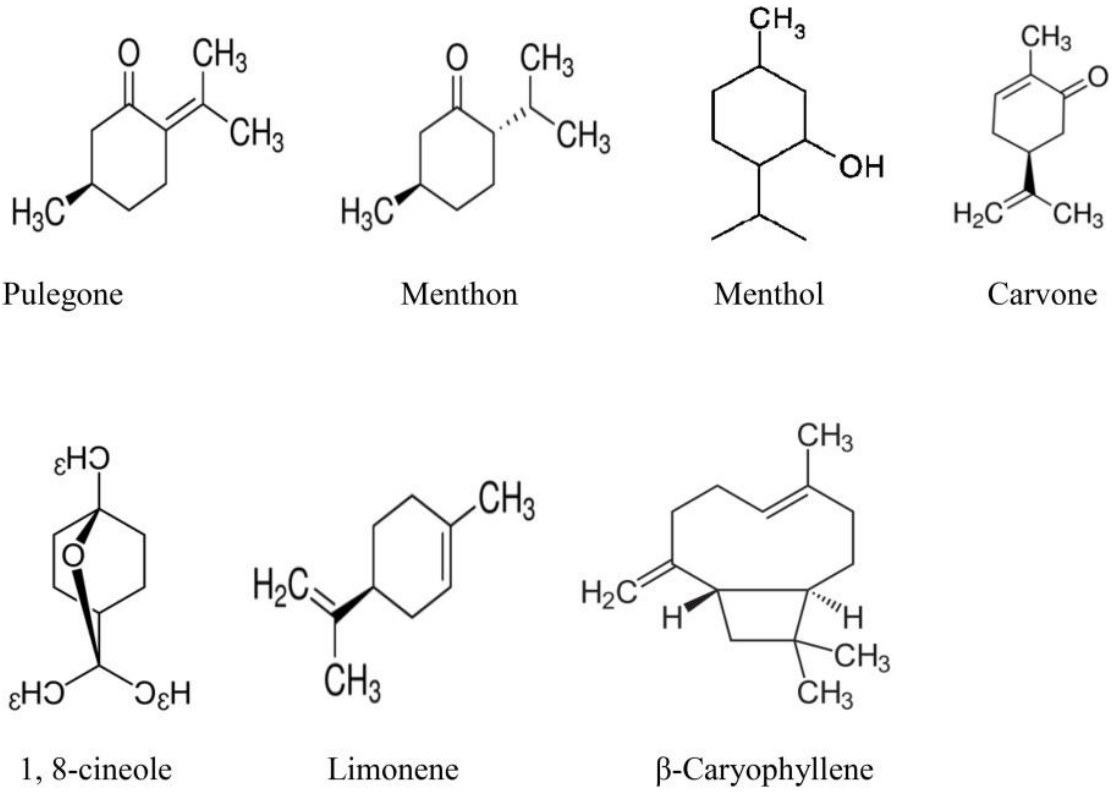

FIGURE 2.10: Essential oils present in Mentha species [144].

2.9 Role of Nanotechnology in Research

The branch of nanotechnology includes the synthesis, production and application of materials that are in the nano-scale range (1-100nm). Nanoparticles have size in nanoscale and large surface area to volume ratio which enables the nanoparticles to reach biological systems with great efficacy [147]. The macroscopic properties of any material can be compared with the individual molecules and their interactions at the nanometer scale. Controlling fundamental molecular interactions at the nanometer range helps manipulate the physical, chemical and biological properties of the materials [148].

With the advancements in material and engineering sciences, nanotechnology has been exploited in numerous fields ranging from chemistry to food sciences and nano-medicine [149]. Two approaches are most commonly employed in the synthesis of nanoparticles bottom-up approach and top-down approach. In the bottom-up approach, materials are constructed at the molecular level later followed by

self-assembly on the principles of molecular recognition, for example, carbon nano tubes. In the top-down approach, materials are built from larger entities without the involvement of atomic level (Figure 2.11) [150].

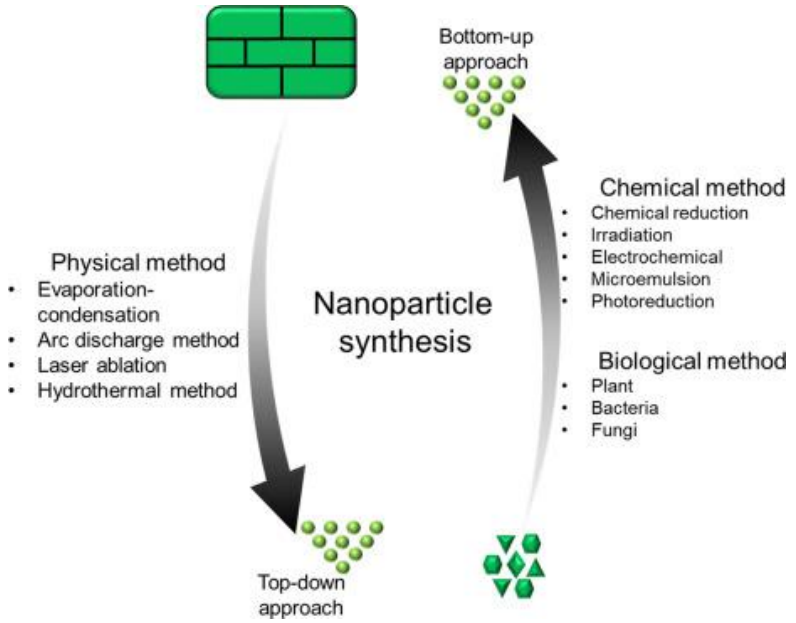

FIGURE 2.11: Approaches of nanoparticle synthesis [151].

Nanoparticles can be prepared by physical, biological and chemical techniques. Each of these techniques has its advantages and limitations. The reaction kinetics of biological nanoparticles are simple as compared to complex chemical procedures. Roots, stems and leaves are utilized for the synthesis process. Plants contain different phytochemicals such as phenols, terpenoids, and amines necessary for reducing metallic ions. Different metallic nanoparticles such as gold, silver, and zinc oxide are being prepared by using the green approach [152].

The development of nanocarriers is justified by the unique structural, magnetic, optical, and electronic capabilities of polymeric particles, metals, and semiconductors, which make them an appropriate drug-delivery vehicle (Figure 2.11) [153]. Biodegradable self-assembled nanoparticles created by nanoscale technologies can be employed as contrast agents in imaging and can be directed to areas afflicted by cancer.

Even though there are now few curative alternatives available for breast cancer patients, developing nanotechnologies offers a new, promising strategy for the

disease's early identification and treatment. Breast cancer imaging, diagnosis, and treatment research can be conducted in an interdisciplinary setting, thanks to nanoparticles [142].

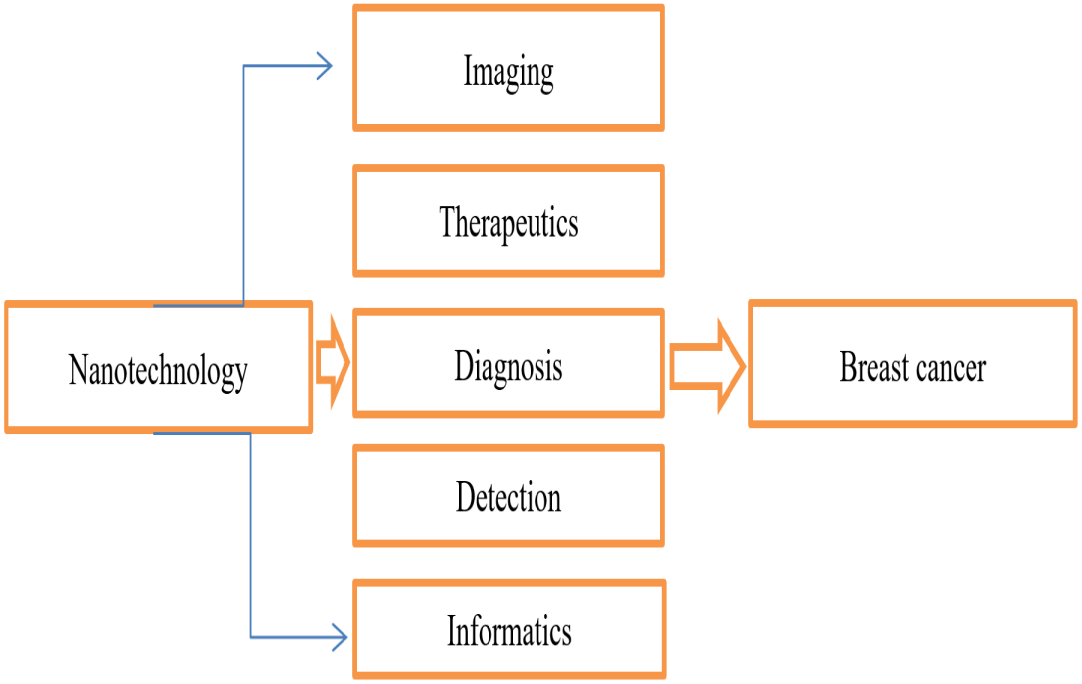

FIGURE 2.12: Applications of nanotechnology in multiple fields [154].

2.9.1 Synthesis of Nanoparticles

2.9.1.1 Physical Methods

Metallic nanoparticles are mostly produced by evaporation, condensation and laser ablation by using a tube furnace at standard atmospheric pressure. The source material is mounted in the center of the furnace which is then converted into the carrier gas. Typical tube furnace requires pre-heating procedures in order to raise the environmental temperature and consumption of huge amount of energy. Moreover, the size of nanoparticles produced is within a narrow range. From currently reliable methods, laser ablation is the most distinctive as well as substantial method which produces pure metallic nanoparticles without the involvement of any chemical substances [155].

2.9.1.2 Chemical Method

2.9.1.2.1 Chemical Reduction

In chemical methods, mostly chemical reduction approach is used which employs using organic and inorganic reducers for synthesis of silver nanoparticles. Various reductants for instance sodium citrate, sodium borohydride and tollens reagent are being used. These reducing agents can convert silver ions into metallic silver. These clusters can then be converted into colloidal metallic silver. The presence of various surfactants plays a dynamic role in stabilizing the synthesized particles and shielding them from sedimentation and agglomeration [156].

2.9.1.2.2 Microemulsion Techniques

The microemulsion technique has numerous applications in various fields because nanoparticles synthesized by this technique are uniform and controllable size [157]. Thus, large amounts of organic solvent and surfactant molecules must be separated from the end product. The major disadvantage of this technique is the utilization of toxic organic solvents. Moreover, nanoparticles must be tested in various physiochemical environments in order to ensure their practical utility [158].

2.9.1.2.3 Microwave Assisted Synthesis

This synthesis technique is very much different and better than conventional oil bath and produces nanoparticles of compatible and uniform sizes. This technique utilizes less energy consumption, better yield and less chemical waste as compared to other chemical methods [159].

2.9.2 Biological Methods

Due to limitations of physical & chemical methods and in order to save environment from hazardous chemicals, biological methods appeared feasible possibilities

for preparation nanoparticles. Biological mediated synthesis of AgNPs proved to be simple, cost-effective yet environment friendly. Recently, a lot of attention and concern has there on the production of AgNPs of particular size using biological systems and biomolecules. The foremost benefit of using the biotic system is the accessibility of biological raw material, the elimination of extra processes which is needed to prevent particle accumulation and the eco-friendly synthesis process which eliminates the need for safety precautions against pollution [160].

2.9.2.0.1 Synthesis of Nanoparticles by Bacteria

The cell membrane and the contents of biological cells are the most adaptable sites for the production of nanoparticles. Since the beginning of life on Earth, biological entities and inorganic materials are in constant contact with one another. Biosynthesis is a phenomenon that occurs when means of an enzymatic or biological process. Microbes often create inorganic compounds on the nanoscale with precise shapes, either intracellularly or extra-cellularly. Owing to their, chemo-osmotic and proton anti-transporters, microorganisms have better survival and grow in high concentrations of harmful metals (Table 2.2) [161].

TABLE 2.2: Types of nanoparticles synthesized by bacteria

S.No	**Name of bacteria**	**Type**	**Size**	**Reference**
1	*Rhodopseudomonas sps*	Ag	6-10nm	[162]
2	*Bacillus megaterium*	Ag, Pb, Cd	10-20	[163].
3	*Streptomyces sp.*	Mn, Zn	10-20nm	[164].
4	*Lactobacillus sporogens*	ZnO2	145.7nm	[165].

2.9.2.0.2 Synthesis of Nanoparticles by Fungi

The synthesis was done mainly by various fungal enzymes which are used in multiple industries such as textile and leather industries. These enzymes have replaced the toxic chemicals used in various industrial processes. These fungal enzymes

are eco-friendly and thus pose less negative environmental effects [166]. The fungal system is a versatile and complex biological system which have the ability to synthesize intracellular and extracellular enzymes. In addition to this, they have several advantages because of their ubiquitous distribution in nature [167]. Various-sized AgNPs (5-50 nm) can be prepared by utilizing various fungal species such as *Fusarium oxysporum*. Moreover, this method is also considerable in the sense that after the reaction process is completed, it does not cause any assemblage of particles for up to a month [154].

2.9.2.0.3 Synthesis of Nanoparticles by Algae

Various algal genera have the potential to prepare gold and silver nanoparticles which is cost-effective and do not involve any hazardous chemical reactions [168]. Various cyanobacteria and eukaryotic genera are used for the synthesis process such as *Lyngbya majuscule, Spirulina subsalsa, Padina pavonica, Spirulina platensis*, and *Sargassum fluitans* [169].

2.9.2.0.4 Synthesis of Nanoparticles by Plants

Since a long time ago, plants have been capable of reducing metal ions and, in this context, they possess strong hyperaccumulating and reductive ability which is being used to extract precious ores of metals from such land where mining is not possible in either way and the process is called as phyto mining. The metals which are being absorbed by plants are later harvested by using various techniques such as sintering and smelting [170].

Whole plants and various plant parts such as roots, leaves etc. can also be used to manufacture metallic nanoparticles [171]. Plants are composed of phytochemicals such as polysaccharides, phenolic compounds, alkaloids, tannins, resins etc. which reduce and stabilize silver ions and are also medically important. These SMs serve as reducers and capping agents in the manufacturing process and environmentally benign nanoparticles can be synthesized.

2.10 Computer-aided Drug Designing

The process of finding new drugs takes ten to fifteen years and can cost up to 2.558 billion USD when medicine is finally brought to market [172]. It is a multi-step process that starts with choosing an appropriate therapeutic target and continues with preclinical and clinical research, hit to lead discovery, lead molecule optimization and validation of the drug target [173]. With a relatively high medication attrition rate, the rate of success in clinical trials is only 13%, despite the significant costs and effort invested in drug development [174].

Despite the substantial expenses and time required to find new treatments, only 13% of clinical trials are successful because to a high medication attrition rate [175]. It is seen for the past decade that there is a growing trend of drug development by computational methods. All over the world leading research organizations and pharmaceutical companies have adopted computer-aided drug discovery (CADD) tools to conduct preliminary trials of drugs. This in turn have resulted in reducing costs and failures in the final stage [176]. The computational techniques uses different software in which the binding of the target protein and ligands can be visualized. This is very important to fully understand the binding affinity due to this reason rational drug design is a crucial part of CADD. The development of supercomputing facilities, parallel processing, and advanced software, algorithms, and tools have also facilitated lead identification in pharmaceutical research [177].

In addition, new developments in machine learning and artificial intelligence (AI) have substantially facilitated the analysis, understanding, and interpretation of massive data pertaining to pharmaceuticals during the drug discovery process [179]. Various techniques are used to find novel inhibitors using chemical databases, such as quantum mechanics, pharmacophore modelling, molecular docking, quantitative structure-activity relationship (QSAR), and statistical learning methods. The drug development process has made substantial use of both the structure and ligand-based categories of CADD drug design approaches in order to identify suitable lead molecules (Figure 2.13) [180].

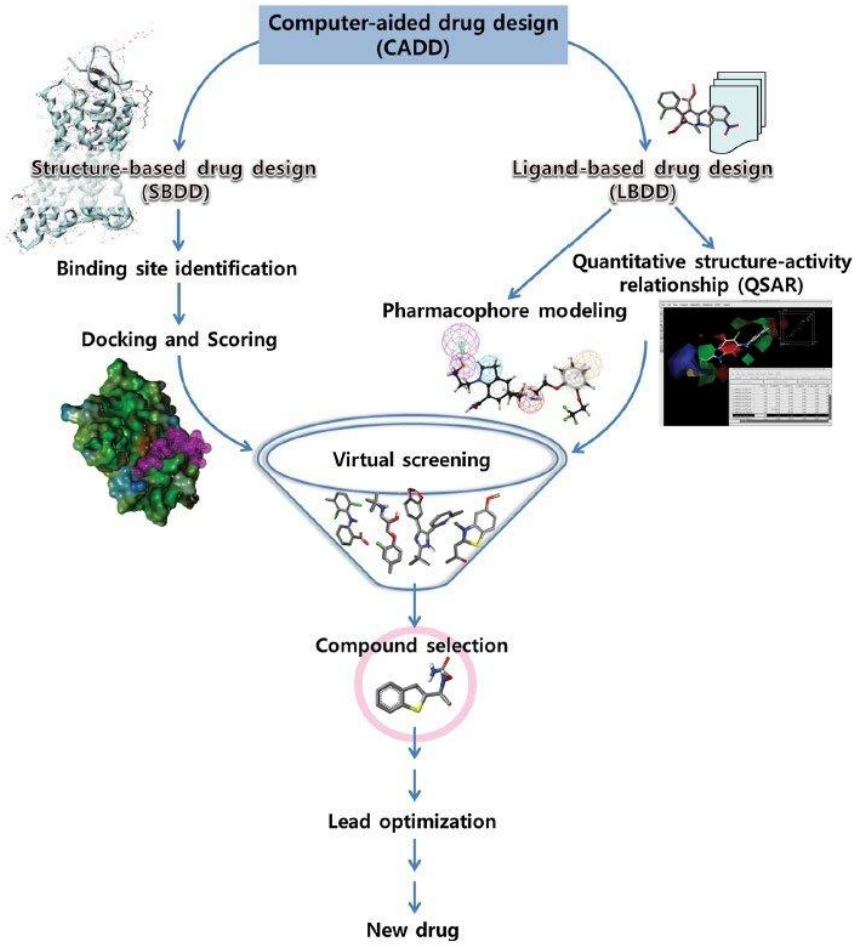

FIGURE 2.13: Types of CAAD [178].

2.10.1 Molecular Docking

Molecular docking is an in silico technique that uses a variety of scoring algorithms to determine the optimal binding pose of a protein-ligand complex and assess its strength in order to choose the best posture that each molecule generates to a rank-order [181]. Through complementarity optimization of factors including hydrophobicity, stericity and electrostatic force docking approaches aim to fit a ligand into the binding site of a target protein. This enables the target protein's binding free energy to be estimated [182]. As a powerful physical technique, molecular dynamics simulation predicts the positions of individual atoms in a molecular system. This may be done to find a relation of position with time by using Newton's equations of motion, which govern interatomic interactions. Using a suitable force field, the forces between interacting atoms are estimated to

determine the system's total energy [183]. MD simulations have been widely used for several reasons. Using any kind of experiment, it is very hard to measure the position and velocity of every atom in the system at any given time. The settings of the simulation are clearly known and may be carefully changed.

Chapter 3

Material and Methods

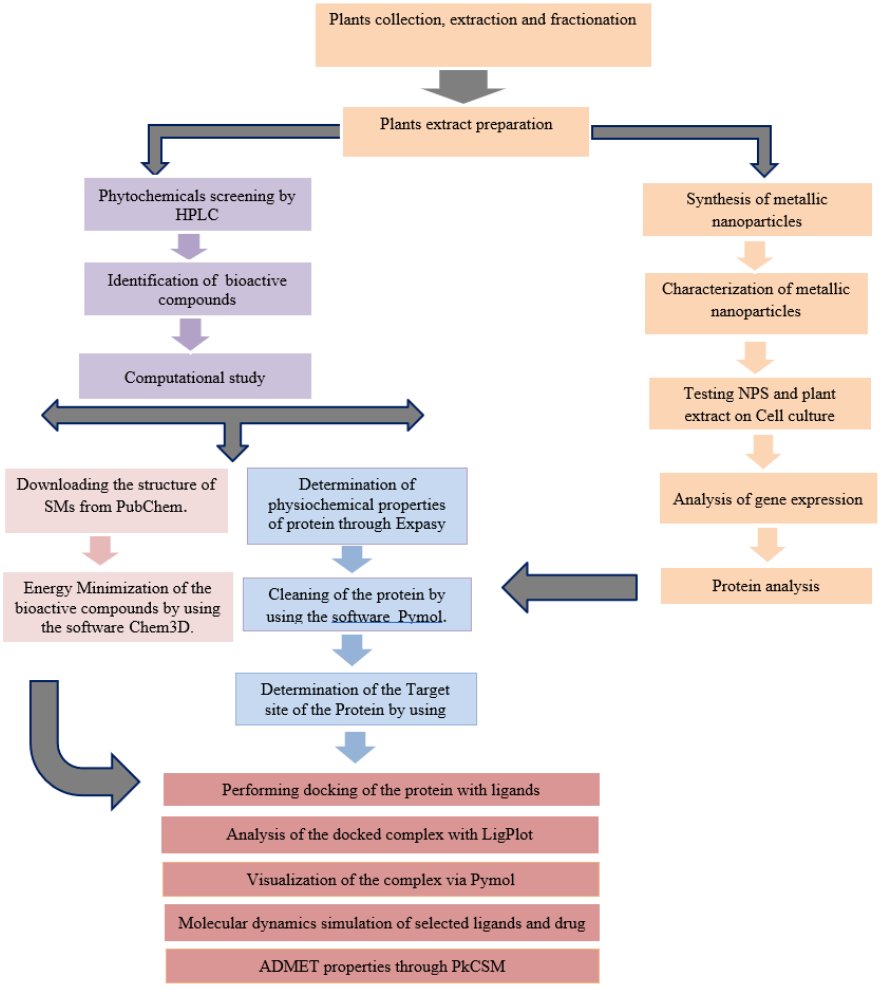

FIGURE 3.1: An Overview of Methodology

All the materials used in the adopted methodology are briefly mentioned here. In all of the experiments, borosilicate glassware was used which was purchased from Pyrex®. At the start of this process, all the glassware was wiped with detergents followed by immersion in a 10% bleach solution. After that at 200 °C, the glass apparatus was dried in the air-dry heating oven. Then it was subjected to sterilization for 20 minutes at 120°C and 15 psi. During the whole experiment, molecular biological grade analytical chemicals purchased from Sigma Chemical Co. were used.

Objective 1: To identify the anti-proliferative role of *Zygophullum arabicum* and *M. longifolia* var. *asiatica* plant extract and their metallic (ZnO) nanoparticles against breast cancer cell lines and their impact on the expression of breast cancer target gene (Rab22A) and its protein along with apoptotic pathway genes and protein.

3.1 Synthesis of Nanoparticles

Table 3.1: List of materials used for nanoparticles synthesis

No	Equipment
1	Muslin cloth
2	Filter paper
3	Electric balance
4	Beakers
5	Magnetic stirrer
6	Spatula
7	Pipette
8	Falcon tube
9	Mortar and pestle
10	Glass beakers
11	Whatman No. 1 filter paper

3.1.1 Preparation of Plant Extract of *Z. arabicum*

Zygophullum arabicum was obtained from the geographical area of district Rawalpindi (33° 17′ 20.4″ N, 73° 6′ 50.4″ E). The plant was verified from QAU herbarium, Islamabad (Voucher No: 133626). Plant material was dried by following the methodology reported by Shahid et al., with slight changes.

Before being processed into leaf extract, fresh *Z. arabicum* leaves were thoroughly cleansed with tap water and then distilled water (d.H_2O) to get rid of any impurities.

The leaves were air-dried at room temperature (around 37°C for three weeks. After the leaves had dried fully, they were pulverized into a powder [184].The following materials (Table 3.2) were utilized for the synthesis of *Z. arabicum* plant extract.

TABLE 3.2: Materials used for the preparation of *Z. arabicum* extract

Equipment/Chemicals	**Final concentration/quantity**
Powdered plant material	5g
Distilled water	50mL

The preparation of plant extract was done by following the methodology reported earlier with slight modification. About 5g of powdered sample of *Z. arabicum* was added to 50 ml of d. H_2O and heated on plate for 20 minutes. First, the mixture was filtered through muslin cloth and afterwards, Whatman filter paper No. 1 was used. The extract was stored at 4°C [185].

3.1.2 Preparation of Zinc Acetate Salt Solution

The materials used for the preparation of the zinc acetate salt solution are mentioned in Table 3.4.

TABLE 3.3: Materials used for the preparation of zinc acetate salt solution

Chemicals	**Quantity**
Zinc acetate salt	25.5mgs
Distilled water	100mL

The 0.25 mM zinc acetate salt solution was prepared in the laboratory. The molar mass of zinc acetate salt was calculated. 25.5 mg of zinc acetate salt was weighed on electric balance. This salt was mixed in 100 mL of distilled water. Afterwards, the mixture was provided continuous stirring at 6000 rpm for about 1 hour. After one hour, stirring was completed and the mixture was ready to use for the later steps.

3.1.3 Synthesis of Nanoparticles of *Z. arabicum*

The following information (Table: 3.4) pertains to the chemicals and glassware used in the synthesis of nanoparticles:

TABLE 3.4: Materials used in ZnO NPs synthesis

Samples	**Quantity/Concentration**
Plant extract	5mL
Zinc acetate dihydrate salt	25.5mg
Distilled water	100mL

The ZnO nanoparticles of *Z. arabicum* were prepared by adopting the methodology by Hussain et al., [186]. To make ZnO NPs using plant extracts of *Z. arabicum*, 5mL of extract was added in 45 mL of a 0.25 mM zinc acetate solution drop by drop, and then the mixture was left undisturbed at 20°C (Table: 3.5). After about one hour, colour change was observed.

TABLE 3.5: Detailed experimental conditions for the synthesis of ZnO NPs using the green synthesis method

Sample	**Precursor**	**Reducing agent**	**Reduction time**	**Stirring**	**Temp**
ZnO NPs	45mL	5mL	30 minutes	Continuous	20°C

3.1.4 Preparation of the Plant Extract of *M. longifolia* var. *asiatica*

M. longifolia var. *asiatica* was collected from Islamabad (33° 44′ 50″ N, 73° 8′ 20″ E). The plant was verified from QAU herbarium, Islamabad (Voucher No: 133626). A brief description of the materials used in the synthesis of *M. longifolia* var. *asiatica* is given in (Table: 3.6)

The preparation of plant extract was done by following the protocol of Aziz et al., (2018) with minor adjustments. A 5g sample of fresh mint leaves was obtained and cleaned in separate batches with distilled water. The leaves were finely chopped using a mortar and pestle, and then 50 mL of sterile distilled water was used to smash them. For fifteen minutes, the ingredients were continuously stirred while boiling. The contents were cooled and then filtered through Whatman No. 1 filter paper having a pore size of 25 μm. The resulting extracts had a dark yellow colour and were employed as stabilizers and reducing agents and saved for further use [187].

TABLE 3.6: Materials used in *M. longifolia* var. *asiatica* extract preparation

Chemicals	**Quantity**
Plant extract	5g
Distilled water	200mL

3.1.5 Synthesis of Nanoparticles of *M. longifolia* var. *asiatica*

For the preparation of zinc acetate salt solution, the required chemicals along with the procedure are mentioned in section 3.1.2. Zinc acetate dihydrate was synthesized in distilled water to a 0.25 mM solution, which was then reduced in a 9:1 ratio with the obtained plant extract. The plant extract was added to the reaction dropwise after the prepared 10 mM solution of the metal precursor was heated to 60°C and stirred constantly.

The reaction was then allowed to stand for two hours while stirring and heating continuously. The solution's colour changed to indicate the formation of NPs, which was confirmed by the UV characterization. The synthesized NPs were then repeatedly rinsed with ethanol and distilled water. Further characterization was done when the particles were dried at 50–600°C in a hot air oven [188].

3.2 Characterization of Synthesized Nanoparticles

3.2.1 UV-Vis Spectroscopy

The UV-Vis analysis of both nanoparticles was carried out at the Department of Material Science and Engineering, IST Islamabad by adopting the following method. The synthesized NPs were characterized using UV-Vis spectroscopy. The spectrum scan was performed using a single beam spectrophotometer (VWR UV-1600) coupled to "Multi-Wavelength Professional" computer software. The analysis was performed in the wavelength range of 300–900 nm. For every scan, distilled water was used as a blank [189]. The following steps were followed

- First of all, the electric balance was cleaned with 70% ethanol.

- Afterwards, 10 mg of the powdered ZnO nanoparticles of both plants were weighed on a weight balance and methanol was selected as a solvent.
- Optical clarity was required for the solvent (spectroscopic grade) in the studied area. The solvent-induced absorbance less than 1A was guaranteed.
- Using a typical quartz cuvette for optical measurements, the nanoparticles were diluted in methanol to a low concentration and sonicated using a tiny ultrasound bath to help ground the crystals. This was a preliminary step before adding the nanoparticles to the solvent.
- It was made sure that the laser beam could pass through exactly 1 cm of solution to rule out air bubbles inside the cell or solution that had leaked out of the cell.
- The cell was cleaned before being placed inside the spectrometer.
- When reporting a standard UV/VIS spectrum, the wavelength at maximum height (8max) and the molar absorptivity were used to identify each peak's position [190].

3.2.2 FTIR Analysis

Fourier transform infrared spectroscopy (FTIR) analysis was aimed to characterize the role of chemicals and metabolites which acted as reducing and capping agents in the nanoparticle's synthesis. It pairs infrared (electromagnetic radiation) with bonding in molecules in the form of stretching and bending vibrations. According to spectral analysis, various functional groups such as amide (-CO-NH2), carbonyl (-CO), and hydroxyl (-OH) are implicated in the reduction, capping, and stability of NPs [191].

The FTIR analysis of both nanoparticles was carried out at the Department of Material Science and Engineering, IST Islamabad by adopting the following method [192]. The attenuated total reflection Fourier Transform Infrared spectroscope

(Thermofisher Nicolet Summit Pro) equipped with software OMNIC paradigm was used for the analysis with the following steps.

- The transmittance spectrum was measured at a resolution of 4 cm^{-1} spanning from 4000 cm^{-1} to 400 cm^{-1}.
- OPUS software was opened and signed in using the ATR.
- In a drop-down menue tab 'Measure' was selected to perform cleanliness test.
- Then sample file was selected and all the measurement parameters were adjusted accordingly. A single measurement icon was selected.
- Then pre-defined experiment file was uploaded and the file path was defined in the Advanced tab.
- Afterwards, the tab "Check Signal" was selected.
- The chamber was purged to remove as much of the CO_2 peak as feasible before running a background.
- After completing the purge, an Interferogram was selected followed by "Save Peak Position".
- ATR background attenuation occurred between 2000 cm^{-1} and 2500 cm^{-1} as a result of the diamond platform.
- After placing the sample on the diamond stage, the clamp was pressed down.
- Single Channel Measurement was chosen from the basic menu. The completion of the scans was noted at the bottom of the screen.
- The sample was removed, the diamond stage was cleaned and data was saved.

3.2.3 X-ray Diffraction (XRD) Pattern Analysis

The unique and characteristic X-ray diffraction (XRD) pattern of each crystalline material can be used as a fingerprint to evaluate the crystallinity of the material.

Cards number standards databases are kept by the Joint Committee on Powder Diffraction Standards (JCPDS) and are used to identify crystalline materials. It provides information about phase impurities in the substances [193] [194]. XRD analysis was performed at Government College University, Faisalabad. This was done by using the XRD powder system, D8 Advance Bruker Germany in reflection mode using Cu Kα radiation (λ=1.54 $\mathring{A}$; U=40 kV, I=40 mA, line focus). The analysis was performed by following the methodology as reported in the literature [192]. The following steps were followed. To reduce scattering, a dispersion of GSH-coated ZnO nanoparticles and NIST's microcrystalline LaB6 standard powder (SRM 660b) were put on a single crystal sample holder made of silicon.

The sample was air dried and then measured throughout a range of 20 to 90° 20, for a time interval of 12s. This resulted in a total measurement duration of 24 hours. Diffrac. Suite EVA V1.2 from Bruker was used to perform qualitative phase analysis using the cubic ZnO (4-0783)62 and LaB6 (34-0427) 63 patterns from the ICDD database. The Rietveld technique was used to measure average crystallite size (CS) and lattice parameters (a) from diffraction peak broadening. The Rietveld approach uses LaB6 as a reference material. This approach improves and modifies the experimental parameters and displacement of the sample.

3.2.4 Scanning Electron Microscopy (SEM)

The aim of Scanning electron microscopy (SEM) analysis was to analyze the shape, size, aggregation & dispersion of nanoparticles. The SEM analysis of ZnO nanoparticles was carried out at the Department of Material Science and Engineering, IST Islamabad. The procedure was adopted as reported in the literature [195].

- First of all, SEM sample stub was properly autoclaved & nanoparticles were sprinkled on it gently & they were sealed with double sided sticky tape.
- A hand blower was used to blow away the loose particles that remained on the edges of the stub. It was ensured that these particles were properly blown away to ensure the safety measures

- In the last step, samples were sputtered with gold and they were ready for the analysis.
- High-energy electron beams were used for the analysis of samples. They had a voltage between 100 and 30,000 volts. The emission of electrons emission was achieved using a heat source.
- There are scan oils which enabled the electron beam to travel in straight lines to certain spots. This was continued until the specimen's surface produced a rectangular raster. Due to this reason, the image of the specimen was created point by point.
- Electron detector was used to find the signals or electrons that the scanned material had released. The process of creating SEM images involved the use of both backscattered electrons (BSE) and secondary electrons (SE). It was used to magnify images more than 10,000 times.
- The high voltage of the electron gun ranging between (15-30kV) was employed because it can penetrate underneath the surface and provide information about the sample interior as compared to the low voltages.
- The size of the ZnO nanoparticles was determined and the data was saved in the system and USB drive.

3.2.5 EDX Analysis

EDX analysis was used to determine elemental composition & their proportion in the sample. An electron beam was bombarded on the sample and the X-rays emitted were detected using an EDS X-ray detector. ZAF correction, where Z is the atomic number, A is absorbance, & F is fluorescence, was applied during EDX programming to resolve the specimen. To determine the final measurement of each element in the sample, data were collected from the perfectly formed particles that were exposed on top of the plate [196]. The EDX analysis of both ZnO nanoparticles was carried out at the Dept of Material Science & Engineering

IST Islamabad.

3.3 Cell viability (MTT) Assay

To reveal the dose-dependent cytotoxic effects of ZnO NPs and respective plant extracts, MTT assay was used by adopting an already reported method with slight modifications [197]. A brief detail of the chemicals and their quantity is mentioned below in (Table: 3.7).

TABLE 3.7: Reagents used in cell viability assay (MTT assay)

S. No.	Chemicals	Quantity
1	MCF cancer cell lines	ATCC
2	96-well micro-plates	Sigma-Aldrich
3	MTT cell growth assay kit (CT02)	Sigma-Aldrich
4	DNEM (D5796)	500mL Sigma-Aldrich
5	Dimethyl Sulfoxide (GK2245)	100mL Glentham Life Sciences

The steps followed included

- MCF-7 cell line was cultured in a 96-well micro-plate using DMEM media, with a density range of 1×104 cells per well. The plate was left for 24 hours to allow cells to attach.
- After a further night of incubation, the cells were subjected to several doses of ZnO NPs (20, 40, 60, 80, and 100 μg/mL).
- Following exposure, a 5-mg/mL MTT dye solution was added to each well for four hours.
- Cells treated with DMSO (Sigma-Aldrich) were used as a control group.

- The cells were incubated for 72 hours. In the next step, they were treated with 10 μL of the 5 mg/mL MTT solution which was obtained from MTT kit (Sigma-Aldrich). Afterwards, they were incubated for an additional three hours.

- After 3 hrs of incubation, the formazan crystals were yielded. These crystals were dissolved in 100 μL of the lysis solution. The lysis solution was obtained from the MTT kit.

- A microplate reader (BioRad, xMark Microplate Spectrophotometer) was employed to record the absorbance at 570 nm.

- The percentage viability of viable cells was calculated by the following formula: % of viable cells= OD of sample/OD of control $\times$ 100

- The average of the 3 separate experiments was used to express results [198].

3.3.1 Statistical Analysis

The data was examined using the GLM process and the ANOVA in SPSS software. Each experiment was conducted in triplicate and the mean $\pm$ standard deviation was used to represent the findings.

3.4 Gene Expression Studies by Real-Time qPCR

The expression of the targeted gene Rab22A and apoptotic genes was assessed using real-time qPCR. RNA extraction and cDNA synthesis were performed according to the reported methodology with some modifications [199]. The primers of the studied genes are listed in Table 3.9. The basic steps are as follows:

- In the first step, the cells were lysed. This was done by treating them with RNX solution (Trizol reagent). This solution was prepared by adding 200 μL of chloroform in 1 mL of RNX solution.

- In the following step, these prepared samples were subjected to centrifugation at 12000 rpm for 30 minutes.
- The transparency of the solution was achieved to the maximum level by performing the above step thrice and later the clear solution was added to a new vial.
- The volume of supernatant was recorded
- The same volume of isopropanol as the supernatant was added to a fresh vial, and it was centrifuged for 15 minutes at 12,000 rpm.
- After centrifugation was done, the pellet was saved and the supernatant was discarded. In the next step pellet was dissolved with DEPC water.
- The quality and amount of RNA were thoroughly monitored and the Revert AidTM First Strand cDNA Synthesis Kit (Fermentas, Germany) procedure was followed for cDNA synthesis.
- The mixture was incubated by adding 1 μL of DNAse, 1 μg of RNA, and 1 μL of 10$\times$ buffer for 30 minutes at 37°C.
- The next step was to inactivate DNAse activity. For this purpose, 1 μL of EDTA was added to the mixture followed by incubation for 10 min at 65°C.
- Subsequently, 2 μL of Reverse Transcriptase (RT) enzyme, 2.5 μL of MgCl2, 2.5 μL of dNTP mixture, 1 μL of RNasin and 5 μL of 5 $\times$ buffer was added.
- The reaction mixture was then placed in a thermocycler and heated to 42°C for sixty minutes.
- Another important step is to deactivate the reverse transcriptase enzyme. Samples were added and heated to 70°C for ten minutes in a thermocycler for this purpose. The product was kept at -20°C.
- The Syber green technique was used to determine the expression of Rab22A, bax, caspase-3, caspase-8 and caspase-9 genes in MCF-7 cells treated with ZnO NPs after 24 and 48 hours respectively.

- The β-actin gene served the purpose of internal control.
- The final volume was considered 30 μL as follows; 13.5 μL of Master mix (Bioneer, Korea), 3 μL of synthesized cDNA of β-actin, Rab22A, bax & caspase 3, 8 and 9 genes, 3 μL of forward and reverse primers for each gene, 10.5 μL of DEPC water.
- The optimal temperature programme consisted of conditions mentioned in Table 3.9.
- Following the reaction, the Ct data was retrieved from the device and the rest software used the Ct method to quantify the expression of the gene.
- In the next step Graph Pad and SPSS version 19 were used to plot the gene expression.

TABLE 3.8: Specific primer sequences used for real-time PCR

Genes	**Primer sequence**
Rab22A	F: GTCCCTTAGCACCAATGTACTATC
	R: AATGGCAACTACAATATTAGGTGG
bax	F: CCCGAGAGGTCTTTTTCCGAG
	R: CCAGACCATAGCACACTCGG
Caspase 3	F: ACATGGCGTGTCATAAAATACC
	R: CACAAAGCGACTGGATGAAC
Caspase 8	F: GACAGAGCTTCTTCGAGACAC
	R: GCTCGGGCATACAGGCAAAT
Caspase 9	F: CATATGATCGAGGACATCCAG
	R: TTAGTTCGCAGAAACGAAGC
β***-actin***	F: GAGACCTTCAACACCCCAGCC
	R: AGACGCAGGATGGCATGGG

TABLE 3.9: Cycling conditions for real-time-qPCR

Step	**Cycle number**	**Temperature (°C)**	**Duration (min)**
Primitive denatured	1	95	10
Denatured		95	20
Connecting primers	40	62	15
Expansion of primers		72	15
Melting stage or temperature gradient of 72 to 95 (°C)	1	95	5”

3.4.1 Statistical Analysis

The experiment was run in triplicate. Mean and standard error was calculated and Two-way ANOVA was used to evaluate the data statistically using SPSS 19 software.

3.5 Determination of Protein Expression by ELISA

ELISA was performed by adopting the following protocol [200].

- In the first step, a 96-well microtitration plate was taken and coated with monoclonal antibody (mAb).
- In the next step, the plates were washed with PBS four times. After thoroughly washing the plates were saturated with BSA for 2 hrs.
- Again, the plates were washed with PBS thrice followed by the addition of 100μL of samples containing bax, casp-3, 8 and 9 and Rab22A proteins along with the control (beta-actin).

- These proteins were deposited in the wells and left for 3 hours. This was done to achieve the binding of proteins with specific mAb. Again, the plates were washed with the PBS buffer and the proteins which were not bound were washed off.

- In the next step, biotinylated mAb was added. This was again followed by washing with PBS thrice. In the next step, streptavidin-HRP was added. It was prepared by adding 100 μL of streptavidin-HRP in 1/1000 in PBS and 1% BSA was added and allowed to rest for 30 minutes.

- The plates were again washed with PBS buffer three times. In the final step, 100 μL of Horse radish peroxidase substrate was added and it was allowed to stand for 15 minutes in the dark.

- Finally, 100 μL of H2SO4 was added and the reaction was allowed to stop. Absorbance was recorded at 450 nm on a plate reader device

.

3.5.1 Statistical Analysis

Data were statistically analyzed by SPSS.20 and graphs were generated using GraphPad Prism 6 (GraphPad Software).

Objective 2: Characterization of extracts of *Zygophullum arabicum* and *M. longifolia* var. *asiatica* plants for identification of bioactive compounds.

3.6 Phytochemical Screening by HPLC

HPLC analysis was performed at Central High Tech Lab, Government College University Faisalabad.

3.7 Preparation of Plant Extract

The chemicals or reagents such as water, formic acid, acetonitrile, and methanol along with the standards such as gallic acid, ferulic acid, benzoic acid, vanillic acid, salicylic acid, quercetin, rutin, coumarin, chlorogenic acid, kaempferol and sinapic acid of HPLC grade were purchased from Sigma Aldrich. To remove all moisture, the plants were dried for 20 days at 25°C in the shade. Plant parts were ground into a fine powder with a 60-mesh diameter using an electric grinder. 50 g of the sample powder was weighed and dissolved in 250 mL of methanol, covered with aluminium foil and left overnight. The next day centrifugation was performed for 3-4 minutes and the sample was filtered through Whatman filter paper. The supernatant was allowed to evaporate. The filtration of extracts was done using Whatman filter paper No. 1823 once the methanol had evaporated after three days of repose. The sample powder was scraped and the resulting extracts were packed and kept at about 4°C.

3.8 Preparation of Standards

Methanol was used to prepare standard stock solutions of flavonoids and phenolic compounds i.e. gallic acid, caffeic acid, ferulic acid, benzoic acid, vanillic acid, salicylic acid, quercetin, rutin, coumarin, chlorogenic acid, kaempferol and sinapic acid at the concentration of 1mg/mL. Afterwards, different dilutions were prepared in series i.e. 0, 0.5, 1, 1.5, 2, 2.5, 3, 3.5 μg/mg for the standard calibration curve from which the analysis of flavonoids and phenolic compounds was performed.

3.9 Instrumentation Conditions for HPLC

Liquid chromatography consisted of phase C18 column (5 μm, 250 $\times$ 4.6 mm) accompanying oven set at 30 °C. Data analysis was performed using software

version 4.2. 6410 on an HPLC system (Perkin Elmer, USA) that was connected to a Flexer Binary LC pump and UV/VIS LC detector (Shelton CT, 06484 USA). The mobile phase consisted of two components:

- Solvent A (water/ formic acid) (0.1%)
- Solvent B (acetonitrile/ formic acid) (0.1%).
- The gradient elution system was 95% A (5 min), 90% A (10 min), 50% A (35 min), 95% A (10 min) and 95% A (5 min). The injection volume is 20 μL and the flow rate is 1 mL/min.

3.10 HPLC/DAD Analysis

Screening of secondary metabolites was carried out by HPLC with DAD. This technique was adopted to compare the retention times of the detected secondary metabolites with the standards. It was done according to the reported methodology with some modifications [201]. It was ensured that the sample and standards were filtered using a millipore membrane so that they did not cause any damage to the column and thereby may not reduce the efficacy of the results. Agilent model 1260 with a DAD detector was used to separate secondary metabolites by HPLC. External calibration with standards was used to complete the quantification process. Chem Station software (Agilent, Germany) was employed to save the chromatograms and apply their treatments.

The phenolic compounds and flavonoids identification was achieved by the comparison of detected peaks with established references based on their wavelengths and retention periods. The standard solutions helped to achieve calibration of the HPLC equipment. This also facilitated to identify the peak corresponding to each molecule in the samples. The peaks were integrated and the surface was subsequently documented. At their maximum absorption wavelength, the compounds that have been chosen for calibration were examined. Various concentrations within each range were examined in the HPLC to produce a calibration line.

The efficiency of the separated components was evaluated using HPLC, with the separation factor and resolution being utilized.

Objective 3: To analyze the role of identified bioactive compounds of *Zygophullum arabicum* and *M. longifolia* var. *asiatica* against breast cancer-targeted gene (Rab22A) by computational approaches.

3.11 In silico Analysis of Detected Flavonoids Against Target Protein Rab22A

Molecular docking is a technique that examines the arrangement and direction of molecules within the binding site of a macromolecular target. Search algorithms provide potential poses, which are then sorted using scoring methods [202]. It helps to predict the molecular behaviour of target protein binding. This tool is widely employed for drug discovery. The top software used for best scores in docking are AutoDock, Vina, MOE-Dock, FLexX and GOLD respectively [203]. This study comprised the following steps.

3.11.1 Preparation of Ligands for Molecular Docking

For the selection of active ligands, HPLC was done to find out the bioactive compounds present in both plant species which were actually selected as ligands for the docking process. The structures of ligands of both plants, identified through HPLC were downloaded from the PubChem database. Minimization of ligand's energy was carried out by Chempro software chem12 [109]. Before beginning any further modelling tasks in structure-based protein-ligand modelling, all ligands were properly prepared with the appropriate 3D geometries, bond order, accessible tautomer, and ionization states [204, 205]. The ligand's MM2 energy was minimized by Chem3D ultra. After the energy minimization step, sdf format of the ligand structure was saved.

3.11.2 Retrieval and Analysis of Protein Structure

The structure of Rab22A was downloaded from the available resource of the protein data bank (PDB). With the DOI https://doi.org/10.2210/pdb1Z0J/pdb and the PDB ID IZ0J structure of Rab22A was downloaded. The target protein's sequence IZ0J was obtained in FASTA format from the UniProt protein sequence database (https://www.uniprot.org), with accession number Q9UL26 and a residue length of 194 amino acids, respectively. The physical and chemical characteristics of the Rab22A proteins were determined using the Expasy ProtParam tool (http://web.expasy.org/protparam/). This tool helped to determine multiple parameters such as molecular weight, theoretical pI, GRAVY etc. The fundamental units of protein folding, structure, evolution, and design are called protein domains. Functionally significant domains and conserved sites were identified via the InterPro database (https://www.ebi.ac.uk/interpro/) [206]. The linear chain consisting of 194 amino acids was considered as reference chain and remaining all protein constituents such as water molecules, ions and residues were removed by using the pymol software (v1.7.4.5) [207].

3.11.3 Molecular Docking by CB Dock and Analysis of Docked Complex

Using a curvature-based cavity identification method, CB-Dock helped to analyze the particular protein and predicted its binding areas. After that, docking was carried out by the program Autodock Vina which is a cutting-edge technology. Autodock and AutoDock Vina are two of the most popular free and open-source software for molecular docking simulations [208].

LigPlot+ is a computational program that makes the 2D schematic presentation of protein and ligand complexes from PDB file input [209]. In current research work, analysis of the docked complex was done by ligplot+ protein-ligand interaction software which automatically generated a diagram of protein ligand interactions.

These interactions were modified through hydrophobic and hydrogen bonds. The ligplot+ generated a 2D representation of the protein-ligand complex [210]. The complex file, in PDB format, was opened in Ligplot+ and the H-bonds and hydrophobic interactions of docked molecules were examined. The RMSD and RMSF values were calculated [211].

3.12 Molecular Dynamics (MD) Simulation

In this study, molecular dynamics (MD) simulations were conducted using GROMACS 2022 [212]. The selected Rab22A protein and lead compounds of both plants along with the reference drug were included in the simulation system. The preparation, simulation, and analysis processes are described as follows.

3.12.1 System Preparation, Energy Minimization and Equilibration

To avoid self-interactions, the protein-ligand complexes were arranged in a cubic manner with a minimum gap of 1.0 nm between the protein and the edges. To neutralize the system's charge, counterions were introduced after the system was solvated using the SPC/E water model [213]. This step ensured that the electrostatic interactions would be accurately modelled throughout the simulation.

- **Energy Minimization**
  - To eliminate steric clashes or high-energy interactions, steepest descent algorithm was used to do energy minimization of the solvated system.
  - When any atom's maximal force was below 1000 kJ/mol/nm, the minimization was said to have converged.
- **Equilibration Phases**
  - **NVT Equilibration**

    * The first step was to ensure that the number of particles, volume and temperature should remain constant for the first 100 ps of the equilibration process.
    * The V-rescale thermostat was used. Its function was to maintain the temperature at 300 K, This can be achieved with a coupling constant of 0.1 ps [214].

  – **NPT Equilibration**
    * An NPT ensemble (const number of particles, pressure, & temp) was employed for the second equilibration phase lasted for 100 ps.
    * Using the Parrinello-Rahman barostat the pressure was kept at 1 bar. This was achieved by using a coupling constant of 2.0 ps [215].

3.13 Production MD Simulation

A 100ns production MD simulation was conducted for each protein-ligand complex.

- Periodic Boundary Conditions (PBC): PBC was applied in all directions to mimic an infinite system.
- Electrostatic Interactions: Using the Particle-Mesh Ewald (PME) approach, long-range electrostatics were computed with a 1.0 nm cutoff distance for the short-range interactions [216].
- Bond Constraints: A 2 fs time step was enabled by constraining all bond lengths using the LINCS algorithm [217].

3.14 Analysis of MD Simulation Results

Various analyses were performed on the MD simulation trajectories to assess the stability, flexibility, and interactions of the protein-ligand complexes. The analyses included:

1. Root Mean Square Deviation (RMSD): RMSD analysis was done for the protein backbone to monitor structural stability over time. A stable plateau in RMSD indicates equilibrium.

2. Root Mean Square Fluctuation (RMSF): RMSF was done for each residue to identify flexible and stable regions in the protein structure.

3. Hydrogen Bonds (H-bonds): The hydrogen bond number between the protein and the ligands was analyzed to understand the key interactions.

4. Radius of Gyration (Rg): Rg was calculated to assess changes in protein compactness over time.

5. Solvent Accessible Surface Area (SASA): SASA was computed to evaluate the exposure of the protein surface to the solvent.

6. The analyses were conducted using built-in GROMACS tools, and the results were visualized using GROmancer, an in-house web-based tool.

3.15 Toxicity Prediction by ADMET Properties

SwissADME was used to determine the pharmacokinetics properties, also known as the ADMET properties and the drug-likeness predictions. The free online resources structure.bioc.cam.ac.uk/pkCSM and http://www.swissadme.ch/index.php were used to determine the drug-likeness and ADMET properties of all ligands [218].

Chapter 4

Results

This chapter covers all the phases which are involved in the designed study program starting from the identification of plant material, green synthesis of ZnO NPs and their characterization by using UV-Vis spectrophotometer analysis, SEM (Scanning electron microscope, XRD (X-ray Diffraction Spectroscopy), and EDX (Energy-dispersive X-ray Spectroscopy).

Biological evaluation of prepared ZnO NPs was also carried out by performing various biochemical assays including MTT assay, gene expression analysis, and protein analysis by ELISA. The different secondary metabolites present in our selected plants were quantified by the HPLC-DAD system and based on these results computational approaches were used for the discovery of novel drug candidates targeting the Rab22A gene in breast cancer.

The results are as under:

Objective 1: To identify the anti-proliferative role of*Zygophullum arabicum* and *M. longifolia* var. *asiatica* plant extract and their metallic (ZnO) nanoparticles against breast cancer cell lines and their impact on the expression of breast cancer target gene (Rab22A) and its protein along with apoptotic pathway genes and protein.

4.1 Synthesis of ZnO Nanoparticles

The change of colour from brown to light yellow and brown to transparent white indicated the synthesis of ZnONPs of *Z. arabicum* and *M. longifolia* var. *asiatica* respectively (Figure 4.1 A & B).

FIGURE 4.1: Synthesized ZnO NPs of (A) *Zygophullum arabicum* and (B) *Mentha longifolia* var. *asiatica*

4.2 Characterization of ZnO Nanoparticles

4.2.1 UV-Vis Analysis

After the synthesis of ZnO nanoparticles, their optical characteristics were assessed using a UV-Vis spectrophotometer. Zinc oxide nanoparticles of *Zygophullum arabicum* and *Mentha longifolia* var. *asiatica* showed an absorption peak between 295 nm as indicated in Figure 4.2.

The characteristic absorbance peak of ZnONPs synthesized from *M. longifolia* var. *asiatica* was observed at 345 nm (Figure 4.2). SPR (surface plasma resonance) is responsible for maximum absorption in the range of 400-500 nm in UV-Vis spectrometry.

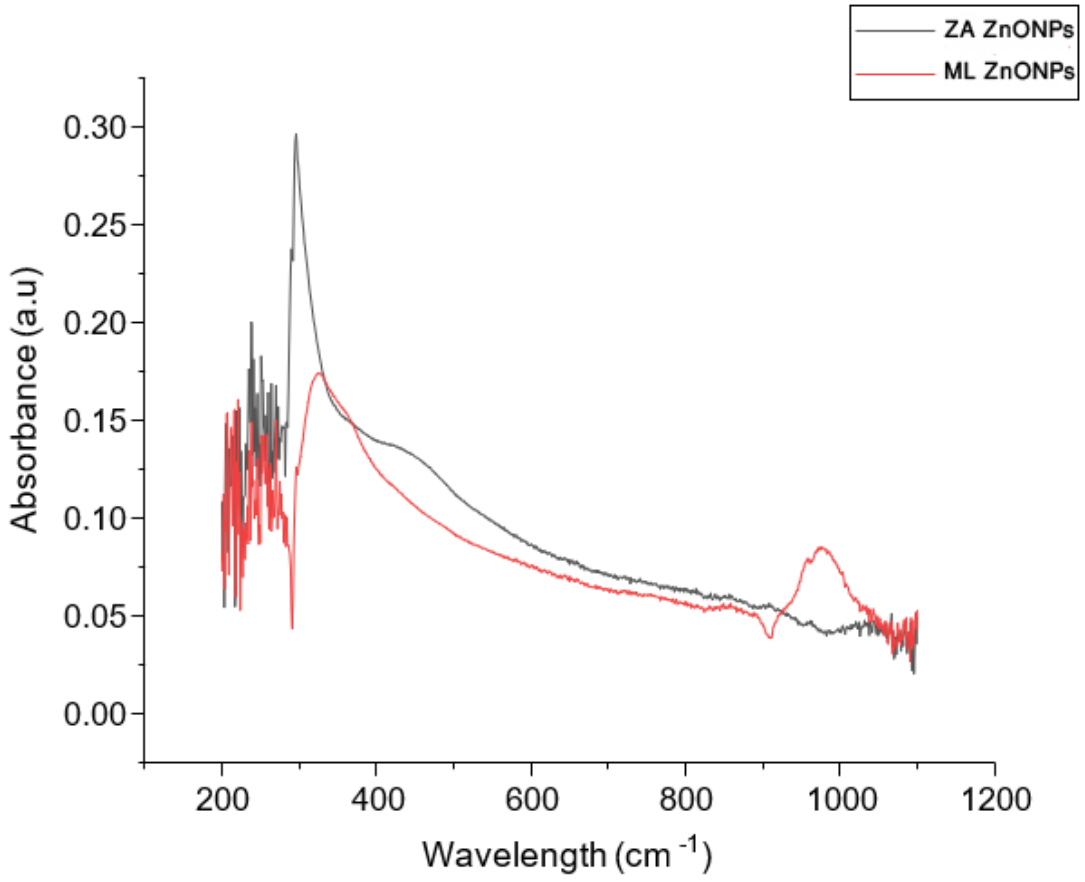

FIGURE 4.2: UV-vis spectroscopy of ZnO nanoparticles from *Z. arabicum* and *M. longifolia* var. *asiatica*

4.2.2 Scanning Electron Microscopic (SEM) Analysis

The morphology of the synthesized nanoparticles was assessed using a SEM (JEOL-JSM-6490LATM) at 20Kv voltage and a maximum frequency of 2838 cps. The average size of synthesized nanoparticles along with S.E. was determined after finding the individual particle sizes in the field. SEM revealed the size of *Z. arabicum* ZnO NPs to be 25 ± 4 nm with a spherical shape (Figure 4.3) as compared to nanoparticles of *M. longifolia* var. *asiatica* having a size of 35 ± 6 nm with a hexagonal shape (Figure 4.4). The working of SEM by bombarding a beam of highly activated electrons on the sample resulted in the production of a large number of signals. This electrical interaction with the material revealed the exterior morphology (texture), chemical composition, crystal structure, and orientation of the constituent materials that comprised the sample.

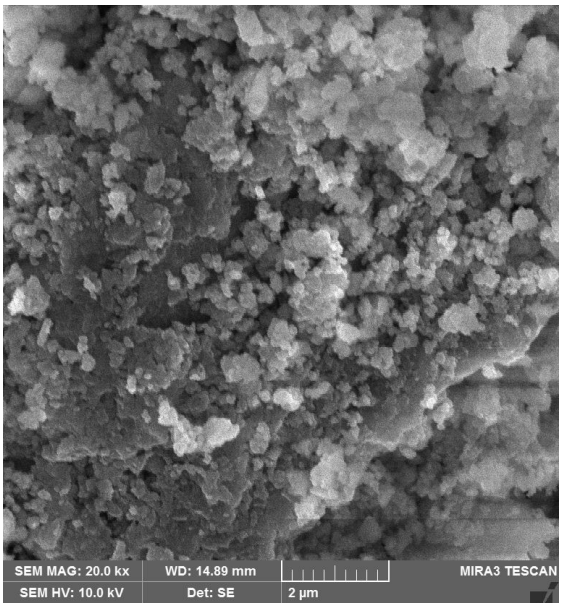

FIGURE 4.3: SEM analysis of *Z. arabicum* ZnO nanoparticles

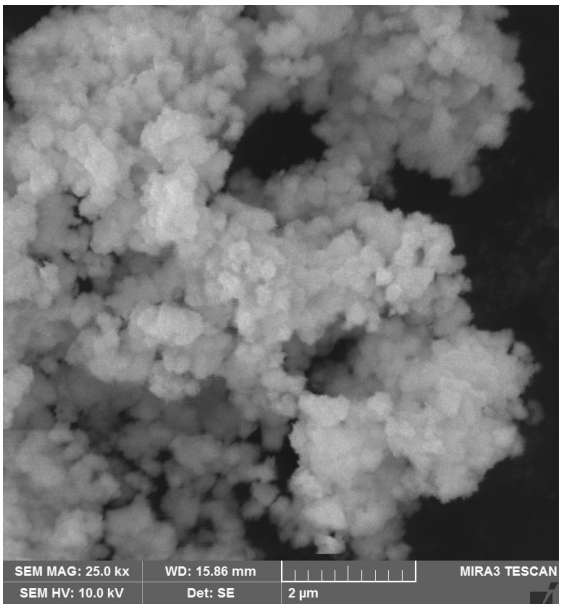

FIGURE 4.4: SEM analysis of *M. longifolia* var. *asiatica* ZnO nanoparticles

4.2.3 FTIR Analysis

The FTIR spectrophotometer was used to perform FTIR analysis in order to identify the different biomolecules that were present in the aqueous extracts of both plants and were involved in the creation of nanoparticles. The FTIR spectroscopy was done to validate the functional groups present in both plants which were responsible for the reduction of zinc ions into ZnONPs. The major bands of the

FTIR spectrum of *Z. arabicum* were observed at 2970, 2888, 2832, 2370, 2318, 1379 and 1067 cm^{-1}. The minor bands were observed at 2160, 1561, 1375, 873, 600 and 594 cm^{-1} (Figure 4.5). The major bands corresponding to 2970-2832 cm^{-1} indicated the presence of the C-H group of aldehydes suggesting the presence of saturated compounds. The bands at 2370-2318 cm^{-1} indicated the presence of hydroxyl O-H and methyl group monstrating the presence of alcohols. A distinct band at 1067 cm^{-1} indicated the presence of the C-O group of polyols. These groups are responsible for the reduction of metallic zinc.

FTIR spectroscopy was also carried out for ZnONPs synthesized from *M. longifolia* var. *asiatica*. The major bands were observed at 3649, 2989, 2969, 2900, 2365, 2025 and 1383 cm^{-1}. The minor bands were observed at 1558, 1570, 1370, 1261 and 852 cm^{-1} (Figure 4.6). The major bands indicated the presence of O-H, C-H and C-O functional groups. The major band at 3649 cm-1 showed the presence of bending of the N-H group indicating the presence of proteins. The bands at 2989, 2969 and 2900 cm^{-1} indicated the presence of C-O groups whereas bands at 2365 and 2025 cm^{-1} indicated stretching bond C-C of alkynes. The band at 1383 cm^{-1} corresponds to the iso-propyl functional group of hydroxyl flavones.

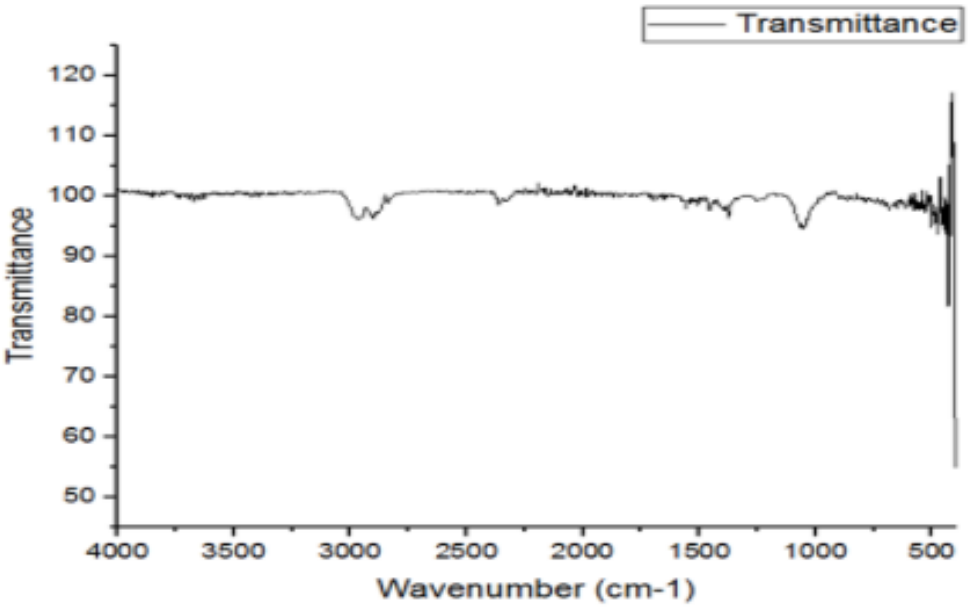

FIGURE 4.5: FTIR analysis of *Z. arabicum* ZnO nanoparticles

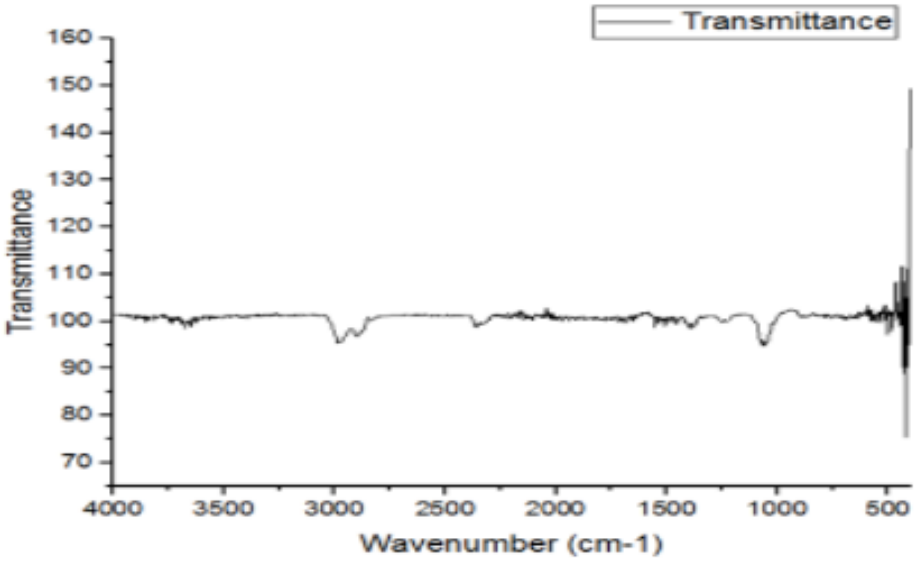

FIGURE 4.6: FTIR analysis of *M. longifolia* var. *asiatica* ZnO nanoparticles

4.2.4 EDX Analysis

The chemical and elemental composition of the synthesized ZnO NPs of *Z. arabicum* and *M. longifolia* var. *asiatica* was done by using energy-dispersive X-ray spectroscopy. According to the EDX spectrum of both nanoparticles, zinc was the primary component in both samples, with no other impurities present (Figures 4.7 & 4.8).

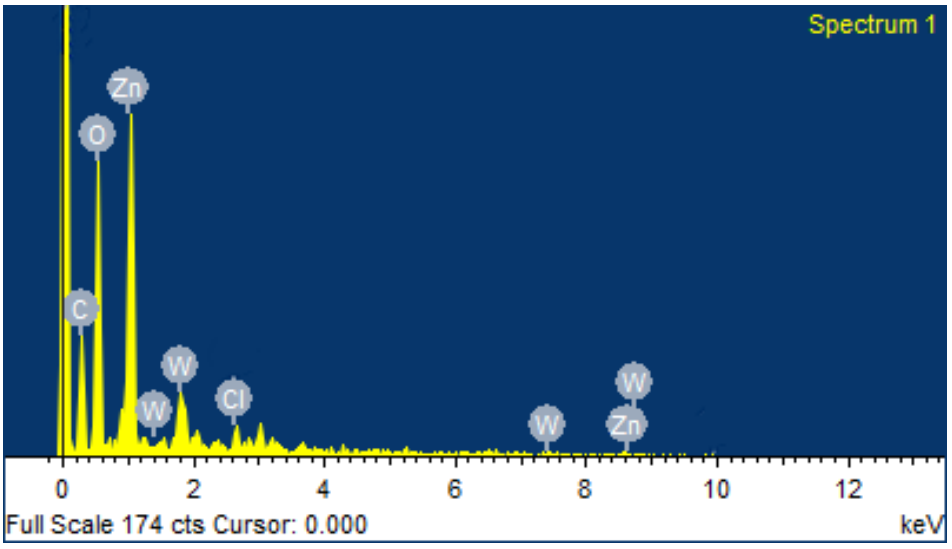

FIGURE 4.7: EDS spectra of *Z. arabicum* ZnO nanoparticles

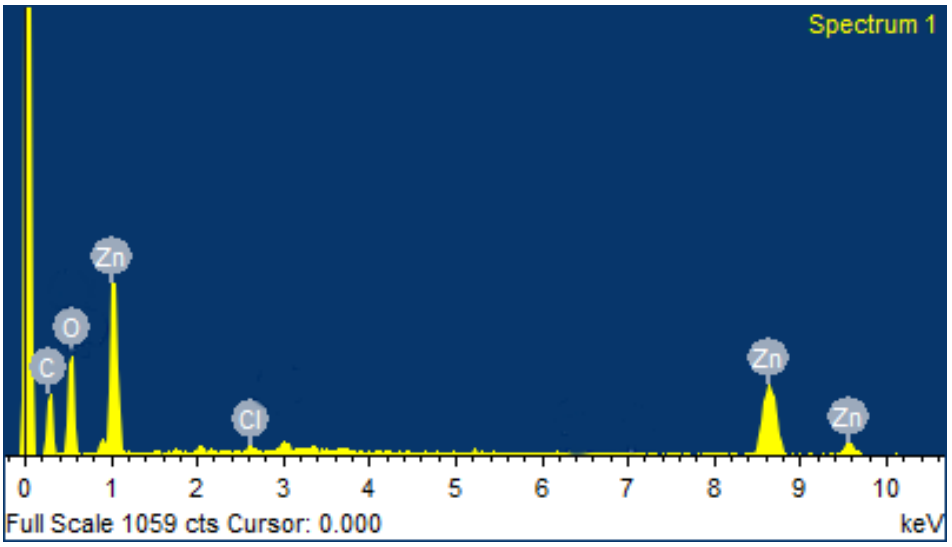

FIGURE 4.8: EDS spectra of *M. longifolia* var. *asiatica* ZnO nanoparticles

4.2.5 XRD Analysis

Phase identity and crystalline alignment of the produced ZnO nanoparticles were ascertained using the X-ray crystallography technique. The XRD pattern of ZnONPs was observed by using index POWDER-X software and matched with standard JCPDS, 36–1451 data.

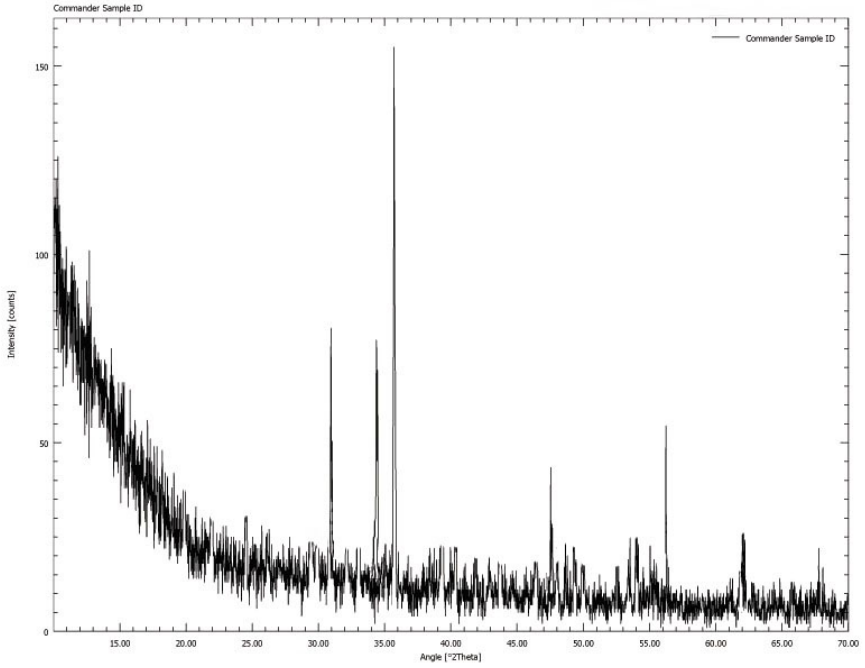

FIGURE 4.9: The XRD pattern of *Z. arabicum* and *M. longifolia* var. *asiatica* ZnO nanoparticles

The result showed the diffraction peaks of ZnONPs at 31.34, 34.50, 36.32, 47.60, 56.68, and 62.94 (Figure 4.9) matching with lattice parameters of (100), (002), (101), (012), (110), (013), which indicated the crystalline nature of the nanoparticles. The X-ray emission from the samples was caused by the beam's energy in the 10–20 KeV range. The electron beam moved across the samples and images were obtained for the synthesized ZnONPs. Additionally, the crystallite characteristics of the produced nanoparticles were computed using $D = 0.9\lambda/\beta \times \cos\theta$, the Debye-Scherrer relation.

4.3 Cell viability (MTT) Assay

The cytotoxicity of *Z. arabicum* and *M. longifolia* var. *asiatica* ZnO NPs was assessed against the MCF-7 breast cancer cell line. Plant extract and nanoparticles at varying concentrations (20, 40, 60, 80, and 100 μM) demonstrated strong cytotoxicity. The percentage of cell viability of the MCF-7 cell line exposed to extracts and ZnONPs of *Z. arabicum* and *M. longifolia* var. *asiatica* showed variations (Figure 4.10). Incubation of MCF-7 cells with 20-100 μM of ZnONPs and respective plant extracts showed decreased cell viability in a dose-dependent manner (Figure 4.11). With increasing concentrations of plant extracts and NPs, cell viability was found to be decreased.

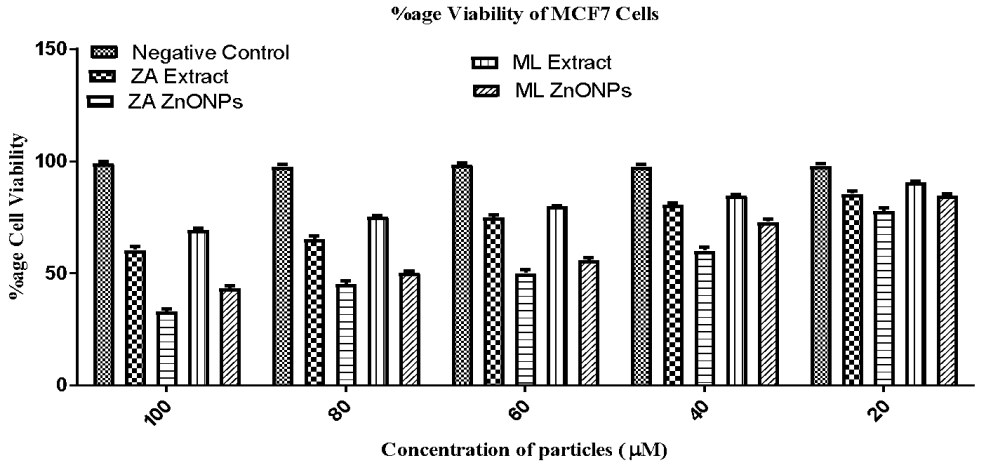

FIGURE 4.10: AGraphical representation of% cell viability of plant extract and ZnO NPS of *Z. arabicum* and *M. longifolia* var. *asiatica*

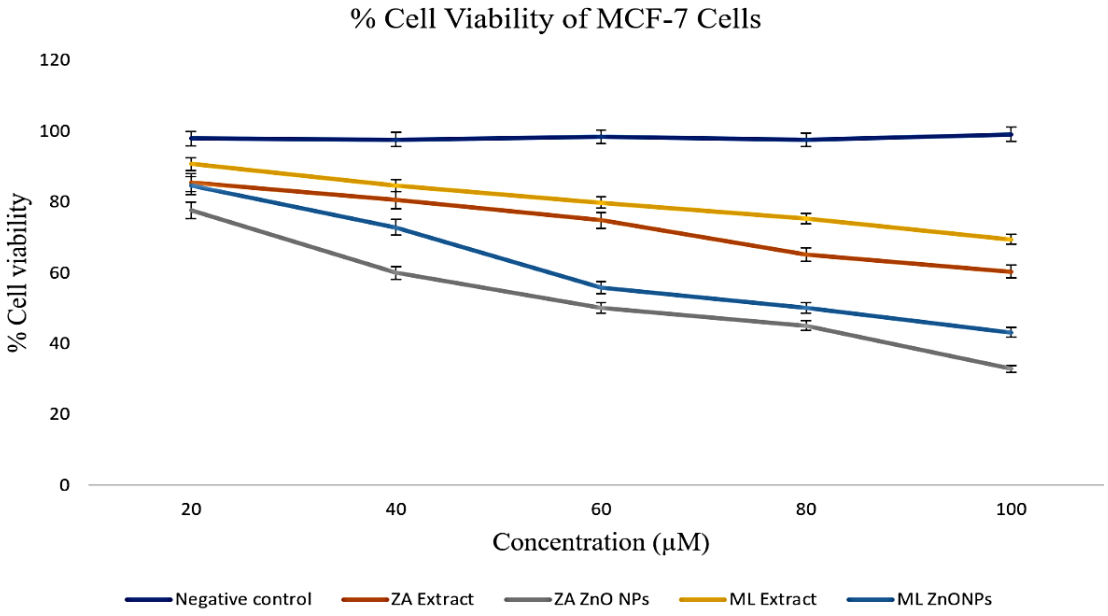

FIGURE 4.11: Decreased cell viability of MCF-7 cell line treated with plant extract and ZnONPS of *Z. arabicum* and *M. longifolia* var. *asiatica* in a dose-dependent manner. Error bars indicate the standard error (SE) of three means, asterisk represents the significant difference in data compared with control at *P $<$ 0.05, **P $<$ 0.01 and ***P$<$ 0.001. ZA=*Zygophullum arabicum*, ML= *Mentha longifolia* var. *asiatica*

.

The lowest cell viability of treated cells was observed at 100 μM of ZnONPs of *Z. arabicum*, which was 32.8%, whereas for the extract of *Z. arabicum*, it was 60.3%. On the other hand, in the case of treatment with the extract and ZnONPs of *Mentha longifolia* var. *asiatica*, the cell viability was found to be 69.4% and 43.2% respectively. ZnONPs of studied plant species were found to be more effective in lowering the viability of breast cancer cell line as compared to the respective plant extracts. The IC50 value of *Z. arabicum* and *M. longifolia* var. *asiatica* ZnONPs was also found to be lower as compared to that of their respective extracts. Moreover, *Z. arabicum* extract and nanoparticles showed higher cytotoxicity (IC50 64.01 μM and 51.68 μM respectively) as compared to those of *M. longifolia* var. *asiatica* extract and respective nanoparticles (IC50 107.9 μM and 88.02 μM respectively. The cytotoxicity results were also found statistically significant (Table 4.1), which shows the analysis of variance for the factors affecting the viability of MCF-7 cells. All of these factors, including the

type of sample (extracts and their ZnONP), concentration of these samples and interaction of both of these factors were found to have a significant impact on the viability of MCF-7 cells with p-value <0.0001.

TABLE 4.1: Analysis of variance for factors affecting the viability of MCF-7 Cells

Source of Variation	**Df**	**Sum-of-squares**	**Mean square**	**F Value**	**P Value**	**Significant**
Interaction	16	2605	162.8	42.28	<0.0001	Yes
Types of sample	4	18200	4550	1182	<0.0001	Yes
Concentration	4	6417	1604	416.7	<0.0001	yes
Residual	50	192.5	3.850			

4.4 Gene Expression Studies

The apoptotic role of plant extracts and synthesized ZnONPs was also studied by the expression of Rab22A, bax and caspases genes as illustrated in Fig 4.12. *Z. arabicum* nanoparticles and respective plant extract showed greater potential in down-regulating the Rab22A gene expression as compared to the nanoparticles and plant extract of *M. longifolia* var. *asiatica*. Rab22A which is primarily involved in endocytic recycling and membrane trafficking of endosomes is a major drug target for treating multiple malignancies. The level of this gene significantly declined in the breast cancer cells treated with ZnONPs and plant extracts of both plant species as compared to untreated cells. This may be attributed to the fact that this gene is considered an oncogene and participates in the carcinogenesis of breast cancer. The present study also observed the up-regulation of the bax gene, which is involved in the apoptotic pathway. Plant extract and ZnONPs of *Z. arabicum* showed greater apoptotic potential by up-regulating bax gene expression as compared to plant extract and NPs of *M. longifolia* var. *asiatica* in treated MCF-7 breast cancer cells in comparison with the control group. Moreover, Cells

treated with plant extract and ZnONPs of *Z. arabicum* showed greater expression of caspase 3, caspase 8 and caspase 9 as compared to those treated with extract and NPs of *M. longifolia* var. *asiatica*. These results indicated that *Z. arabicum* has more apoptotic potential by up-regulating the apoptotic genes in comparison to *M. longifolia* var. *asiatica*.

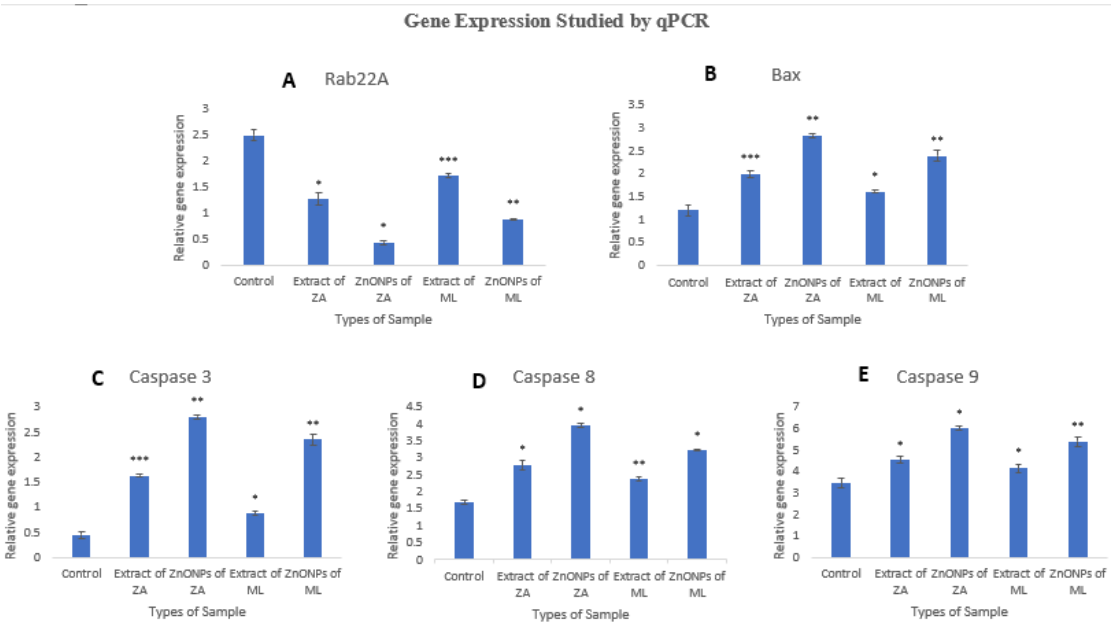

FIGURE 4.12: Gene expression studies: level of Rab22A, bax and caspase 3, caspase 8 and caspase 9 genes determined by real time q-PCR. Error bars indicate the standard error (SE) of three means, asterisk represents the significant difference in data compared with control at *P $<$ 0.05, **P $<$ 0.01 and ***P$<$ 0.001. ZA=*Zygophullum arabicum*, ML= *Mentha longifolia* var. *asiatica*

4.5 Protein Analysis by ELISA

ELISA was used to determine the protein levels of the aforementioned genes. The level of Rab22A, bax, and initiator caspase (caspase 9) and executioner caspases (caspases 3 and caspase 8) proteins were studied in MCF-7 cells treated with *Z. arabicum* and *M. longifolia* var. *asiatica* ZnONPs and plant extracts (Figure **??**). It was observed that Rab22A protein level was decreased while bax protein and caspases protein levels were increased in treated cells as compared to the control group. The results also showed that the level of studied proteins was higher in the cells treated with *Z. arabicum* as compared to *M. longifolia* var. *asiatica*

in comparison to the control group. This confirmed the role of plant extract and ZnONPs in the activation of cell death in cancer cells by activating a series of caspase reactions.

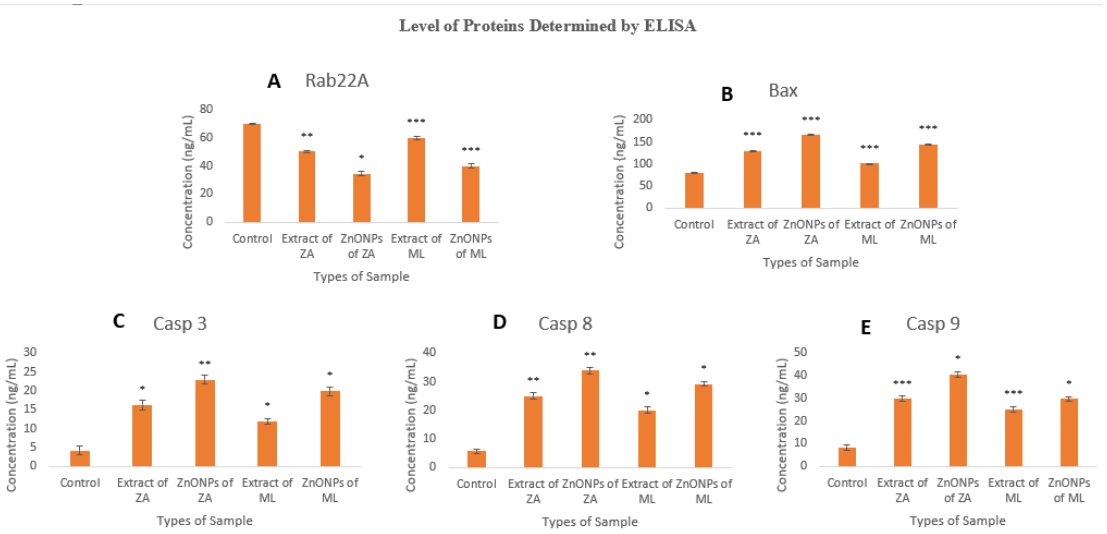

FIGURE 4.13: Determination of protein levels: Rab22A, bax and caspases protein levels determined by ELISA. Error bars indicate the standard error (S.E.) of three means, asterisk represents the significant difference in data compared with control at *P $<$ 0.05, **P $<$ 0.01 and ***P$<$ 0.001. ZA=*Zygophullum arabicum*, ML= *Mentha longifolia* var. *asiatica*

.

Objective 2: Characterization of extracts of *Zygophullum arabicum* and *M. longifolia* var. *asiatica* plants for identification of bioactive compounds.

4.6 Determination of Bioactive Compounds by HPLC

The phytochemical screening of methanolic extract of both plant extracts was done using HPLC (Figure 4.14). By contrasting the fragmentation patterns and retention durations of different compounds with those of reference compounds, different phytocompounds were found. The presence of eight secondary metabolites was highlighted in the extract of *Z. arabicum* which were chlorogenic acid, gallic

acid, coumaric acid, salicylic acid, quercetin, benzoic acid and rutin (Figures 4.15 & 4.16). Whereas, in *M. longifolia* var. *asiatica* extract, identified secondary metabolites included chlorogenic acid, gallic acid, kaempferol, sinapic acid, salicylic acid, coumarin, quercetin, 3-Hydroxy butyric (HB) acid and rutin (Figure 4.17 & 4.18). The highest concentration in *Z. arabicum* was of chlorogenic acid followed by benzoic acid and the minimum concentration was that of gallic acid. The maximum concentration in *M. longifolia* var. *asiatica* was of 3-chlorogenic acid followed by gallic acid and the lowest concentration was that of rutin.

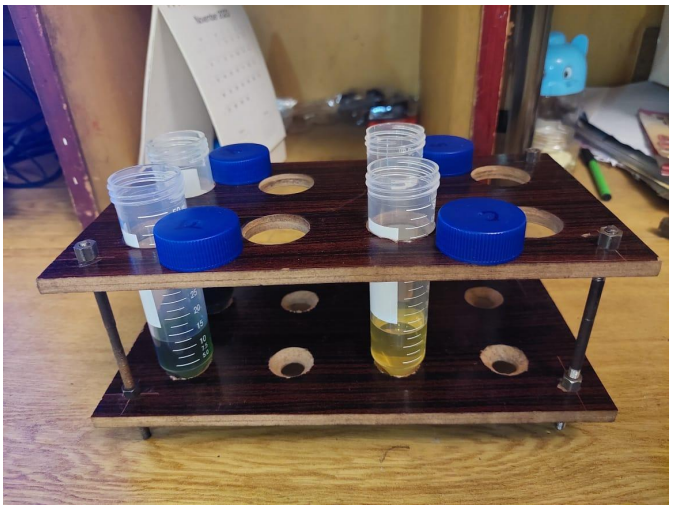

FIGURE 4.14: Preparation of methanolic extract of Z.arabicum and *M. longifolia* var. *asiatica* ZnONPs for HPLC analysis

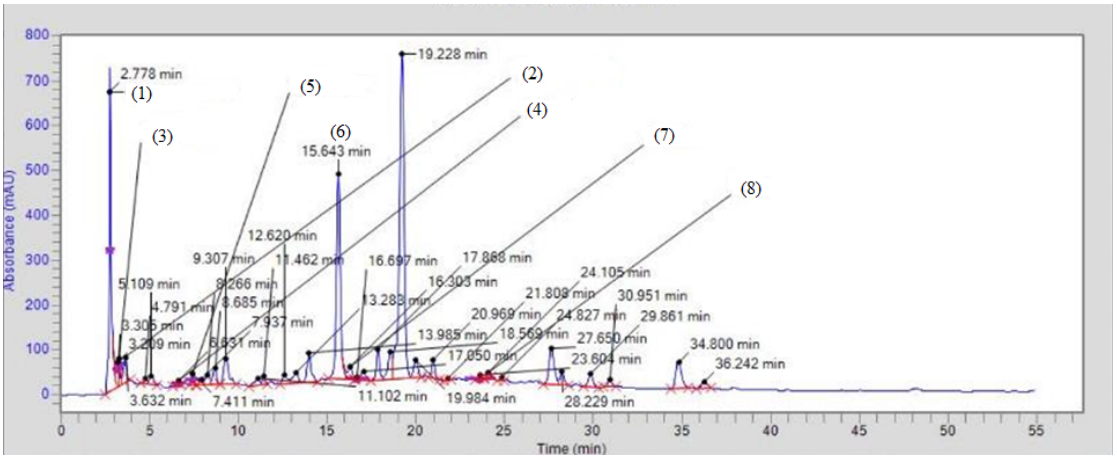

FIGURE 4.15: HPLC profile of *Z. arabicum* methanolic extract

Objective 3. To analyze the role of identified bioactive compounds of*Zygophullum arabicum* and *M. longifolia* var. *asiatica* against breast cancer-targeted gene (Rab22A) by computational approaches.

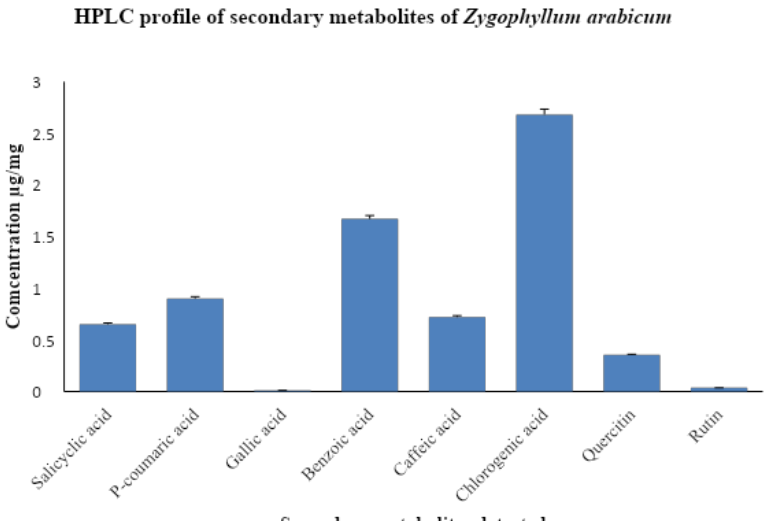

FIGURE 4.16: Graphical representation of HPLC results of *Z. arabicum* methanolic extract

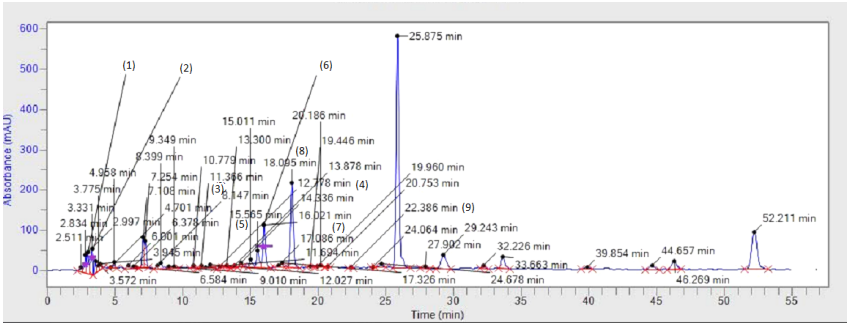

FIGURE 4.17: HPLC results of *Mentha longifolia* var. *asiatica* methanolic extract

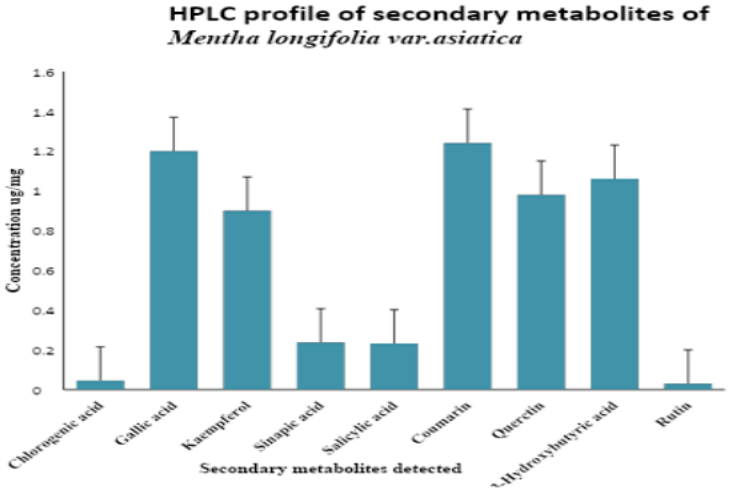

FIGURE 4.18: Graphical representation of HPLC profile of *Mentha longifolia* var. *asiatica* methanolic extract

4.7 Computational Study

4.7.1 Ligands preparation

The secondary metabolites identified through HPLC were selected as ligands for the molecular docking studies. The ligand structures were retrieved from the PubChem database. This database is a public repository containing information about thousands of compounds which can be utilized in numerous machine learning and data science initiatives for drug repurposing, computational toxicology, virtual screening, and other applications. After downloading the sdf structures of ligands and other relevant information from PubChem the primarily step of energy minimization of ligands was carried out. This step is very crucial for the overall success of docking. For this purpose, chem3D ultra was used and the energy was minimized. After the energy minimizatuion step, sdf structures were saved again (Table 4.2).

TABLE 4.2: Ligands of *Zygophullum arabicum* & *Mentha longifolia* var. *asiatica*

S. No.	**Name**	**Ligands CID No.**	**Molecular formula**	**Molecular weight g/mol**	**Structure**
1.	Chlorogenic acid	1794427	C16H18O9	354.311	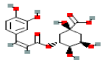
2.	Gallic Acid	370	C7H6O5	170.12	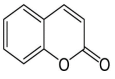
3.	Coumarin	4114	C9H6O2	146.145	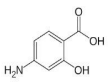
4.	Salicyclic acid	338	C15H10O5	270.24	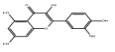
5.	Quercetin	5280343	C15H10O7	302.238	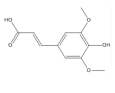

6.	Kaempferol	5280863	C15H10O6	286.239	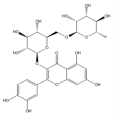
7.	Sinapic acid	637775	C11H12O5	224.212	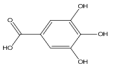
8.	Rutin	5280805	C27H30O16	610.521	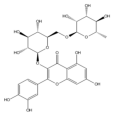
10.	Benzoic acid	243	C7H6O2	122.12	
11.	3-HB acid	441	C4H8O3	104.1	
12.	Palbociclib drug	5330286	C30H50O	426.7g/mol	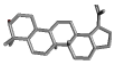

4.7.2 Protein's Primary Sequence Retrieval

The primary sequence of protein Rab22A was retrieved from the protein data bank (PDB). Rab22a is a GTPase-binding protein having PDB ID IZ0J and consisting of 194 amino acids. The archive holdings of the PDB contain more than 155,000 atomic-level protein, DNA, and RNA structures that have been experimentally characterized utilizing macromolecular X-ray crystallography, three-dimensional electron microscopy, and nuclear magnetic resonance spectroscopy. The FASTA sequence of Rab22A was retrieved from https://www.rcsb.org/ and is as follows:

>AAF00047.2 GTP-binding protein RAB22A [Homo sapiens] MALRELKVCLL-GDTGVGKSSIVWRFVEDSFDPNINPTIGASFMTKTVQYQNELHKFLIWDTA GQERFRALAPMYYRGSAAAIIVYDITKEETFSTLKNWVKELRQHGPPNIVV AIAGNKCDLIDVREVMERDAKDYADSIHAIFVETSAKNAININELFIEISRRIP-STDANLPSGGKGFKLRRQPSEPKRSCC

4.7.3 Physiochemical Properties Analysis

The physicochemical properties of the selected protein were determined by the protoparam which is a tool of Expasy (Table: 4.3)

TABLE 4.3: Physiochemical properties of Rab22A

Property	**Value**
Number of Amino Acids	194
Molecular Weight	21,855.06
Instability Index (II)	51.51
Extension Coefficient 1	24,200
Extension Coefficient 2	23,950
Theoretical PI	8.32
Positively Charged Particles	26
Negatively Charged Particles	24
GRAVY	-0.272

4.7.4 Identification of Functional Domains and 3D Structure of Protein

The identification of multiple domains of selected protein was carried out by the Interpro an online database which characterized protein based on its functional domains (Figure 4.19).

The results showed that Rab22A contain two domains i.e small GTP binding domain IPR005225 and small GTP binding protein domain fam TIGR00231. The results indicated that this protein belongs to the homologous superfamily P-loopNTPase.

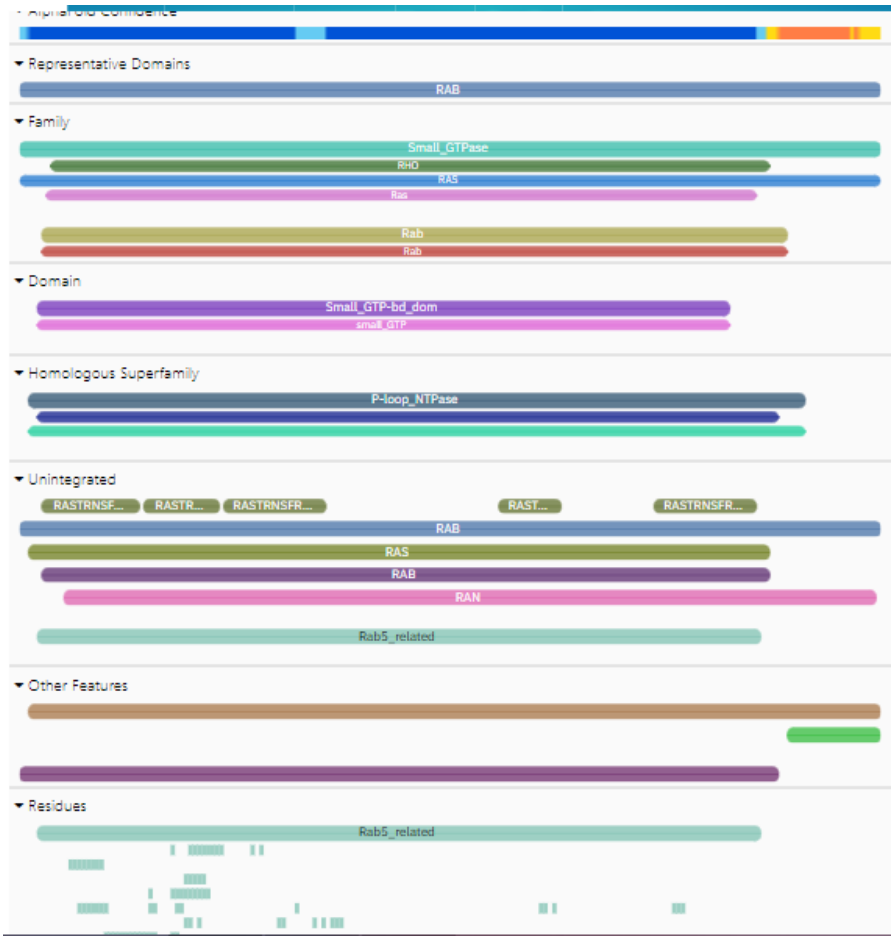

FIGURE 4.19: Identification of functional domains of Rab22A by Interpro

4.7.5 Refining of Protein Structure

The protein structure with PDB ID IZ0J was downloaded from the Protein Data Bank (PDB) (Figure 4.20) stored and then viewed using Pymol software. It was found that it contained water molecules which were removed. All the unnecessary structures were removed and it was properly refined and saved for later use (Figure 4.21). To obtain an accurate protein that might serve as a template for molecular docking and molecular dynamics modelling this was an extremely important step.

4.7.6 Molecular Docking

The CB Dock, an approachable blind docking web server, was utilized for docking studies. It used a cutting-edge rotating cavity detection technique to compute

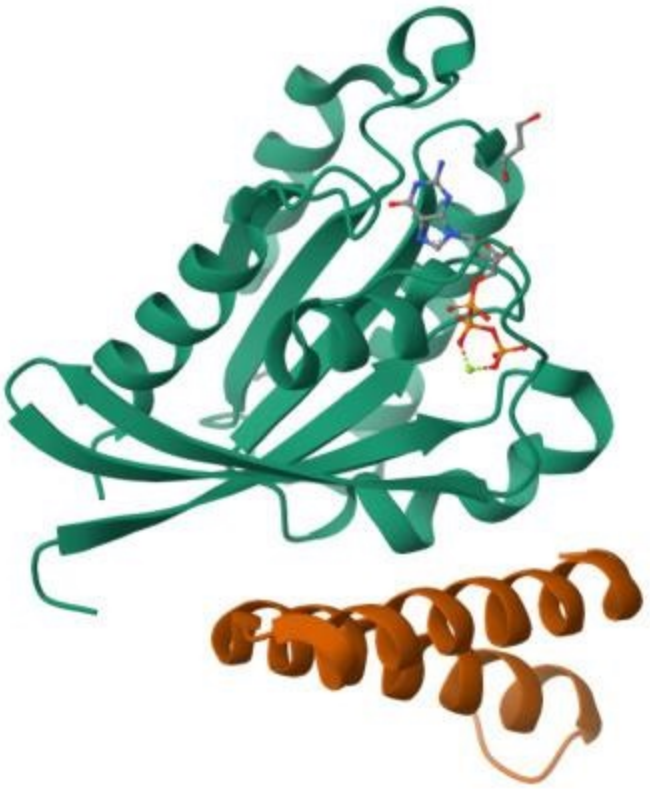

FIGURE 4.20: 3D structure of Rab22A protein obtained from Protein Data Bank

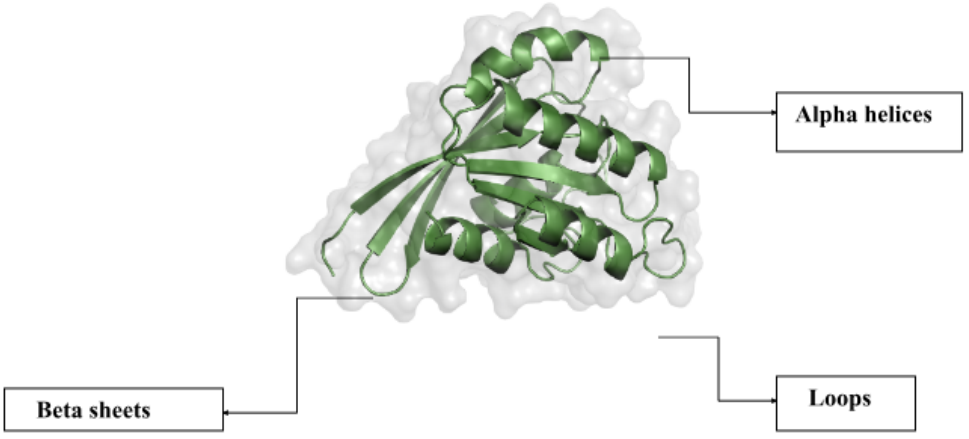

FIGURE 4.21: Refined 3D structure of Rab22A protein by Pymol software

centres and sizes. Moreover, it also determined a binding site for a particular protein and docked it using the Auto dock Vina docking tool. Rab22A was used as a receptor in molecular dockings, while specific compounds identified through

the HPLC of *M. longifolia* var. *asiatica* and *Z. arabicum* were used as ligands.

Following the submission of input files (ligand files in sdf format and receptor files in pdb format), file verification was done. CB-Dock converts the input files to pdbqt format files using OpenBabel and MGLTools. CB-Dock forecasted receptor cavities and determined the sizes and centres of the top N (n=5 by default) cavities. The submission files for docking were received for each size and centre. After N rounds of computation, the final findings were shown. NGL viewer draws the interactive 3D structures. The greatest affinity score of the receptor-ligand interaction was used to select the best confirmation out of the five that were considered.

Chlorogenic acid and 3-hydroxybutyric acid were selected from *Z. arabicum* and *Mentha longifolia* var. *asiatica* respectively as they had the lowest vina score. The reference anti-breast cancer drug palbociclib was used as a reference drug for comparison with the selected ligands. The best poses shown by the ligands and drug are shown in Figures 4.22, 4.23 & 4.24. Ligands of both selected plants with the best vina score value with Rab22A receptor are shown in Tables 4.4, 4.5, 4.6 and 4.10

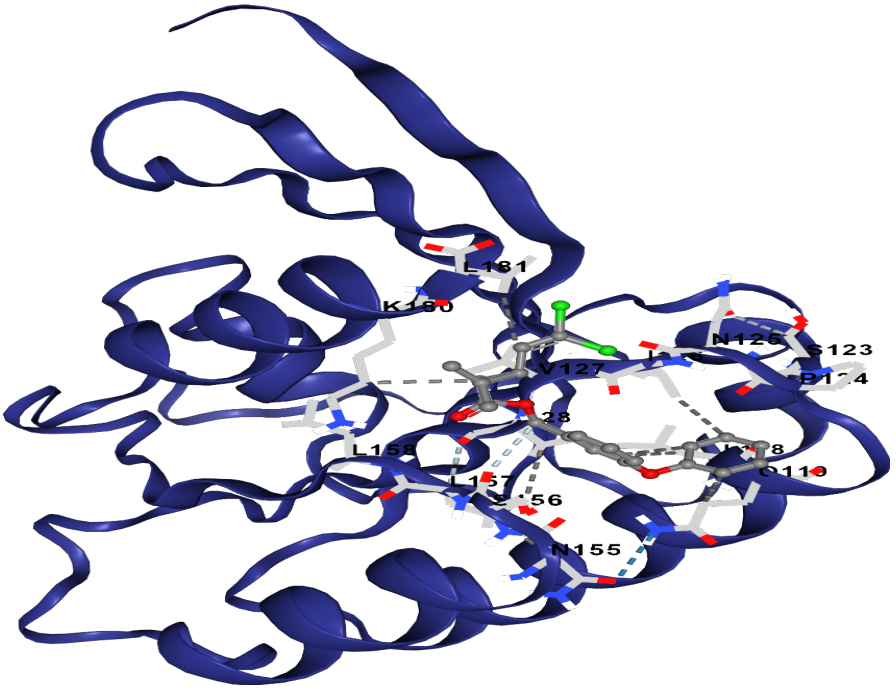

FIGURE 4.22: Best docking pose of 3-hydroxybutyric acid

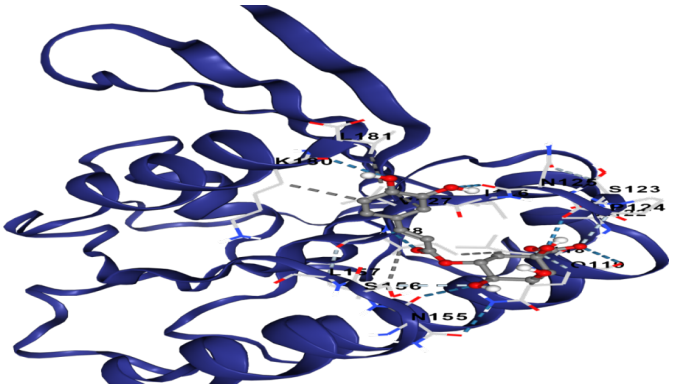

FIGURE 4.23: Best docking pose of chlorogenic acid

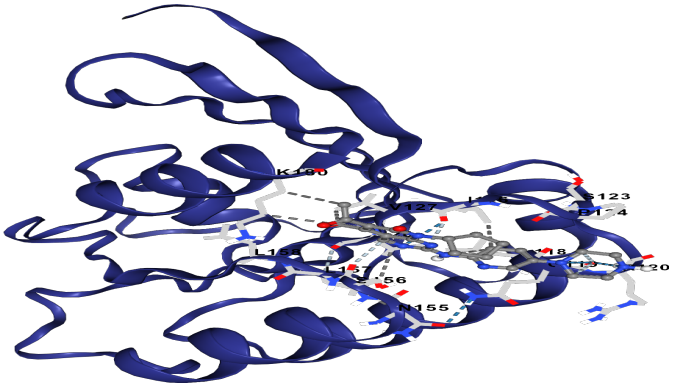

FIGURE 4.24: Best docking pose of palbociclib drug

TABLE 4.4: Docking results of selected ligands of *Mentha longifolia* var. *asiatica* and standard drug against Rab22A protein

S. No	Ligands	Grid Map	Max Energy Kcal/mol	Min Energy Kcal /mol
1	Chlorogenic acid	-9.8	274	354.311
2	Gallic Acid	-6.4	209	170.12
3	Coumarin	-6.5	493	146.145
5	Salicylic acid	-6.3	415	354.31
6	Quercetin	-9	493	302.238
7	kaempferol	-8.6	274	286.239
8	Benzoic acid	-5.8	279	127.1
9	Sinapic acid	-4.8	493	224.212
10	Rutin	-9.9	279	610.521
11	Palbociclib	-8.9	493	447.5

TABLE 4.5: Docking results of selected ligands of *Mentha longifolia* var. *asiatica* and standard drug against Rab22A protein

S. No	Ligands	Grid Map	Max Energy Kcal/mol	Min Energy Kcal /mol
1	Chlorogenic acid	16	22.8823	9.8942
2	Gallic Acid	14	-3.4919	-4.3164
3	Coumarin	16	9.5426	5.150
4	Salicylic acid	12	25.84	6.13
5	Quercetin	14	14.9427	5.3551
6	kaempferol	16	21.7643	6.4005
7	3-hydroxybutyric acid	14	7.9939	3.4983
8	Sinapic acid	11	45.7516	8.3398
9	Rutin	16	39.5842	-2.9537
10	Palbociclib	16	89.786	66.5207

TABLE 4.6: Docking results of selected ligands of *Zygophyllum arabicum* and standard drug against Rab22A protein

S. No.	Ligands	Vina Score	Molecular Weight g mol
1	Chlorogenic acid	-9.8	354.311
2	P-coumaric acid	-6.5	146.145
3	Gallic Acid	-6.4	170.12
4	Benzoic acid	-6.7	122.2
5	Caffeic acid	-6.7	180.159
6	Salicylic acid	-6.3	270.24
7	Quericitin	-6.5	302.238
8	Rutin	-7.2	610.521

TABLE 4.7: Docking results of selected ligands of *Zygophyllum arabicum* and standard drug against Rab22A protein

S. No.	Ligands	Grid Map	Max Energy Kcal/mol	Min Energy Kcal /mol
1	Chlorogenic acid	16	22.8823	9.8942
2	P-coumaric acid	16	9.5426	5.150
3	Gallic Acid	14	70.3460	9.4645
4	Benzoic acid	16	1.9678	-4.2209
5	Caffeic acid	16	1.9678	-4.2209

4.7.7 Analysis of Ligands and Target Protein Interaction through Lig-Plot+

The docking results were analyzed by PyMol Edu (v1.7.4.5) and LigPlot+ (v.1.4.5). Ligand-target protein interactions were predicted with the help of Lig-Plot Plus (v.1.4.5). The LigPlot+ used a graphical system which automatically generated several 2D interaction diagrams (Figures **??**, **??** and **??**).

These two-dimensional diagrams illustrated the hydrophobic interactions and hydrogen-bond interaction pattern between the ligand and the side- or main-chain components of the target protein (Table 4.8 & 4.9).

TABLE 4.8: Findings of interaction between ligands and standard drug molecule with target protein

S. No	Ligands	Binding energy	Number of hydrogen bond	Amino acids
1	Chlorogenic acid	-9.8	5	4
2	Hydroxybutyric acid	-6.7	1	0
3	Palbociclib drug	-8.9	2	3

TABLE 4.9: Findings of interaction between ligands and standard drug molecule with target protein

S. No	Ligands	HBS distance	Hydrophobic interaction
1	Chlorogenic acid	2.94, 2.93, 2.80	Ser 51(A) Ala56(A) Thr52(A) Lys 42(A) His 46(A) Leu 38(A) Gln 49(A) Phe 48(A) Ser 34(A)
2	Hydroxybutyric acid	1	Val 127(A) Lys 180 (A) Ser 156(A) Ile 128(A) Gln 119(A) Aer 123(A) Pro 124(A)
3	Palbociclib drug	2.80, 2.89, 2.94	Thr 52(A) Ser 34(A) Pro 30(A) Lys 33(A) Gln 49(A) Ala 77(A)

4.8 Molecular Dynamics Simulation

The stability of particular ligand-protein complexes was assessed by molecular dynamics simulation. The results showed that chlorogenic acid forms a stable complex with the targeted protein (Figure 4.25 & 4.26). The ligand is bound tightly in the pocket of the protein and it also shows various interactions forming hydrogen bonds and other hydrophobic interactions. In comparison to chlorogenic acid, hydroxybutyric acid also forms a stable complex (Figure 4.27 & Figure 4.28). This complex is however considered to be less stable because there are no hydrogen bonds and other interactions such as carbon, hydrogen bond or pi bonds which makes the complex more stable. The complex of palbociclib drug and Rab22A was also stable but there are fewer hydrogen bonds as compared to chlorogenic

acid. This complex is more stable than the hydroxybutyric acid complex (Figure 4.29 & 4.30).

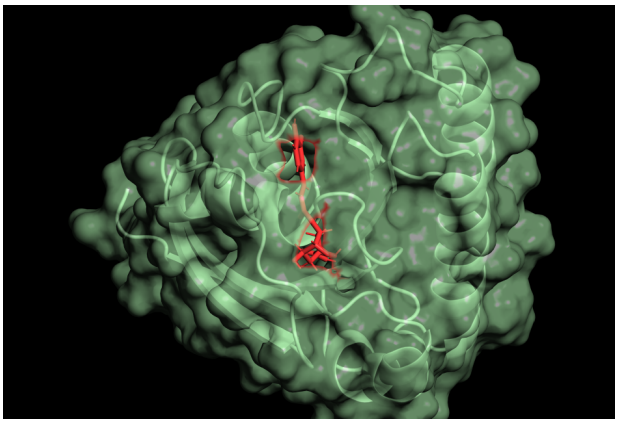

FIGURE 4.25: Best docked pose of chlorogenic acid and Rab22A complex by Chimera

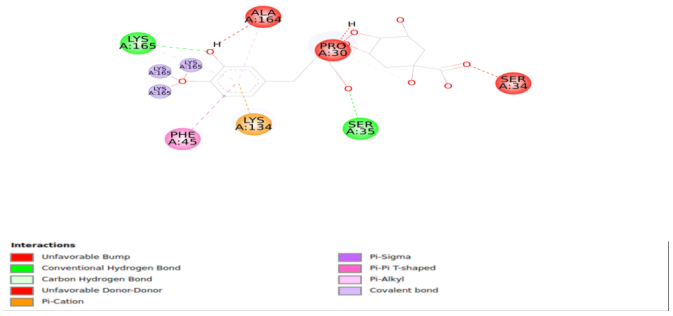

FIGURE 4.26: Electrostatic interactions of the best-docked pose of chlorogenic acid and Rab22A complex viewed via GROMACS 2022.1

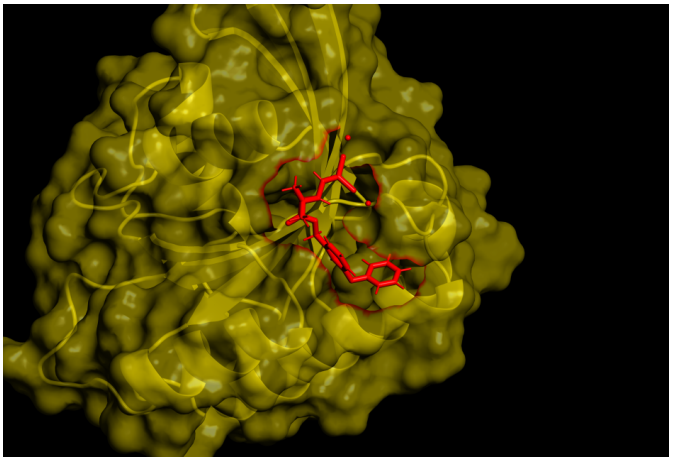

FIGURE 4.27: Best docked pose of 3-hydroxybutyric acid and Rab22A complex by Chimera

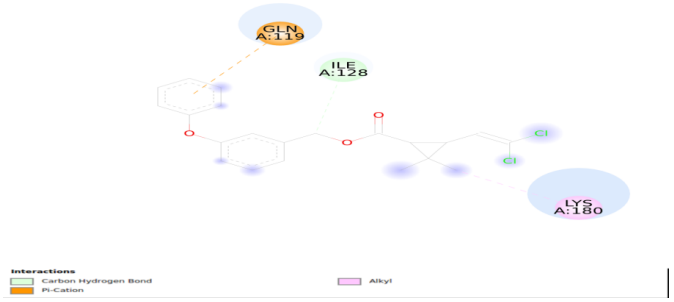

FIGURE 4.28: Electrostatic interactions of the best-docked pose of 3-hydroxybutyric acid and Rab22A complex viewed via GROMACS 2022.1

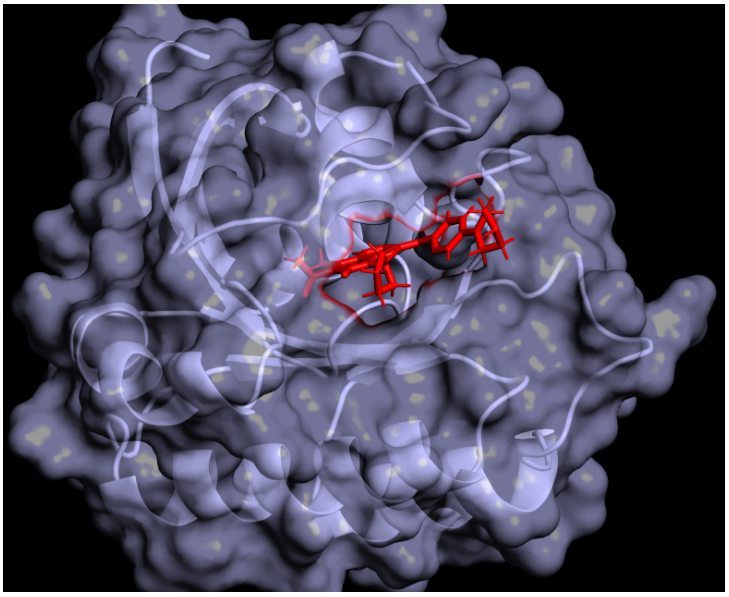

FIGURE 4.29: Best docked pose of palbociclib and Rab22A complex by Chimera

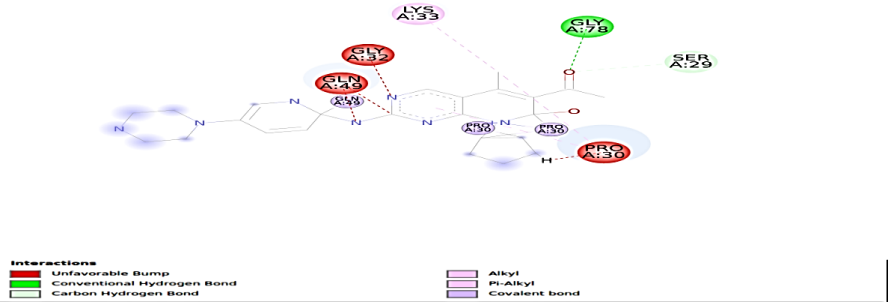

FIGURE 4.30: Electrostatic interactions of the best-docked pose of palbociclib and Rab22A complex viewed via GROMACS 2022.1

4.8.1 Root Mean Square Deviation (RMSD)

Protein conformation changes during various simulation paths were demonstrated by the quantification of the degree of atomic differences between the reference structure and subsequent frames. These results showed that chlorogenic acid remains stable till 20 ns after 25 ns it shows a greater peak (Figure 4.31). Stability was uniform till 50 ns and afterwards, it again showed fluctuations. Hydroxybutyric acid remained unstable from the start and after 10 ns it shows instability suggesting that this ligand is not properly bound with reference protein (Figure 4.32). Palbociclib remained stable till 50 ns & showed fluctuations afterwards (Figure 4.33). The complex of chlorogenic acid showed less RMSD which suggests that it has more rigid structure as compared to the other two ligands (Figure 4.34).

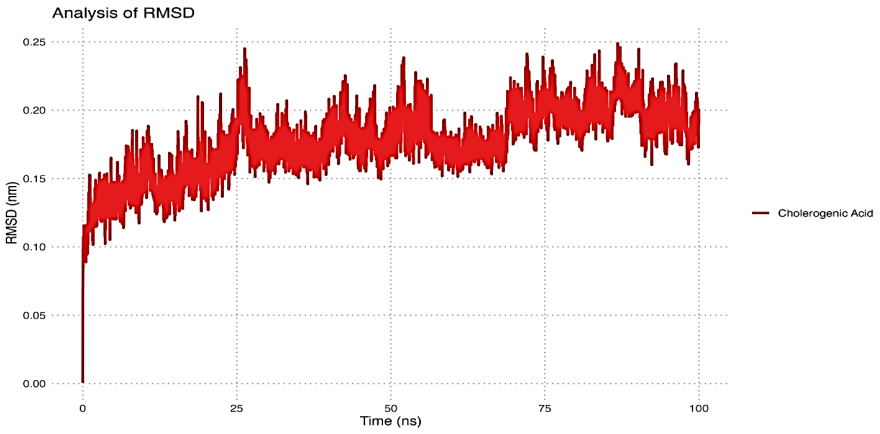

FIGURE 4.31: RMSD plot of chlorogenic acid

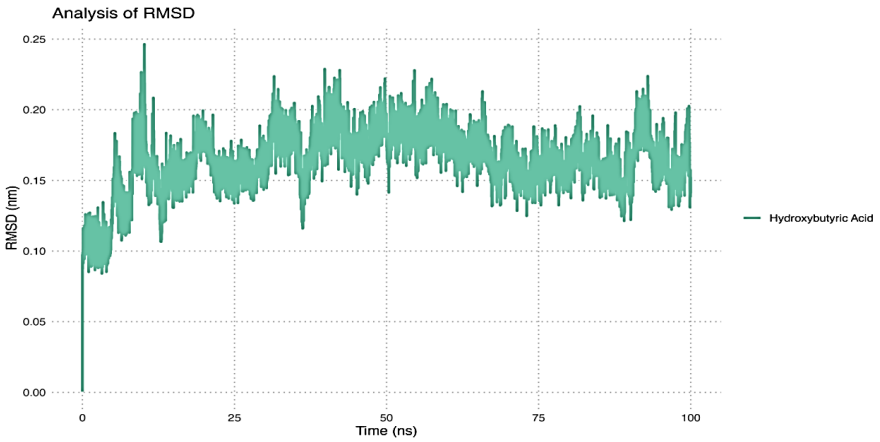

FIGURE 4.32: RMSD plot of 3-hydroxybutyric acid

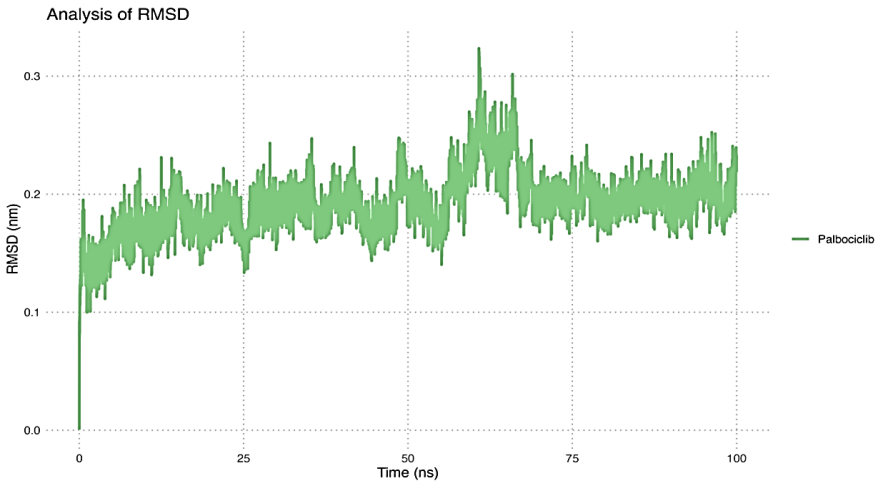

FIGURE 4.33: RMSD plot of palbociclib

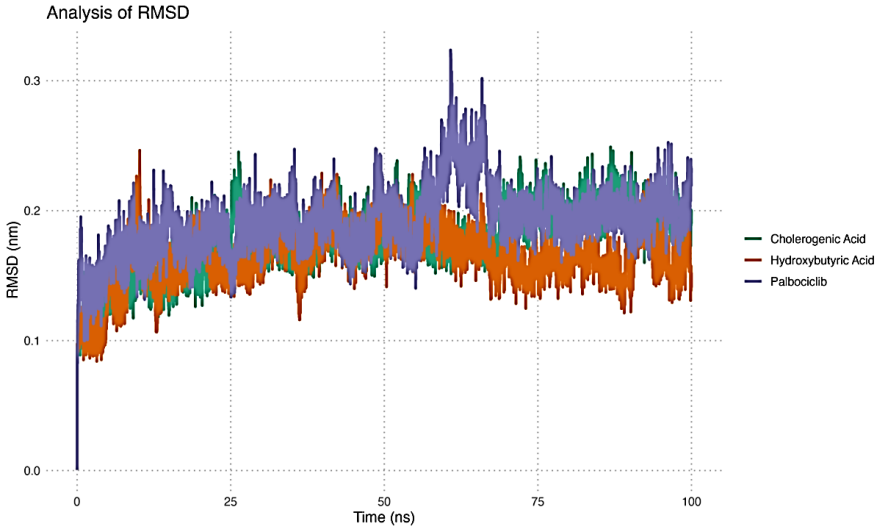

FIGURE 4.34: Comparative RMSD plot of chlorogenic acid, 3-hydroxybutyric acid and palbociclib

4.8.2 Root Mean Square Fluctuation (RMSF)

RMSF provides insight into average deviation of atoms from their mean positions during simulation period. The RMSF of each ligand-protein complex was performed to confirm the conformational changes that took place during simulation trajectories. It can be inferred from the results that all three ligands showed significant fluctuations and displacements during simulation cycles.

Based on these findings, it appears that all three complexes had slight oscillations during the MD simulation trajectories following the production steps. This shows that they have significant correlations with critical residues. Chlorogenic acid presented values less than 0.5 $\mathring{A}$ for Lys, Ala, Ser and Pro residues (Figure 4.35). The significant displacement for hydroxybutyric acid was at 0.3 $\mathring{A}$ and after that significant peaks were observed which shows that the structure was relatively unstable (Figure 4.36).

The drug palbociclib also showed less conformational changes as the highest fluctuation was observed at 0.2 $\mathring{A}$ and the structure was stable (Figure 4.37). The comparative results showed that chlorogenic acid and palbociclib drug have fewer fluctuations which indicates the stable nature of these complexes (Figure 4.38).

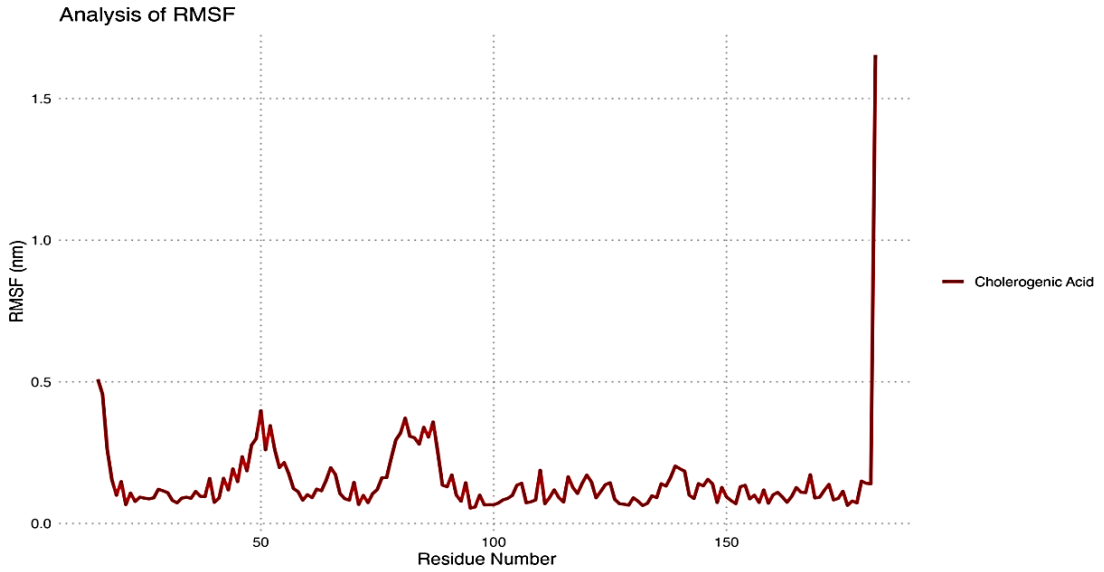

FIGURE 4.35: RMSF analysis of the chlorogenic acid-Rab22A complex

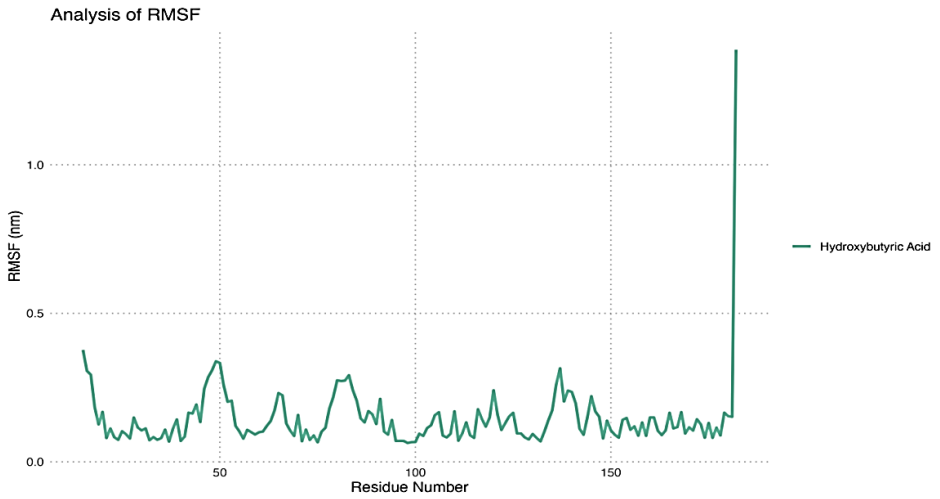

FIGURE 4.36: RMSF analysis of the 3-hydroxybutyric acid-Rab22A complex

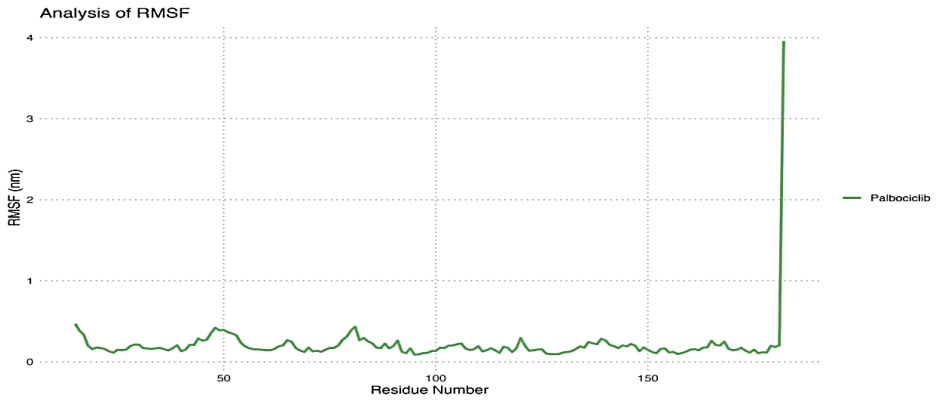

FIGURE 4.37: RMSF analysis of the palbociclib-Rab22A complex

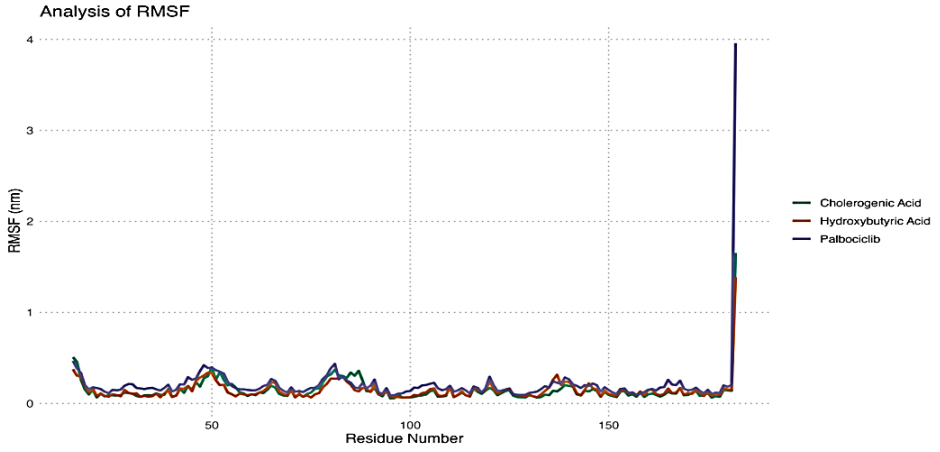

FIGURE 4.38: Comparative RMSF analysis of chlorogenic acid, 3-hydroxybutyric acid and palbociclib-Rab22A complexes

4.8.3 Hydrogen Bonds Analysis

Intermolecular hydrogen bonding is also a sign of stability for the protein-ligand complex. The results showed that chlorogenic acid showed changes in the network of hydrogen bonding which also fluctuated the number of interactions. The hydrogen bonds remained 6 and rose to 7 from 0-12 ns and declined to 4 till 40 ns. The hydrogen bonds again showed a spike and number increased from 4 to 8 till 50 ns.

Afterwards, there was again decline which persisted till 100 ns (Figure 4.39). The number of hydrogen bonds for hydroxybutyric acid remained steady during the simulation trajectories from 0-100 ns. The spike was seen twice where the number rose to two H-bonds during 40 and 85 ns respectively which is a sign of low stability (Figure 4.40).

Palbociclib showed hydrogen bonding for relatively shorter intervals of time with one H-bond (Figure 4.41). The results suggested that it is an unstable complex. The comparative results suggest that chlorogenic acid is the most stable ligand as compared to the other two as it showed maximum hydrogen bonding during regular intervals of time (Figure 4.42).

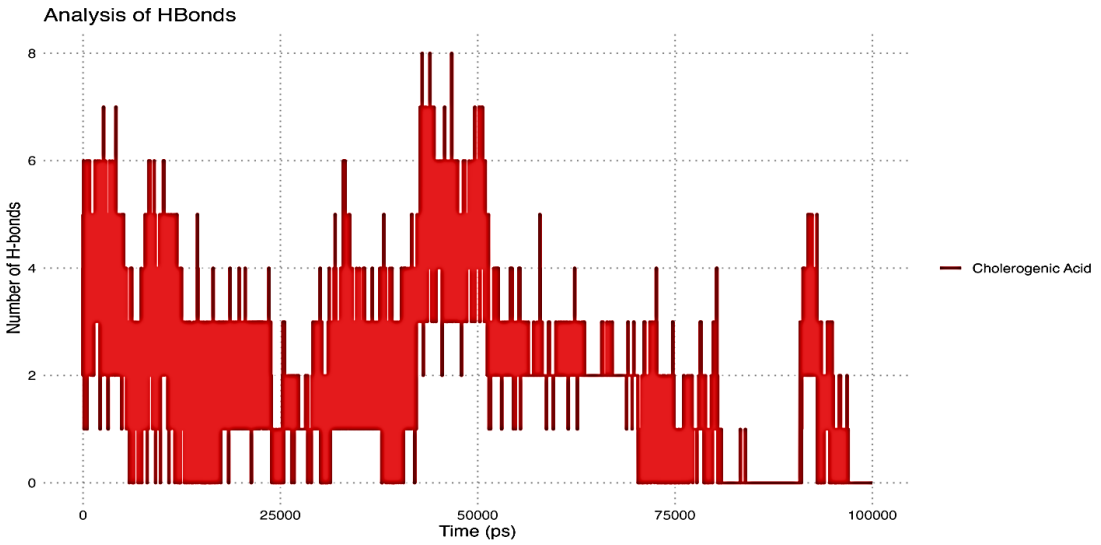

FIGURE 4.39: Hydrogen bond analysis of chlorogenic acid

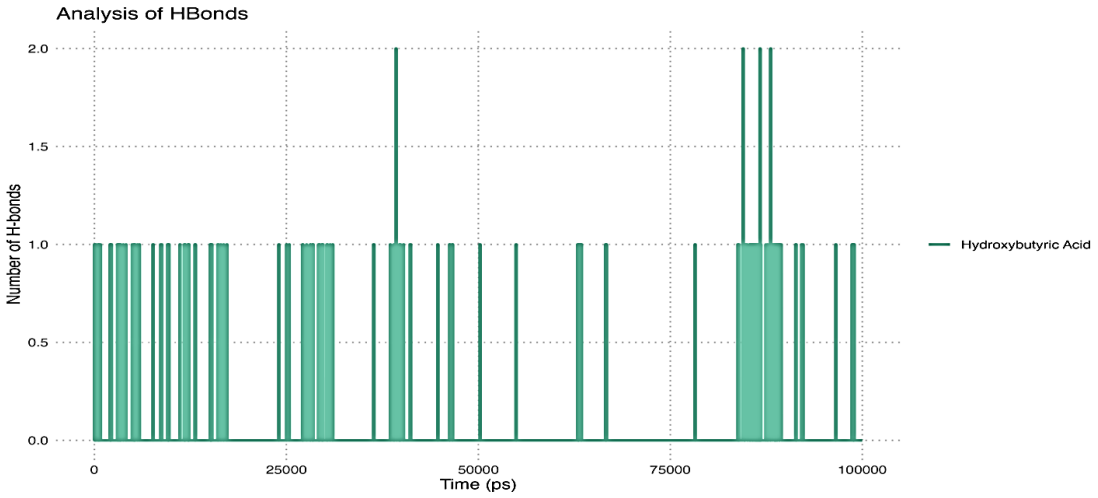

FIGURE 4.40: Hydrogen bond analysis of 3-hydroxybutyric acid

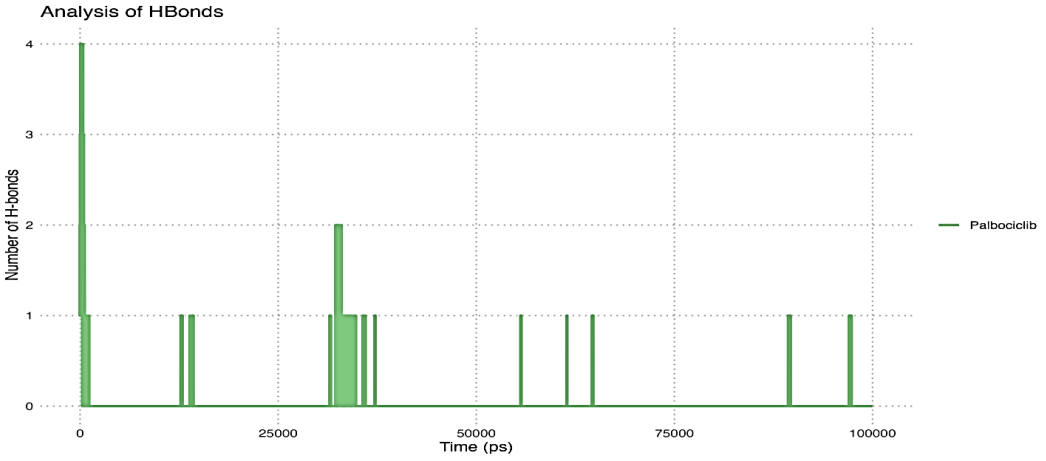

FIGURE 4.41: Hydrogen bond analysis of palbociclib

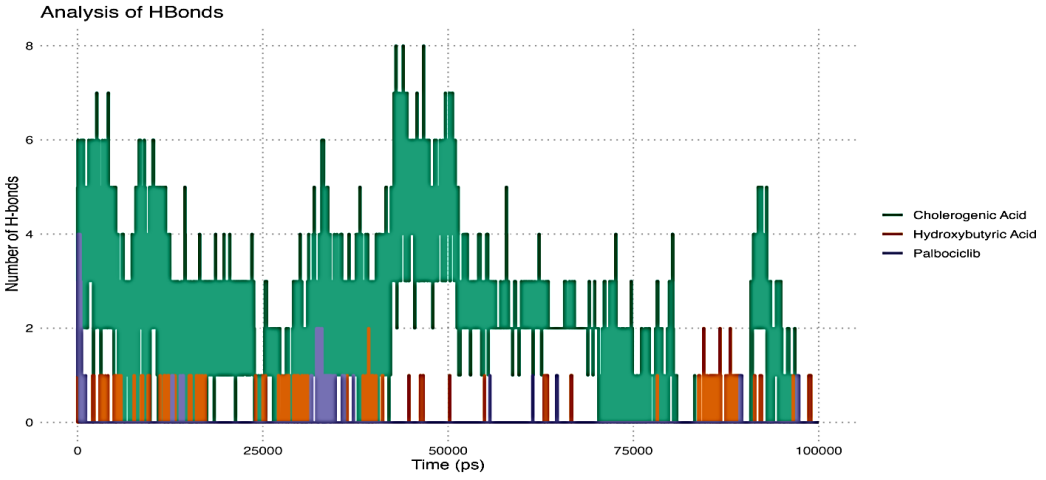

FIGURE 4.42: Comparative hydrogen bond analysis of ligands and drug

4.8.4 Radius of Gyration (Rg)

Using the radius of gyration, protein backbone compactness over simulation cycles was determined. The value of Rg for chlorogenic acid remained 1.6 nm from 0-80 ns and it shows an increase after 80 ns. This indicated that the complex has a stable structure. However, at 85 ns the value of Rg increased from 1.7 nm and it continued to increase to 100 ns where it reached above 1.7nm (Figure 4.43). The complex of hydroxybutyric acid showed variations throughout the simulation period. The value of Rg was 1.6 nm from 0-25 ns and it showed a sudden spike after that the value rose above 1.7 nm at 30 ns. This trend continued till 50 ns. The Rg value again declined from 50-100 ns where it remained under 1.6 nm (Figure 4.44). The palbociclib complex showed higher values of Rg throughout the simulation period. The Rg was above 1.7 nm from 0-25ns. After 25 ns the Rg value rose above 1.8 nm which declined occasionally during certain periods but mostly it remained at 1.8 nm till 100 ns (Figure 4.45). The comparative results also suggest that among the three complexes, chlorogenic acid shows less radius of gyration value from 0-100 ns which shows signs of stability and compactness of the complex whereas, the palbociclib complex showed greater values which indicates that this complex was not stable throughout simulation period (Figure 4.46).

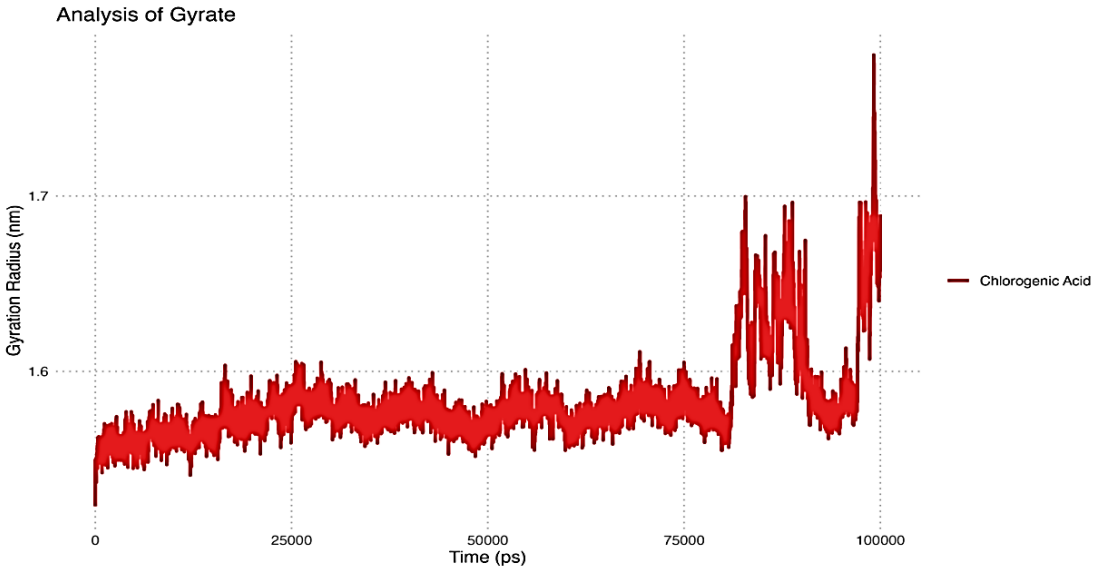

FIGURE 4.43: Radius of gyration plot of chlorogenic acid

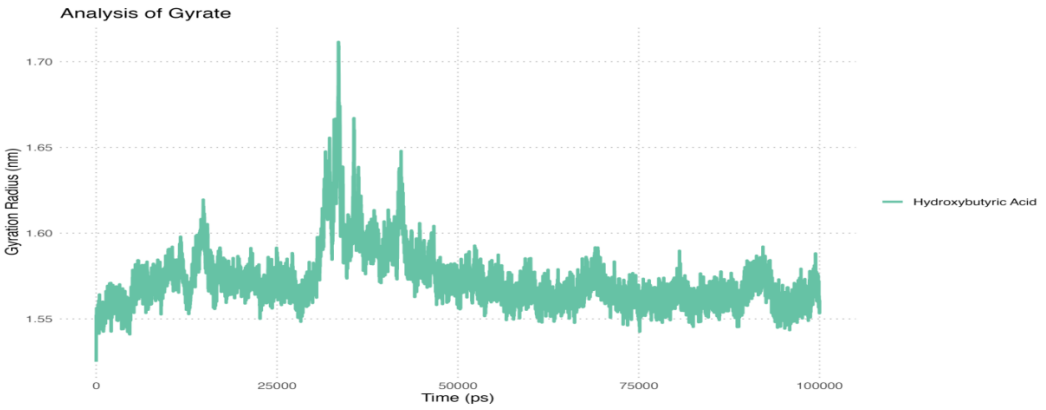

FIGURE 4.44: Radius of gyration plot of 3-hydroxybutyric acid

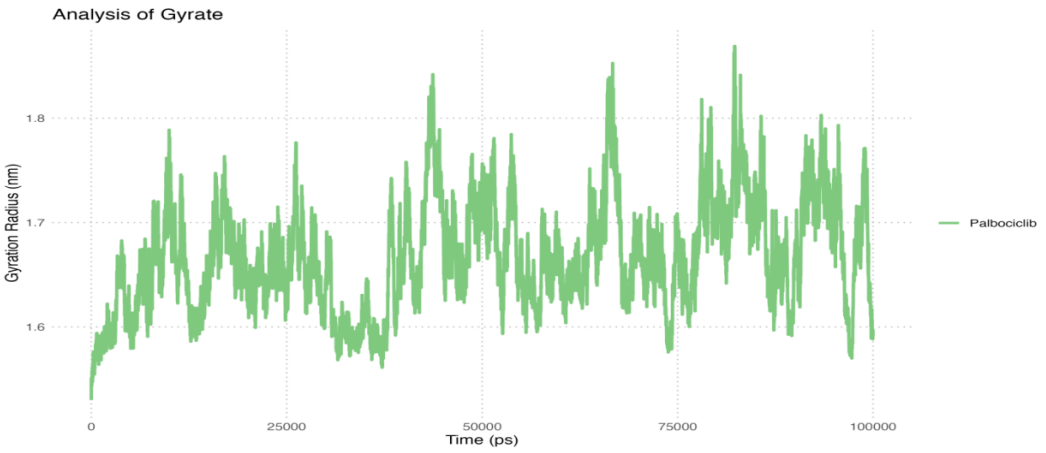

FIGURE 4.45: Radius of gyration plot of palbociclib

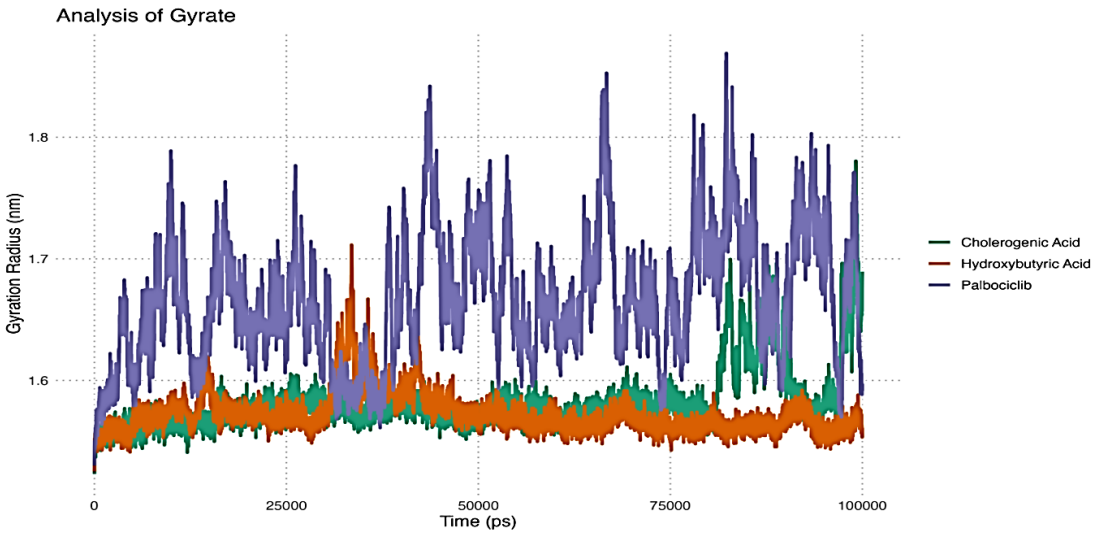

FIGURE 4.46: Comparative analysis of radius of gyration plot of ligands and reference drug

4.8.5 Solvent Accessible Surface Area (SASA)

SASA determines the measure of the area of any protein which is accessible to solvent molecules for their interaction. Chlorogenic acid shows an increase in the trend of surface area from 0-25 ns where the area remains at 105 nm. After 25 ns the value slightly decreases and remains 100-105 nm till 40 ns. The value of SASA again decreases from 40-60 ns and remains below 100 nm. The SASA again increases from 60-80 ns where it remains above 105 nm and shows a slightly decreasing trend from 80-100 ns (Figure 4.47).

For hydroxybutyric acid, the value of SASA remains stable from 0-25 ns where it remains between 100-105 nm and a spile was observed after 50 ns where it jumps above 105 nm till 40 ns. Afterwards, there was a decrease and the SASA dropped from 105 nm and remained under 100 nm from 40-100 ns (Figure 4.48). Palbociclib shows increased surface area throughout the simulation period from 0-100 ns where the value remained between 100-105 nm mostly and above 105 nm occasionally (Figure 4.49). The comparative results showed that chlorogenic acid shows more SASA values as compared to hydroxybutyric acid when they are compared with the reference drug palbociclib which means that chlorogenic acid exposes more area to solvent molecules which makes it an excellent candidate for drug binding (Figure 4.50).

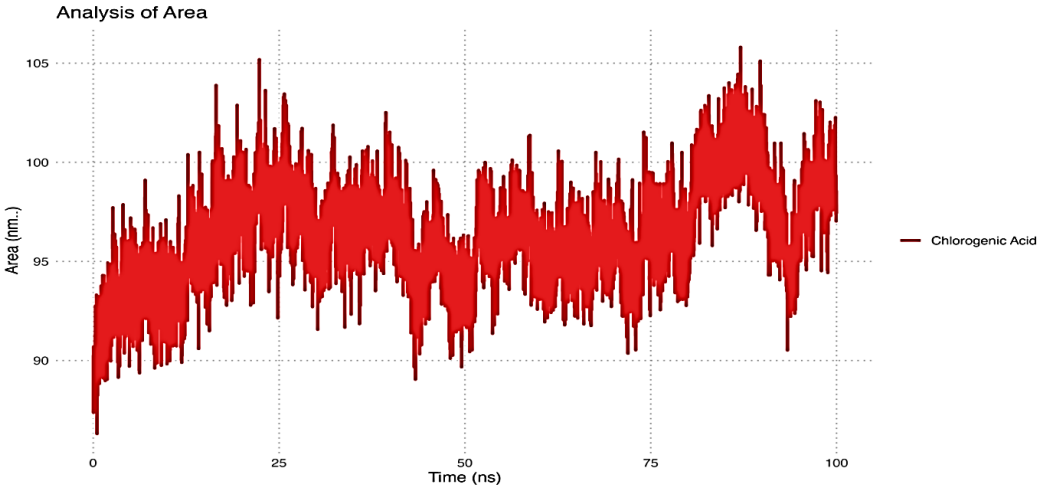

FIGURE 4.47: Solvent accessible surface area (SASA) analysis of chlorogenic acid

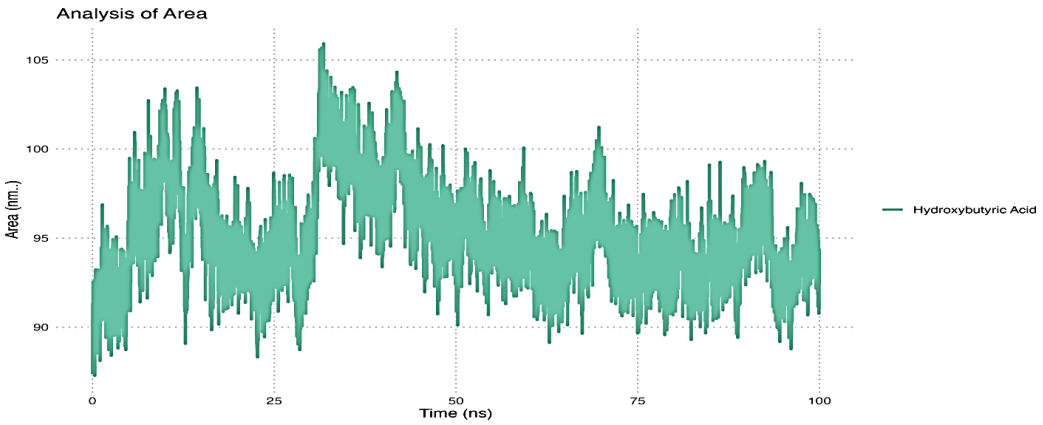

FIGURE 4.48: Solvent accessible surface area (SASA) analysis of 3-hydroxybutyric acid

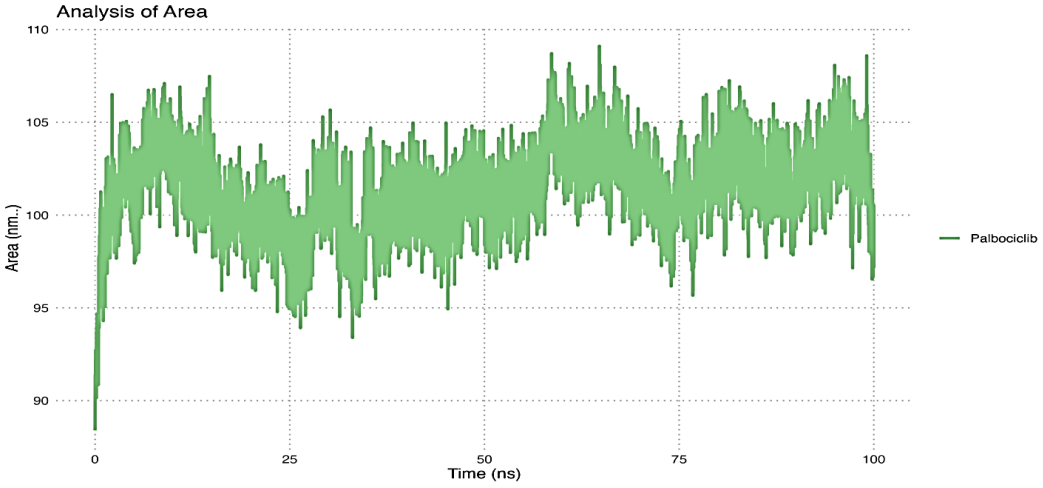

FIGURE 4.49: Solvent accessible surface area (SASA) analysis of palbociclib

4.9 ADMET Properties of Ligands

Certain parameters are used to distinguish between drug-like molecules and those that are not. These parameters are Lipinski's RO5 and the ADMET characteristics test. The initial RO5 guidelines address the four physicochemical parameters which are:

- Molecular weight $\leq$500
- log P$\leq$5
- H-bond acceptors$\leq$10

FIGURE 4.50: Comparative analysis of solvent accessible surface area (SASA) of ligands and reference drug

- H-bond donors≤5

These rules are related to compounds that are orally active. If a compound satisfies three or more of the RO5, it is said to have a drug resemblance. If a substance violates more than two of these rules, it is considered poorly absorbed. Results are summarized in Table 4.10

TABLE 4.10: ADMET properties of selected ligands

Drug likeliness properties	**Ligands and drug**		
	Chlorogenic acid	**3-Hydroxybutyric acid**	**Palbociclib**
Log P-value	-1.7	-0.5	1.8
Molecular weight	352.29 g/mol	104.10 g/mol	447.5g/mol
Hydrogen bond acceptor	9	3	8
Hydrogen bond donor	4	2	2
Bond (Rotatable)	4	2	5
Surface area	141.587	41.584	191.809

Drug likeliness properties	Ligands and drug		
	Chlorogenic acid	3-Hydroxybutyric acid	Palbociclib
Water solubility	-2.449	0.363	2.817
Caco2 Permeability	-0.84	1.103	2.005
Intestinal absorption (Human)	36.377	80.048	83.374
Skin permeability	-2.735	-2.764	-2.737
P-glycoprotein substrate	Yes	No	Yes
P- glycoprotein I inhibitor	No	No	Yes
P- glycoprotein II inhibitor	No	No	No
VDss (Human)	0.581	-0.765	1.537
Fraction unbound (human)	0.658	0.759	0.242
CNS Permeability	-3.856	-3.029	-3.147
BBB permeability	-1.407	-0.34	0.486
CYP2D6 substrate	No	No	No
CYP3A4 substrate	No	No	Yes

Drug likeliness properties	Ligands and drug		
	Chlorogenic acid	3-Hydroxybutyric acid	Palbociclib
CYP1A2 inhibitor	No	No	No
CYP2C19 inhibitor	No	No	No
CYP2C9 inhibitor	No	No	No
CYP2D6 inhibitor	No	No	No
CYP3A4 inhibitor	No	No	No
Total clearance	0.707	0.541	0.663
Renal OCT2 substrate	No	No	No
Renal OCT substrate	No	No	No
AMES Toxicity	No	No	No
Max. tolerated dose(human)	-0.314	0.964	0.033
hERG I inhibitor	No	No	No
hERG II inhibitor	No	No	Yes
Oral rat acute toxicity (LD50)	1.973	1.38	2.539
Oral rat chronic toxicity (LOAEL)	2.982	2.939	1.247
Hepatoxicity	No	No	Yes
Skin sensitization	No	No	No

Drug likeliness properties	Ligands and drug		
	Chlorogenic acid	3-Hydroxybutyric acid	Palbociclib
T. Pyriformis toxicity	0.285	-0.436	0.285

ADMET profiling was employed for determining the physiochemical and pharmacokinetics properties of selected ligands. This was done by an online tool pkCSM. ADMET characteristics such as water solubility, $CaCO_2$ permeability, intestinal absorption, P-glycoprotein substrate, and P-glycoprotein I & II inhibitors are among those that predict the absorption of oral drugs. Chlorogenic acid shows less water solubility and $CaCO_2$ permeability as compared to the reference drug and 3-hydroxybutyric acid. Low water solubility is the key to drug absorption. Compounds that fall between -4 and 0.5 log mol/L are regarded as appropriate. 3-hydroxybutyric acid has more intestinal absorption as compared to chlorogenic acid but less as compared to palbociclib. Chlorogenic acid palbociclib are p-glycoprotein substrate but 3-hydroxybutyric acid is not.

According to the P-glycoprotein I/II inhibitor model, the substance may or may not be a P-gb I/II inhibitor. These inhibitors have the potential for high absorption and decrease P-gp's pumping activity. Chlorogenic acid and 3-hydroxybutyric acid are not P-glycoprotein I/II inhibitors as compared to palbociclib which is a p-glycoprotein I inhibitor but not p-glycoprotein II (Table 4.10).

The distribution properties are described in Table 4.7 which shows that chlorogenic acid has less VDS value compared to 3-hydroxybutyric acid and reference drug. The Fu value of chlorogenic acid and 3-hydroxybutyric acid was found to be more than palbociclib which showed that the selected ligands have more efficacy than synthetic drug considering unbound friction in plasma. In order for medications targeting the central nervous system (CNS) to reach their molecular target, they need to pass through the blood-brain barrier (BBB). Conversely, for

drugs having a peripheral target, low or no BBB penetration might be required to avoid CNS side effects. Molecules which show log BBB > -1 were classified as BBB+. The BBB value is highest for the palbociclib followed by chlorogenic acid and 3-hydroxybutyric acid respectively. CNS permeability is more for chlorogenic acid as compared to the other two. The models for several isoforms of cytochrome P450, a crucial liver detoxification enzyme, are CYP1A2, CYP2C19, CYP2C9, CYP2D6, and CYP3A4. To aid in xenobiotics' excretion, this enzyme oxidizes them. This enzyme deactivates the majority of medicines, although it can also activate some medications. Results are shown in Table 4.10. While two other substances, chlorogenic acid and 3-hydroxybutyric acid, were not anticipated to be substrates of these isoforms, palbociclib demonstrated itself to be a substrate of CYP3A4 isoforms. When predicting toxicity characteristics, the overall clearance of chlorogenic acid was higher followed by palbociclib drug and 3-hydroxy butyric acid respectively. It predicts the removal of the drug from a particular organ. The selected compounds, along with the reference drug, all exhibit negative results for Renal OCT2 substrate. This shows that they do not interfere with the OCT2 transporter's function, which is essential for the elimination of pharmaceuticals and endogenous chemicals.

According to the toxicity properties, the Maximum Tolerated Dose (MRTD) can be used to assess the threshold of a chemical's hazardous dose in humans. This will assist in determining the maximum dosage at which medications should be started in phase 1 clinical studies. MRTD is given as a logarithm (log mg/kg/day). If a substance's MRTD is 0.477 log (mg/kg/day) or more, it is considered high, and if it is 0.477 log (mg/kg/day) or less, it is considered low. Chlorogenic acid shows the lowest MRTD value as compared to 3-hydroxybutyric acid. The pharmaceutical industry has removed numerous compounds due to their inhibition of hERG channels. Palbociclib is classified as a hERG II inhibitor, but the two lead compounds are not hERG I II inhibitors (Table 4.10).

The lethal dose of a substance (LD50) is the total amount administered all at once that results in 50% of test animals (rats) dying. The hazardous potential of a possible substance is predicted by its LD50 (in mol/kg). More than the other

chosen substance, but less than palbociclib, is the LD50 value of chlorogenic acid. The goal of LOAEL is to determine the minimum concentration of a substance required to cause an observed negative outcome. Its value is same for both the selected compounds but high as compared to the drug. The log (mg/kg-bw/day) expression illustrates the pharmacological importance of extended exposure to low-to-moderate chemical concentrations. It is also important to know that hepatotoxicity refers to the liver damage caused by the drugs, it also poses a serious safety risk for drug development. Palbociclib shows positive results for hepatotoxicity while both compounds stand "no" for this model. Skin hypersensitivity is a possible side effect of products treated topically. It yields negative findings for both the chosen medication and lead compounds. One protozoa bacterium, *T. pyriformis* is employed as a hazardous endpoint (IGC50) due to its toxicity, which can impede growth by 50%. The value of chlorogenic acid is the same as that of palbociclib whereas, 3-Hb acid shows less value (Table 4.10).

4.9.1 Lead Compound and Synthetic Drug Comparison

There were two lead compounds which were selected after studying and analyzing their vina score and simulation results i.e. chlorogenic acid from *Z. arabicum* and 3-hydroxybutyric acid from *M. longifolia* var. *asiatica*. After comparing their ADMET properties with the standard drug palbociclib. It was found that chlorogenic acid was a better drug candidate as compared to 3-hydroxybutyric acid and palbociclib.

Chapter 5

Discussion

The current research work was carried out to perform a comparative study to determine the anticancer potential of two pharmacologically significant plant species *Zygophullum arabicum* and *Mentha longifolia* var. *asiatica* extracts and their ZnO nanoparticles against breast cancer targeting Rab22A gene which is a major gene of endocytic pathway and a hallmark of a variety of cancers including breast cancer. During this study, the green method of nanoparticle synthesis was adopted to synthesize ZnO nanoparticles of both species.

In vitro tests were conducted on MCF−7 breast cancer cell lines to evaluate the antiproliferative effect of the synthesized ZnO nanoparticles. The findings were compared statistically. Additionally, the impact of ZnO nanoparticles was also studied on the Rab22A gene by studying the expression of this targeted gene by real−time qPCR and compared statistically. Furthermore, Rab22A protein expression was also determined by ELISA on the treated cells in comparison to control cells. Furthermore, the apoptotic role of ZnO nanoparticles was also studied on different apoptotic genes and their protein expression was determined by real−time qPCR and ELISA respectively. This study also encompasses the identification of secondary metabolites from the methanolic extract of both selected plants by HPLC. The compounds from each plant were identified and then screened using computational assistance for drug discovery. Molecular docking was performed for

the identified compounds from each plant followed by molecular dynamics simulation and the results were compared. The identified lead compounds were then compared with the standard drug based on the ADMET profiling.

5.1 Synthesis and Characterization of Nanoparticles

Any technology developed at the nanoscale with contemporary applications is referred to as nanotechnology. It involves rearranging materials with a size range of 1 to 100 nm [219]. The field of nanotechnology is diverse and interacts with other fields such as applied physics, supramolecular chemistry, mechanical and electrical engineering, pharmaceutical sciences, colloidal sciences, and material sciences. The extension of modern sciences to the nanoscale is known as nanotechnology [220]. Compared to human cells, nanoscale devices are substantially smaller. The ability of nanoparticles to bind to receptors and enzymes both inside and outside of the cell surface is facilitated by their smaller size and comparatively higher surface area over volume [221]. ZnO nanoparticles have been produced by a variety of chemical and physical processes, including sol−gel methods, hydrothermal processes, chemical vapour deposition, precipitations, laser ablations, and physical vapour depositions. All of the aforementioned methods involve the use of highly toxic chemicals and organic solvents which may act as stabilizers but also a major threat to the environment [222]. Green or biological synthesis is the use of a safe, economical, ecologically benign and clean method to create nanomaterials. Unlike conventional chemical and physical approaches for NP synthesis, this process overcomes these limits and prolongs the life of nanoparticles while also being environmentally friendly [223, 224]. The ultimate form and size of the nanoparticle are determined by several active molecules and precursors, including metal salt. Furthermore, the natural reducing, stabilizing, and antibacterial capabilities of nanomaterials are among the advantages of green synthesis [198]. The green approach of nanoparticle synthesis uses living things such as plants, bacteria and

fungi for the synthesis of ZnO nanoparticles. The green synthesis of metal oxide nanoparticles has been made possible by the use of natural materials specifically phytochemicals, which are found in plant parts such as leaves, flowers, and fruits [225]. Over the past ten years, there has been a shift in the use of plant resources for environmentally friendly nanoparticle manufacturing. Certain bioactive substances found in plants include reductase, flavonoids, phenols, alcoholic sugars, terpenes, alkaloids, amino acids, carbohydrates and polyphenolic compounds are responsible for the formation of ZnO nanoparticles because they have a natural origin and are also eco−friendly. These biological materials are frequently less hazardous than toxic chemicals since they are organic and biodegradable [226].

In the current study, ZnO nanoparticles were synthesized from *M. longifolia* var. *asiatica* and *Z. arabicum* aqueous extract. The change of colour indicated the completion of the synthesis process. For *Z. arabicum* colour of the solution changed from colorless to light yellow after 2 hours of incubation. The synthesis of ZnO nanoparticles from *F. cretica* aqueous extracts showed that the solution containing zinc acetate was colourless, but the extract of *F. cretica* was green before mixing. When salt and extract were combined at 90 °C for three hours, a noticeable colour change to light green indicated that the ZnO NPs had been synthesized [227]. The synthesis of nanoparticles from *M. longifolia* var. *asiatica* was also marked by a change in colour from green to transparent white. These findings are in accordance with the previous reports, where ZnO nanoparticles were prepared from M. spicata by using a 0.2M salt solution. The results indicated that the colour of the solution changed to pure white after overnight incubation [228].

Furthermore, the synthesized nanoparticles were investigated for their optical properties by UV−Vis spectrophotometer. The results indicated that *Z. arabicum* showed a characteristic absorbance peak at 295 nm whereas *M. longifolia* var. *asiatica* showed a characteristic peak at 375 nm. These results suggested that both the nanoparticles are free of ionized oxygen because their absorption peaks are not above 500 nm. These results are in accordance with the previous reports [227, 229]. The change of colour was due to the surface plasmon resonance (SPR)

effect, which also validated the stabilization and production of nanoparticles. Because of their significant absorption in the visible spectrum, metallic nanoparticles show surface plasmon resonance (SPR), which is demonstrated by their electromagnetic wave spectra. Visible light caused conductive electrons in nanoparticles to begin oscillating collectively, exhibiting the SPR phenomenon.

SEM analysis was used to determine the size and morphological characteristics of the prepared ZnO nanoparticles. The results revealed the size of ZnO NPs synthesized from *Z. arabicum* to be 25±4nm with a spherical shape. These results correlate with the previous findings. In a particular study, the synthesis of ZnO nanoparticles from *F. cretica* revealed that fine, transparent ZnO NPs were formed. These particles had a size ranging from 65−80 nm and they were spherical [230]. In another study, thyme leaf extract was used to prepare ZnO nanoparticles. SEM analysis indicated that the size of nanoparticles was in the range of 39.4–51.86 nm [231]. The finding of another research showed the size of ZnO NPs to be 10−110 nm which were synthesized from a plant extract of another Fagonia species [227]. Our results are in accordance with the previous reports which suggest that size was measured uniformly without any ambiguity. In the current research, the size of ZnO NPs synthesized from *M. longifolia* var. *asiatica* was also determined using SEM. The results suggest ZnO NPs have a size range of 35±6nm with a hexagonal shape. These findings are in accordance with the previous reports [232].

In another comparative study, the synthesis of ZnO NPs was carried out from Neem and mint extract and the results showed that the size of nanoparticles was 25.5 and 26.1 respectively. These results also suggest that the size of ZnO NPs synthesized from *Z. arabicum* was small as compared to *M. longifolia* var. *asiatica* which means that the former nanoparticles have more ability to penetrate deep in the tissues and are efficient nanocarriers as compared to the later one. This may be attributed to the fact that particles showed greater surface area to volume ratio when their sizes decreased. In comparison to a larger molecule, this would suggest that more of the medication is located closer to the particle's surface which would result in fast drug release [233].

FTIR analysis was carried out to determine the presence of various functional groups and the interaction of synthesized nanoparticles with the capping agent. The FTIR spectra showed that major bands were in the range of 2970-1067 cm^{-1} and the minor bands in the range of 2160− 594 cm^{-1} for *Z. arabicum*. The major bands between 2970−2832 cm^{-1}, 2370−2318 cm^{-1} and 1379−1067cm^{-1} showed C−H, O−H and C−O stretch for aldehyde, alcohol and polyol groups respectively. In a previous study, the synthesis of ZnO nanoparticles was carried out by using *F. cretica* extract showing the FTIR spectra in the range of 3500−50 cm^{-1} [227].

These oxygenated compounds along with the aldehydic groups present in the alcoholic and phenolic compounds play a major role in the synthesis of ZnO nanoparticles by acting as stabilizing agents. The two peaks at 2915.842 cm^{-1} and 2929.34 cm^{-1} indicate C−H stretching modes of vibrations in alkanes. In a particular study, synthesis of gold nanoparticles from Fagonia extract, FTIR peaks were observed between 1000 cm^{-1} and 1200 cm^{-1} which indicate that C−N, C−X and C−O bonds exist for amines, fluorides and alcohols respectively [234]. In another study, the synthesis of nanoparticles from F. indica extract revealed an FTIR signal at 1524 cm^{-1}, corresponding to a compound's nitro group and a peak at 1228 cm^{-1}, corresponding to the acyl group [235]. FTIR spectroscopy was also carried out for ZnO NPs synthesized from *M. longifolia* var. *asiatica*. The major bands were observed in the range of 3649−1383 cm^{-1}. The characteristic peak was observed at 3649 which indicates the presence of N−H group of proteins. Another major band was in the range of 2989 cm^{-1} which corresponds to the C=H functional group. Another study revealed that FTIR spectra of gold and silver nanoparticles synthesized from mint showed a characteristic peak at 2955 cm^{-1} which showed the existence of the C−H group in monoterpenes such as limonene. These were responsible for the reduction of gold and silver nanoparticles. In another particular report, FTIR spectra in the range of 2900−2800 cm^{-1} also validate our results and indicate the presence of the C−H group [236].

In a particular study, synthesis of ZnO NPs was carried out from the aqueous extract of Mentha piperita. The FTIR analysis showed that there was a weak peak at 2974 cm^{-1} which could be due to the C−H stretching vibration. Another

major peak detected at 2360 is indicative of the C≡C bonds. The minor bands were observed at 1558, 1570, 1370, 1261 and 852 cm^{-1}. According to published reports, the bands located at 1591, 881, and 1382 cm^{-1} are ascribed to the functional groups of aromatic rings found in organic molecules. According to the literature, the bands at 3440 and 2890 $cm^{-1}$are caused by primary and secondary amine stretching vibrations, O–H stretching of alcohols and C–H stretching of alkanes [237].

The chemical and elemental composition of the synthesized ZnO NPs of both plants were ascertained by using energy−dispersive X−ray spectroscopy coupled with a scanning electron microscope. The EDX spectrum suggested that the Zn is the primary component along with oxygen in both samples without the presence of any contaminants. These results are in accordance with the previous reports in which the EDX spectrum of ZnO nanoparticles synthesized from *M. longifolia* L. yielded 78.5% zinc and 21.5% oxygen [232]. In another study, it was reported that EDX analysis of ZnO nanocomposite revealed that zinc and oxygen elements were present with zinc in the major proportion i.e. 79% [229] [31]. XRD was performed for the ZnO NPs of both plants to determine the crystalline alignment phase composition and phase identification.

The result showed the diffraction peaks of ZnO NPs at 31.34°, 34.50°, 36.32°, 47.60°, 56.68°, 62.94° matching with lattice parameters of (100), (002), (101), (012), (110), (013), which indicated the crystalline nature of the nanoparticles. In a particular study, it was reported that ZnO nanoparticles synthesized from Mentha piperita showed Braggs peaks and corresponded to 28.5°, 32.3°, 39.7°, 43.6°, 46.4°, 50.2° and 55.3° which corresponded to (211), (202), (110), (114), (412), (204), and (112) which indicate that sample was crystalline [195]. These findings are in accordance with already published reports in which ZnO displayed crystalline structure at (101) orientation [238]. In another report, MnO NPs of *F. cretica* showed a crystalline nature and the XRD patterns showed distinct peaks at 2θ = 28.78°, 37.66°, 42.14°, 49.90° and 56.44 (JSPDF 44−0141) [239]. These findings are in robust accordance with the previous available data [184].

5.2 Cytotoxic Analysis of ZnO Nanoparticles

Despite tremendous advancements in science and technology in medicine, cancer still has few effective therapeutic options. The precise mechanisms underlying cancer metastasis and recurrence remain unclear, although they significantly increase disability and mortality [240]. According to the reports of the Global Cancer Observatory (GCO) 30 million people would lose their lives worldwide by 2030 due to cancer. Apart from its high death rate, cancer imposes a significant financial strain on both society and the families of cancer patients. Therefore, it is imperative to work towards cancer prevention and treatment [241]. Imaging methods, laboratory tests, and morphological analysis of tissues and cells are among the modern methods for diagnosing cancer; the latter is usually thought to be quite reliable in the majority of cases. Many issues with current chemotherapy include low solubility, short half−life, cytotoxicity, lack of selectivity and stem−like cell proliferation.

Different therapies such as photodynamic therapy (PDT), photothermal therapy (PTT), targeted therapy, molecular therapy, chemodynamic therapy (CDT) and nanomaterial−based chemotherapy are currently used in cancer treatment to address these drawbacks. Furthermore, a significant amount of research has been done recently on a range of cancer treatment methods including molecular therapy, immunotherapy, apoptotic regulations and anti−angiogenesis therapy. The advancement of nanotechnology resulted in the lessened side effects of chemotherapy when using nanomedicines for cancer treatment. Numerous studies have been conducted in this area [242]. In targeted therapy, the specificity of chemical drug complexes can be improved by certain nanomaterials with a high surface−to−volume ratio, reducing their toxicity to normal cells and enhancing their capacity to combine with biomolecules or residues. With targeted delivery, specific cancer cells are intended to be precisely targeted; this can be done by active or passive targeting. Active targeting is carried out through conjugation with aptamers, peptides, antibodies, and small molecules. Enhanced permeability and retention EPR effect is

used in passive targeting. Targeted delivery helps reduce toxicity in normal cells, protect drugs from deterioration and increase the solubility of drugs [243].

The cytotoxic potential of ZnONPs synthesized from *Z. arabicum* and *M. longifolia* var. *asiatica* was assessed against the MCF−7 breast cancer cell line. Different concentrations of nanoparticles and plant extract showed potent cytotoxicity. The lowest cell viability of treated cells was observed at 100 μM of ZnONPs and plant extract of *Z. arabicum* was 32.8%, and 60.3% respectively. In the treatment with the extract and ZnONPs of *Mentha longifolia* var. *asiatica*, the cell viability was found to be 69.4 % and 43.2 % respectively. ZnONPs of studied plant species were found to be more effective in lowering the viability of breast cancer cell lines as compared to the respective plant extracts. The IC50 value of ZnONPs of both plant species was found to be less as compared to that of their respective extracts. In a previous study, the effect of solid nanoparticles from two mint varieties *M. longifolia* and M. pulegium were studied on human melanoma A−375 and MCF−7 breast cancer cell lines. Nanoparticles in different concentrations i.e. 150, 300, 600, and 1200 μg/mL were studied on MCF−7 cell lines. The results showed that M. pulegium nanoparticles were more potent and showed less cell viability as compared to *M. longifolia* nanoparticles [244].

A comparative study revealed that MDA−MB231 cell lines were subjected to treatments with iron oxide nanoparticles at 0, 10, 50, 100, 250, and 500 μg/mL, all of which have shown notable cytotoxicity. After the 24−hour incubation period, there was a rapid decline in cancer cells with the increase in the concentration of nanoparticles [245]. Another study reported the effect of gold and silver nanoparticles on HePG2 cell lines. It was observed that increasing the concentration of both nanoparticles i.e. 0.1−2mg/mL, decreased the viability of cells. After 24h incubation it was found that both nano−formulations showed significant anticancer activity but gold nanoparticles were more effective comparatively as compared to silver nanoparticles. Two possible pathways have been postulated to explain biological nanoparticles' anticancer effect. First, the apoptotic pathway causes oxidative stress and DNA fragmentation in the malignant cell and is dependent on elevated ROS levels. Second, DNA and proteins can interfere, which affects how

cell chemistry works. Thirdly, mitochondrial dysfunction and cell permeability are altered when biological NPs interact with cell membranes [246].

In a particular study, the cytotoxic effect of methanolic extract of *F. arabica* was evaluated against breast, oral and lung cancer cell lines. The extract showed promising results against MCF−7 cancer cell lines followed by oral and lung cancer cell lines. The plant extract also showed considerable cytotoxicity. The MTT assay findings displayed abnormal morphological features, including nuclear condensation, apoptotic cells, turgidity, and membrane blabbing. Based on the aforementioned findings, we can infer that *F. arabica* may be cytotoxic due to mechanisms such as apoptosis and cell necrosis [131].

In another study, phytochemicals of F. indica were screened and their anticancer potential was determined by MTT assay on HepG2 cell lines. The results showed that 50% cytotoxic concentration (CC50) of (FIWM) was recorded as 128.3±2.43μg/ml. The maximum cytotoxicity was found after 30h of incubation [247]. In another study, the effect of AgNPs synthesized from F. indica was studied on MCF-7 cell lines, results showed that there was per cent dependent growth inhibition as compared to untreated cells. Different concentrations of nanoparticles i.e. 5, 10, 20, 25, 50, 100 and 200 μg/mL were used. The IC50 for AgNPs was found to be 12.35 μg/mL ascompared to 25.09 μg/mL of the untreated cells [248].

5.3 Gene Expression Analysis of Rab22A, Bax and Caspases

Breast cancer (BC) is the most common type of cancer and the second largest cause of cancer−related deaths among women worldwide. According to the report of Cancer Statistics 2020, there are over 42,000 predicted fatalities and 276,480 new cases of cancer which are expected [249]. Even though early diagnosis and treatment have improved, the death rate from breast cancer is still high in wealthy nations. To improve breast cancer treatment, diagnosis, prognosis, and further

research on the disease's pathophysiology is still required. Tumour cells that have entered the tissue are often what cause a solid tumour to begin and die. In order to investigate a possible cause of tumour spread, tumour cell migration has been extensively explored. There are no biomarkers to predict the spread of breast cancer to other organs. Investigating important variables and processes that mediate the migration and spread of breast cancer helps to direct early detection and treatment, which lowers the death rate and improves prognosis [250].

In order to guarantee that cargo is delivered to the right location, Rab22A, a member of the RAS oncogene family, regulates membrane characteristics as well as vesicle budding, delamination, motility, and fusion. During the initial stages of endosome formation, Rab22A is mentioned and it controls vesicle transit. Rab22A functions as a crucial coordinator of intracellular transport mechanisms and is essential to cellular trafficking. The transport of molecules between different cellular compartments is crucially regulated by this little GTPase protein. To keep the cell functioning and organized properly, it must play a complex role in cellular trafficking pathways. Rab22A's complex involvement in cellular trafficking emphasizes how crucial it is to preserving the general well−being and capacity of cells. It emphasizes how crucial it is to comprehend its mechanisms in order to further our understanding of cellular biology and may create targeted therapeutics for related ailments, as its ability to regulate the movement of vesicles and their payload is essential for a variety of cellular functions [251].

In the current study, the level of expression of the Rab22A gene in breast cancer was studied by the ZnO nanoparticles synthesized from two therapeutic plants *M. longifolia* var. *asiatica* and *Z. arabicum*. The study was conducted in vitro in MCF−7 cancer cell lines. The results showed that the expression of the Rab22A gene was decreased more significantly in plant extract and ZnO particles of *Z. arabicum* as compared to *M. longifolia* var. *asiatica* extract and nanoparticles. The experiment was run with the IC50 of plant extracts of both plants and their nanoparticles, it was observed that expression was significantly decreased with the plant extract and ZnO nanoparticles of *Z. arabicum*. These findings correlate with the previous research in which the relationship between Rab22A and

clinical data was examined in over 700 cases of breast cancer and it was found that extracellular vesicles coated with Rab22A promoted the infiltration and migration of breast cancer in hypoxic environments. As a result, Rab22A may be a promising target for therapeutic intervention in breast cancer [20]. In another research, upregulation of the Rab22A gene results in over production of melanoma cell growth suggesting its possible role as an oncogene [113]. In another study, it was found that the expression of Rab22A was also upregulated in HCC cell lines and samples [252]. Hypoxia promotes MV generation and HIF−dependent growth in metastatic breast cancer. Hypoxia in metastatic breast cancer promotes MV synthesis and HIF−dependent Rab22A gene expression [253].

5.4 Protein Expression Analysis of Rab22A, Bax and Caspases

The stimulatory effects of ZnO nanoparticles and plant extracts of *Z. arabicum* and *M. longifolia* var. *asiatica* were also studied on the expression of bax gene. Bax forms a complex with BCL2 family members and functions as a proapoptotic protein. In the current study, ZnO nanoparticles of both plants and their extracts showed upregulation of the bax gene. However, the extract of *Z. arabicum* and its nanoparticles showed more promising results as compared to *M. longifolia* var. *asiatica* extract and nanoparticles. These results correlate with previous research, in which iron oxide nanoparticles showed an increased expression ratio of BAX/BCL in MCF−7 cancer cell lines [254].

The expression of caspase−3, caspase−8 and caspase−9 genes were evaluated to determine the apoptotic potential of synthesized ZnO nanoparticles and the plant extracts. It was observed that ZnO nanoparticles synthesized from *Z. arabicum* and its plant extract showed higher caspase gene expression as compared to the extract and ZnO nanoparticles of *M. longifolia* var. *asiatica*. It suggests the apoptotic role of *Z. arabicum* ZnO nanoparticles. Caspases play a pivotal role in apoptosis execution by coordinating cellular devastation via a proteolytic process.

The cysteine proteases belong to a family of at least twelve proteases which are mostly expressed as inactive enzymes. Caspases−3 serves as a marker to verify the process of apoptosis because they are involved in the last molecular stages.

In a particular study, it was documented that in comparison to control cells, ZnO−NP treatment significantly increases the protein levels of BAX, caspase−3, and caspase−9 in bone cancer cells. Control cells showed a lower apoptotic rate. It was reported that cell viability increases in dose dose−dependent manner. The rate of apoptosis was higher in the cancer cell lines which were treated with 50 μg/mL of ZnO nanoparticles as compared to those cell lines which were given 30 μg/mL of sample. This treatment significantly downregulates the anti−apoptotic proteins such as BCL−2 and ultimately increases the expression of mRNA and various proteins of cell cycle such as p53 and bax in epidermal cancer cells. In another study, ZnO nanoparticles were given orally to rats, it was observed that the expression of p53 proteins was upregulated in renal tissues. Various mechanisms are involved in the induction of apoptosis process by reactive oxygen species such as translocation and cleavage of BCL−2 proteins. Antioxidants can prevent the activation of caspase proteins, indicating a ROS−dependent mechanism which is responsible for apoptosis upon treatment with ZnO nanoparticles [255].

Furthermore, ELISA was carried out to determine the protein levels of all studied genes. It was observed that the protein expression was also upregulated likewise the gene expression in the MCF−7 treated cells with plant extract and ZnO nanoparticles of *Z. arabicum*. The expression of Rab22A protein was downregulated. In a particular study, a GSEA analysis was performed to check the role of this gene and its protein in multiple pathways. It was found that Rab22A is not only involved in endocytic recycling but it also regulates various stages of the cell cycle such as E2F targets, G−phase−M−phase checkpoint along with various biological pathways such as mTOR pathway and myc targeted pathways. In a particular study, it was reported that overexpression of mTorc1 signalling facilitates the invasion of Rab1A and the spread of colorectal cancer. Moreover, it has been demonstrated that Rab22A stimulates extracellular signalling to support BC stem cell growth [256]. ZnO NPs can trigger apoptosis in MCF−7, as per the

results of cell cycle analysis ascertained using flow cytometry analysis. Based on the findings, apoptosis was induced at the sub−G1 phase, which was responsible for the reduction of cell growth with IC50 and IC75 of ZnO NPs at 24 hours. ZnO NPs were found to significantly induce apoptosis in MCF−7 cells. In another study, around 26% of treated cells and 2.8% of untreated control cells entered the sub−G1 phase of the cell cycle, respectively. Apoptosis was enhanced to a greater extent by the increase in nanoparticle concentration [257].

ZnO NPs have been shown to have a positive effect on inducing apoptosis in a variety of cancer types, including ovarian, hepatocarcinoma, breast, and bronchial epithelial cells. Exposure to ZnO NPs has been shown to release cytochrome c from mitochondria, generate excessive ROS and block the activity of all antioxidant enzymes. These changes ultimately result in mitochondrial malfunction. These malfunctions may contribute to the imbalance in protein synthesis, especially about apoptotic−related proteins, which may ultimately activate the intrinsic apoptotic pathway also referred to as the mitochondria−mediated apoptotic pathway [258] [259].

However, ZnO−NP treatment in ovarian and cervical tumour cells caused the production of p53, bax, and cytochrome−c when the dose of nanoparticles was increased. In comparison to control cells, HeLa cells treated with ZnO−NPs showed enhanced production of caspase−9, caspase−3, cleaved caspase−9, and cleaved caspase−3. ZnO−NPs demonstrated notable distinctions from control cell models in the induction of comparable alterations in the transcripts of various proteins, including p53, BAX, BCL−2 and CAS−3. The triggering of apoptosis was caused by the formation of ROS, Ca2+ release caused by oxidative stress and loss of membrane potential of mitochondria. ZnO−NP exposure causes tumour cells to become more vulnerable. Moreover, ZnO−NPs have been shown to cause time−dose−dependent damage and genotoxicity from elevated ROS in mouse models. Furthermore, it was also observed that when the male mice were injected with ZnO nanoparticles there was an aberrant release of sperms and various structural changes in seminiferous epithelia were also observed [255]. In another study, MDA−MB231 and MCF−7 cell lines were treated with silver nanoparticles.

After 48h of incubation period, the IC50 values were too low i.e. 6.4 and 6.5 ppm. The western blot analysis showed the induction of apoptosis by ROS generation and upregulation of caspase proteins [260].

5.5 Phytochemical Analysis of *Mentha longifolia* var. *asiatica* and Zygophyllum arabicum

The genus Fagonia includes herbs, shrubs, and shrublets that can grow up to 75 cm in height and 100 cm in width on average. The aqueous extracts of plants in the genus Fagonia have been widely used as medications to treat a variety of ailments, including high fever, diabetes, asthma, stomachache, tooth pain, and renal issues. This genus is rich in flavonoids, saponins, and triterpenes, all of which are beneficial. Numerous researchers have considered the herbal chemistry and biological function of Fagonia species as potential candidates. Their extracts' in vivo pharmacological examination revealed other noteworthy characteristics like cytotoxic and anti−cancer potential [261].

High Performance Liquid Chromatography was used to determine the phytochemical constituents of *Z. arabicum* and *M. longifolia* var. *asiatica*. With High Performance Liquid Chromatography (HPLC), a stationary phase made up of micro spherical particles with diameters of two to five micrometres or materials porous monolith is passed through a column containing a mobile phase made up of a mixture of solvents, either buffered or not of variable force. The methanolic extract was prepared and subjected to HPLC in which 12 standards were used which were chlorogenic acid, gallic acid, 3−hydroxybutyric acid, caffeic acid, vanillic acid, kaempferol, ferulic acid, sinapic acid, salicylic acid, benzoic acid, quercetin, rutin and coumarin. The results showed that the methanolic extract of *Z. arabicum* has 8 phytochemicals out of these 12 in which the highest concentration was of 3−hydroxybutyric acid i.e. and the lowest concentration was of gallic acid. Previously, it has been reported that various saponins, alkaloids, flavonoids and terpenoids were found in the methanolic extract of *F. indica* [262]. In a particular

study, secondary metabolites found in the unhydrolyzed and acid−hydrolyzed extract of *F. cretica* were studied. The results indicated that in the unhydrolyzed extract two significant compounds cauloside A and kaempferol were detected whereas after acid hydrolysis ursolic acid and quinovic acid, and the flavonoid, kaempferol were detected [263]. According to the literature, numerous chemical components including tannins, saponins, flavonoids, terpenes, alkaloids, proteins, hederagenin, ursolic acid, pinitol, etc., have been reported in the genus Fagonia [264]. In another study, it was reported that ethanolic extract of *F. cretica* was screened by HPLC which indicated the presence of various phenolic compounds i.e. ferulic acid and sinapic acid which correlates with our findings [265]. The aqueous extracts of Fagonia species have been employed in various anticancer studies and the results showed that they exhibit antiproliferative and cytotoxic effects. These findings suggest that the phytochemicals found in Fagonia species have strong anticancer potential and they can be used to synthesize different drugs such as camptothecin [266]. In another study, methanolic and aqueous extract of F. indica was subjected to HPLC. It was revealed from the results that methanolic extract contains a greater amount of flavonoids and phenolic compounds as compared to aqueous extract. These phytochemicals were then screened for molecular docking studies to check the binding with CYP3A4 and UGT2B enzymes. Quercetin showed the best binding pose with the CYP34A which means that it could be used as a novel drug target for diabetic patients [267].

The Lamiaceae family, which has 25–30 species total, includes the genus Mentha, which is home to mint. The members of this genus are highly valued in the business and economic spheres and have long been recognized for their therapeutic and aromatherapeutic qualities. Many regions of the world use a variety of Mentha species in traditional medicine and cuisine. Because they have a taste and aroma that is "fresh−like," essential oils from the Mentha species are frequently used to flavour beverages. Mentha species have been the subject of chemical investigations that have produced a variety of significant phytocompounds from many classes, including proteins, free sugars, hydrocarbons, fatty acids, alkaloids, lignans, organic acids, and flavonoids. Additionally, phenolics, flavonoids, and essential oils

are the primary constituents of mint [268].

Methanolic extract of *M. longifolia* var. *asiatica* was prepared to screen the active secondary metabolites by HPLC. The results indicated the presence of 8 phytochemicals which were chlorogenic acid, gallic acid, kaempferol, sinapic acid, salicylic acid, coumarin, quercetin and rutin. The concentration of chlorogenic acid was the highest as compared to the lowest concentration of rutin. The genus Mentha has a high and naturally occurring phenolic and flavonoid content. Its anti−inflammatory and antioxidant properties may be attributed to a variety of chemically active components. In recent research, Mentha arvensis was analyzed for its anticancer potential and the phytochemical screening was performed by HPLC which indicated the presence of luteolin, ursolic acid, rosmarinic acid, and oleanolic acid. These compounds were then assessed for their antibacterial and antidiabetic potential and they showed promising results by various insilico models [269]. In another study, three extracts i.e. hydroethanolic, aqueous and acetonic of *Mentha longifolia* L. were prepared to study their chemical profile by the HPLC−DAD system. The results suggest that gallic acid is the predominant compound in the aqueous extract whereas kaempferol and chlorobenzoic acid were that major compounds in the hydroethanolic and acetonic extract respectively. These findings correlate with our results [270]. In a particular study, five Mentha species were screened to identify various metabolites. The results showed that all five species were pharmacologically active and they contain variety of compounds including flavonoids, organic acids, phenolic acids etc. The major compounds in all the species were chlorogenic acid, rosmarinic acid and sagerenic acid. These compounds were then analyzed on different cancer cell lines to determine their cytotoxic potential and anti−helicobacter effects [271]. In a similar study, the methanolic profiles of *M. piperita* and *M. longifolia* were studied to analyze different phenolic acids by HPLC. The results showed the presence of six phenolic acids in *M. piperita* and nine in *M. longifolia*. In both extracts, rosmarinic acid was the significant compound followed by chlorogenic acid, caffeic acid and o−coumaric acid. These results are also in accordance with our findings [272]. In another study, three Mentha species were screened for determination of

their phytochemical constituents. These species were M. spicata, M. Pulegium and *M. longifolia* L. The results were analyzed quantitatively which showed that ethyl acetate extract of *M. longifolia* L contains phenolic compounds whereas M. Pulegium contains tannins in its EtAc extract. The chloroform extract confirms the presence of flavonoids in all three species respectively [273]. Based upon all these findings, it was concluded that both selected plants have pharmacologically active ingredients which can be validated further in order to design a drug against breast cancer.

5.6 Computational Analysis

Medicinal plants are considered a valuable natural resource for the discovery and development of novel medications and treatments. An estimated $3/4^{th}$ of world's population utilizes plants as a source of traditional medicines because of their ethnopharmacological importance. This practice is mostly employed in underdeveloped nations. Furthermore, a broad range of physiologically active phytochemicals (bioactive compounds), such as alkaloids, terpenoids, polyphenolics, furyl are isolated from plants which are used in the synthesis of various medicines. Plant bioactive compounds have several biological and pharmacological roles, including those of antioxidant, antibacterial, anti−inflammatory and anti−carcinogenic which are primarily responsible for their therapeutic effects [274]. The process of discovering a new medication or identifying a novel drug is expensive, complex, highly dangerous, and time−consuming. It involves many different scientific fields and a wide range of contemporary equipment and procedures. The average time for a new drug to be approved for the market is estimated to be between 10 and 15 years. The whole process of development of new drugs costs around 1.0 billion USD. This cost and duration have a major impact on the lead compound synthesis and testing [275]. To create novel medications that will address both present and future global health issues, a blend of cutting−edge technologies, such as artificial intelligence, and creative drug design will be required. New technologies include

inventive computational and analytical techniques that can be applied to separate compounds from extracts and the requirement to find compounds that have the intended medicinal effect. New chemicals produced from plant extracts can be designed, tested, and subjected to biological testing due to the development of computational tools. Natural products are a great source of chemicals for the design of new, pharmacologically significant molecular products, thus it is not surprising that they will facilitate better drug discovery [276]. In the current research work, Rab22A was selected as a target protein. The 3D structure of this protein was retrieved from the protein data bank. The PDB id of the selected protein is IZ0J and its structure was downloaded in the PDB format. The Protein Data Bank (PDB) serves as a primary repository for retrieving 3D and atomic structures of macromolecular proteins, which are identified through various experiments. PDB offers a vast community of researchers from many scientific fields that have free and easy access to biomolecular structures. It also provides a platform for structural biologists to create a permanent resource that has been carefully chosen to preserve and share their work [277].

After downloading the pdb structure, the physiochemical properties of the selected protein were determined using the protoparam tool. The predicted aliphatic index of Rab22A protein was 51.1%. The amino acid is said to be in the isoelectric point when its positive and negative charge levels remain constant and its net charge is zero. Isoelectric points (pI) of Rab22A were 8.32 suggesting a moderately basic nature of the protein. Aspartate (D), glutamate (E), arginine (R), lysine (K), and aspartate (R) are the total numbers of positively and negatively charged residues, respectively. With a particular amino acid sequence, GRAVY is utilized to computationally analyze several physicochemical properties. Low range GRAVY value of -0.272 indicates its high affinity for water that improves the solubility of a protein [278].

A comparable web server that uses reference databases to annotate sequence domains is called InterPro. To eliminate duplication and retain the pertinent data from each resource in the results, InterPro merged all of the resources into a single entry. Gene Ontology terms, a unique name and accession number, and entry

kinds comprising family, domain, repetition, site, and homologous superfamily are among the many details the web server provides based on its annotation result. Interpro was used to analyze the functional domains of the Rab22A protein. The results indicated that this protein belongs to the superfamily P−loopNTPase [279]. Among the major families found in the proteomes of most cellular organisms, the P−loop NTPase domains appear to be monophyletic. Almost all cellular metabolic and mechanical activities involve these domains such as membrane transport, intracellular trafficking, transcription, replication, repair, as well as the activation of different metabolites [280].

The refinement of protein structure was carried out by using pymol software. PyMOL is a great option for creating sophisticated pipelines for computational protein analysis. The two−pronged molecular graphics viewer and programmatically accessible interface made it particularly suitable for developing Python−based software tools for intricate investigations of biological macromolecules. To study the dynamic behaviors of biomolecules with visual aids it is an ideal source. Numerous PD algorithms have indeed been put into practice in various molecular graphics contexts. Although maintaining and visualizing MD trajectories can be difficult due to their length and size. To overcome this shortcoming, pymol was developed to analyze complex information and render large data files of MD simulation [281].

Molecular docking" allows one to computationally determine the architecture of compounds made up of two or more different molecules. Docking studies aim to predict the intended three−dimensional structures. Only appropriate incentive structures are produced by docking alone. One to identify which structures are more likely to exist in nature, these options are ordered using scoring systems. The affinity of small molecules can be analyzed by docking in the same manner as medically significant therapeutic compound activities can be analyzed. This provides information regarding the affinity and binding nature of compounds with the targeted protein [282]. Protein−ligand docking is a popular method for ligand binding mode and affinity prediction. For computer−aided drug discovery (CADD), protein−ligand docking is a potent technique. Typically, blind docking

is carried out throughout the whole surface of the protein. On the other hand, docking on potential binding sites of the specified protein typically increases blind docking's sampling efficiency and lowers its computing cost. Modern docking software Autodock Vina is used by CB−Dock to carry out docking operations. It predicts binding areas of a given protein. Additionally, it computes the diameters and centres using a cavity identification technique based on curvature [283]. The preliminary step of the CB−dock was to select the ligands. Based on the HPLC data, ligands were selected for both plants and their 2D structures were downloaded from the PubChem database in the SDF format. The preliminary step is energy minimization of the ligands which was done by chempro ultra 12 software because without minimizing energy the results of molecular docking were not accurate. After energy minimization, docking was performed with all selected ligands via CB−dock. Based on vina score, grid map and cavity size, two ligands were selected from both studied plants. Chlorogenic acid was selected from *Z. arabicum* and 3−Hydroxybutyric acid was selected from *M. longifolia* var. *asiatica*. These ligands were selected for molecular dynamic simulation studies along with the reference drug palbociclib. The docking poses for both ligands and the drug were then studied to find the best interaction between the protein and ligand via Ligplot+.

In the current research, molecular dynamics simulation was also carried out with the selected ligands (chlorogenic acid and 3−Hydroxybutyric acid) and reference drug. The simulation was run from 0−100 ns and chlorogenic acid showed low RMSD values compared to 3−Hydroxybutyric acid and palbociclib. The RMSD (Root Mean Square Deviation) metric was utilized to quantify the structural variation between the anchored ligand and the receptor. This metric reflected the spatial difference between the ligand−protein complex structures generated in the redocking and the co−crystallized structure. An excellent match between the chlorogenic acid and the protein's active site was indicated by RMSD values, which varied from 1.4 to 2.0 $\mathring{A}$ [284]. Moreover, the mean structural fluctuations of the protein represented in terms of variations of the mean atomic quadratic deviations are targeted as structural alterations. These can be observed during

simulation trajectories. The results showed mild fluctuations for chlorogenic acid and reference drug as compared to 3−hydroxybutyric acid. These results correlate with the previous findings [285]. Hydrogen bonding is a sign of stability. In the current study, H−bond analysis was also carried out and the results showed that chlorogenic acid showed maximum hydrogen bonds in comparison to the other two ligands. It is evident from the H−bond analysis that the protein's active sites are more firmly and efficiently bound by chlorogenic acid than by 3−Hydroxybutyric acid and palbociclib. The data suggests that chlorogenic acid was a better inhibitor than the other two ligands. The radius of gyration (Rg) was used to quantify how the protein structure folds and unfolds when it binds to ligands. The protein−ligand combination if more unfolded and less compact, it shows a higher radius of gyration. The value remained low for chlorogenic acid which shows that this ligand has higher stability. SASA was also done from 0−100 ns for MD simulation. The result indicated that chlorogenic acid has more SASA values which means that this ligand exposes more surface area for different solvent molecules which makes it an excellent drug candidate because surface area has a major impact on a drug's rate of absorption and metabolism.

Furthermore, the selected ligands (chlorogenic acid, 3−hydroxybutyric acid and palbociclib) were screened for their ADMET properties. In the preliminary stages of drug development, ADMET qualities are important because good drug candidates need to have both suitable ADMET properties at a therapeutic dose and enough effectiveness against the intended treatment target. It is noteworthy that all of the chosen antibiotics and standards have a high likelihood of being absorbed in the human gut, with HIA + values of 83%, and 80%, for palbociclib and 3−hydroxybutyric acid respectively, except chlorogenic acid with HIA− (36%). The VDS and Fu values of the selected drug were less than the ligands which means that these ligands are more effective than standard drugs. BBB is another important distribution property because it predicts whether the drug can reach the central nervous system or not. BBB value was greater for chlorogenic acid as compared to the drug and 3−hydroxybutyric acid. Cytochrome P450 inhibitors,

which are microsomal enzymes, were also employed to forecast the metabolic activities of the chosen therapeutic options. As prospective therapeutic pharmaceuticals, all of the chosen medications are non−inhibitors of cytochrome P450 except palbociclib which is CYP3A4 inhibitor which improves their metabolism. Even though it is anticipated that all of the chosen antibiotics and standards will not biodegrade, they do not cause cancer. The reference drug and the selected ligands are non−AMES−toxic when taking into account their mutagenesis potential and AMES toxicity. Furthermore, type III oral acute toxicity was present in the standard and selected compounds, meaning that they are mildly hazardous even though they do not cause corrosion or ocular irritation. A drug's capacity to suppress hERG carries significant risks since it may cause the myocardium's potassium ion channel to become blocked, disrupting the heart's electrical activity and possibly leading to an early death. It's interesting to note that all of the standards and antibiotics chosen are non−inhibitors of hERG except the standard drug which is a hERG II inhibitor.

These results showed that the ADMET properties of chlorogenic acid are more suitable to be employed as a potent drug as compared to 3−hydroxybutyric acid. These results correlate with the previous research in which chlorogenic acid was found to inhibit α-amylase and α-glucosidase enzymes. Thus, it was concluded that chlorogenic is a potent drug target to treat diabetes and related disorders such as hyperlipidemia [286]. In another study, the derivatives of chlorogenic acid were used to treat breast cancer in an in−silico study. The most promising lead for a future chemical change was chlorogenic acid which had a high binding score. This particular molecule could serve as a chemical template for the subsequent creation of novel chlorogenic acid derivatives with enhanced pharmacological action. Three different functional groups that make up chlorogenic acid can be carefully changed. These groups include ester, hydroxyl, and carboxylic acid groups. The specific modification chosen for this instance was the carboxylic acid functional group present in the quinic acid ring of chlorogenic acid [287].

Chapter 6

Conclusion and Future Work

Breast cancer is the major reason of mortality all around the globe. Breast cancer incidence is also high in the Pakistani population among Asian countries. This trend is increasing with each passing year with multiple risk factors involved. The current research aimed to evaluate the therapeutic potential of two medically valuable plants *Z. arabicum* and *M. longifolia* var. *asiatica* against the breast cancer-targeted gene Rab22A. Plants are rich sources of pharmacologically active ingredients which show anticancer effects. The present study aimed to do a comparative analysis to determine the ZnO nanoparticles of both plants and check their cytotoxic and apoptotic potential against the MCF-7 cancer cell line. The current study also aimed to screen the phytochemicals of both selected plants by HPLC. The screened secondary metabolites were analyzed for computer-aided drug design to find their interaction with the Rab22A gene. In addition to this, selected metabolites are used for molecular docking and molecular dynamics simulation. Their ADMET properties were also studied to determine the pharmacokinetic and pharmacodynamics properties of drug candidates.

The observations of the current study shed light on the green synthesis of ZnO nanoparticles from *Z. arabicum* and *M. longifolia* var. *asiatica* which led to the stable synthesis of nanoparticles. The characterization of both nanoparticles was carried out by UV-Vis analysis, SEM, FTIR, EDX and XRD analysis. Based on this analysis, it was found that both nanoparticles are excellent nanocarriers and

can be employed as drug candidates against the Rab22A targeted gene. It was also observed that the plant extract and ZnO nanoparticles of *Z. arabicum* showed significant cytotoxic potential against the MCF-7 cancer cell line as compared to and *M. longifolia* var. *asiatica* extract and nanoparticles.

The efficacy of both nanoparticles was also tested on the gene and protein expression of the Rab22A gene. Amazingly, it was observed that extract and ZnO nanoparticles of *Z. arabicum* showed reduced expression of the Rab22A gene and protein in the MCF-7 cancer cell line as compared to treatment with *M. longifolia* var. *asiatica*. The apoptotic role of these nanoparticles was also evaluated in the present study. It was observed that ZnO nanoparticles and plant extracts of both species showed higher expression of bax, caspase-8 and caspase-9 genes and proteins. The expression was much higher for *Z. arabicum* plant extract and nanoparticles. Thus, this study provides a sound basis that Rab22A gene can be employed as a potential drug target in the treatment of breast cancer.

Furthermore, the methanolic extract of both plants was screened to determine the secondary metabolites of both plants. The methanolic extract of both plants showed presence of 8 phytochemicals for each plant. These screened compounds were then used for molecular docking. Based upon the physiochemical characteristics and other parameters of molecular docking such as cavity size, vina score etc. one lead compound from each plant was selected i.e. chlorogenic acid from *Z. arabicum* and 3-Hydroxybutyric acid from *M. longifolia* var. *asiatica*. These lead compounds were then employed for molecular dynamics simulation studies. The various parameters of simulation such as RMSD, RMSF, hydrogen bond analysis, the radius of gyration and solvent-accessible surface area were determined. It was found that chlorogenic acid was far better than 3-hydroxy butyric acid when they were compared with standard anticancer drugs i.e. palbociclib. The ADMET profiling was also done in a comparative manner which also suggested that chlorogenic acid was a far better choice as an anticancer drug.

These comparative results suggest that both plants have significant medicinal value but secondary metabolites of *Z. arabicum* have more pharmacological significance

and can be used in pharmaceutical industries to prepare anticancer drugs against breast cancer. The selected lead compounds were also compared with standard drug palbociclib and the results suggested that chlorogenic acid was far better than palbociclib. Hence, this compound is a novel drug candidate to be used in the treatment of breast cancer.

6.1 Future Recommendations

Future recommendations of the current study are as follows:

1. In this study, only the effect of ZnO nanoparticles was studied. This can be elaborated and nanoparticles of various metals such as Cd, Au and Fe can be synthesized and studied comparatively.

2. Animal models and clinical trials can be performed to confirm the Rab22A gene as a potential biomarker in the diagnosis and treatment of breast cancer.

3. Other members of the Rab5 superfamily can be explored to find new possible inhibitors of the endocytic pathway.

4. The study of the Rab22A gene and its role as a potential drug target can be explored in a variety of cancers such as liver and lung cancer.

5. The plant extract and metallic nanoparticles of *Z. arabicum* should be studied for other cancer types.

6. Multiple apoptotic markers of intrinsic and extrinsic apoptosis pathways must be studied to confirm the efficacy of *Z. arabicum* extract and nanoparticles as apoptotic agents.

7. The genus Fagonia comprises many novel species, other species can be explored for their anticancer potential.

8. Apart from HPLC other techniques for phytochemicals screening such as GC-MS and LC-MS can be used to confirm the presence of novel metabolites.

9. The role of the Rab22A gene can also be explored in various signalling pathways i.e. PI3K/Akt/mTOR pathway which leads to breast cancer incidence and recurrence.

Bibliography

[1] R.L. Siegel, K.D. Miller, and A. Jemal. Cancer statistics, 2019. *CA: a cancer journal for clinicians*, 69(1):7–34, 2019.

[2] A. Ahmad. Breast cancer statistics: recent trends. *Breast cancer metastasis and drug resistance: challenges and progress*, pages 1–7, 2019.

[3] H. Sung et al. Global cancer statistics 2020: Globocan estimates of incidence and mortality worldwide for 36 cancers in 185 countries. *CA: a cancer journal for clinicians*, 71(3):209–249, 2021.

[4] S.R. Johnston. Acquired tamoxifen resistance in human breast cancer?potential mechanisms and clinical implications. *Anti-cancer drugs*, 8 (10):911–930, 1997.

[5] R.-M. Lu et al. Targeted drug delivery systems mediated by a novel peptide in breast cancer therapy and imaging. *PloS one*, 8(6):e66128, 2013.

[6] G. Kumar et al. Codelivery of phytochemicals with conventional anticancer drugs in form of nanocarriers. *Pharmaceutics*, 15(3):889, 2023.

[7] C.-H. Heldin et al. High interstitial fluid pressure?an obstacle in cancer therapy. *Nature Reviews Cancer*, 4(10):806–813, 2004.

[8] M. Rebucci and C. Michiels. Molecular aspects of cancer cell resistance to chemotherapy. *Biochemical pharmacology*, 85(9):1219–1226, 2013.

[9] P.J. Kaboli et al. Akt-targeted therapy as a promising strategy to overcome drug resistance in breast cancer?a comprehensive review from chemotherapy to immunotherapy. *Pharmacological research*, 156:104806, 2020.

[10] S.A. Narod. Looking for brca1 and brca2 mutations in asian women with breast cancer. *Annals of Translational Medicine*, 11(8), 2023.

[11] M. Ahmad and A.A. Shah. Predictive role of single nucleotide polymorphism (rs11614913) in the development of breast cancer in pakistani population. *Personalized Medicine*, 17(3):213–227, 2020.

[12] V.K. Chaturvedi et al. Cancer nanotechnology: a new revolution for cancer diagnosis and therapy. *Current drug metabolism*, 20(6):416–429, 2019.

[13] T. Yonezawa. Preparation of metal nanoparticles and their application for materials. In *Nanoparticle technology handbook*, pages 829–837. Elsevier, 2018.

[14] H. Barabadi et al. Optimization of myco-synthesized silver nanoparticles by response surface methodology employing box-behnken design. *Inorganic and Nano-Metal Chemistry*, 49(2):33–43, 2019.

[15] J.L. Gray et al. Targeting the small gtpase superfamily through their regulatory proteins. *Angewandte Chemie International Edition*, 59(16):6342–6366, 2020.

[16] R.B. Haga and A.J. Ridley. Rho gtpases: Regulation and roles in cancer cell biology. *Small GTPases*, 7(4):207–221, 2016.

[17] Y. Zhou et al. Rab22a enhances cd147 recycling and is required for lung cancer cell migration and invasion. *Experimental Cell Research*, 357(1):9–16, 2017.

[18] L. Kong et al. Crucial roles of rab22a in endosomal cargo recycling. *Traffic*, 24(9):397–412, 2023.

[19] J.G. Magadan et al. Rab22a regulates the sorting of transferrin to recycling endosomes. *Molecular and cellular biology*, 26(7):2595–2614, 2006.

[20] T. Wang et al. Hypoxia-inducible factors and rab22a mediate formation of microvesicles that stimulate breast cancer invasion and metastasis. *Proceedings of the National Academy of Sciences*, 111(31):E3234–E3242, 2014.

[21] F. Kang et al. O 2-3-aminopropyl diazeniumdiolates suppress the progression of highly metastatic triple-negative breast cancer by inhibition of microvesicle formation via nitric oxide-based epigenetic regulation. *Chemical Science*, 9(34):6893–6898, 2018.

[22] A. Mazurakova et al. Anti-breast cancer effects of phytochemicals: primary, secondary, and tertiary care. *EPMA Journal*, 13(2):315–334, 2022.

[23] N. Nazam et al. Phenolic acids-mediated regulation of molecular targets in ovarian cancer: current understanding and future perspectives. *Pharmaceuticals*, 16(2):274, 2023.

[24] C.L. Poo et al. Effect of traditional chinese medicine on musculoskeletal symptoms in breast cancer: a systematic review and meta-analysis. *Journal of pain and symptom management*, 62(1):159–173, 2021.

[25] S.-Y. Pan et al. Historical perspective of traditional indigenous medical practices: the current renaissance and conservation of herbal resources. *Evidence-based complementary and alternative medicine*, 2014, 2014.

[26] M. Abotaleb et al. Flavonoids in cancer and apoptosis. *Cancers*, 11(1):28, 2018.

[27] A. Kapinova et al. Controlling metastatic cancer: the role of phytochemicals in cell signaling. *Journal of Cancer Research and Clinical Oncology*, 145: 1087–1109, 2019.

[28] A. Nisar et al. Phytochemicals in the treatment of inflammation-associated diseases: the journey from preclinical trials to clinical practice. *Frontiers in Pharmacology*, 14:1177050, 2023.

[29] V.S. Thakur, G. Deb, M.A. Babcook, and S. Gupta. Plant phytochemicals as epigenetic modulators: role in cancer chemoprevention. *The AAPS Journal*, 16:151–163, 2014.

[30] N. Iftikhar et al. Fagonia arabica l.: a review of its phytochemistry, pharmacology and traditional uses. *Combinatorial Chemistry and High Throughput Screening*, 25(7):1187–1199, 2022.

[31] B. Salehi et al. Plants of genus mentha: From farm to food factory. *Plants*, 7(3):70, 2018.

[32] A. Aimila et al. Comparative study on different extraction methods of oil extract from mentha asiatica boriss. and optimization of the extraction process by response surface methodology. *Flavour and Fragrance Journal*, 39 (1):33–44, 2024.

[33] D.L. McKay and J.B. Blumberg. A review of the bioactivity and potential health benefits of chamomile tea (matricaria recutita l.). *Phytotherapy Research*, 20(7):519–530, 2006.

[34] S.R. Abbas and M. Nisar. Herbal significance of horse mint (mentha longifolia) a review. *Journal of Biotechnological Sciences*, 8:138–143, 2020.

[35] X. Bai et al. Chemical constituents and biological activities of essential oil from mentha longifolia: Effects of different extraction methods. *International Journal of Food Properties*, 23(1):1951–1960, 2020.

[36] S. Ying et al. Green synthesis of nanoparticles: Current developments and limitations. *Environmental Technology and Innovation*, 26:102336, 2022.

[37] C. Pandit et al. Biological agents for synthesis of nanoparticles and their applications. *Journal of King Saud University - Science*, 34(3):101869, 2022.

[38] L.M. Coussens and Z. Werb. Inflammation and cancer. *Nature*, 420(6917): 860–867, 2002.

[39] L. Ferrucci et al. Measuring biological aging in humans: A quest. *Aging Cell*, 19(2):e13080, 2020.

[40] S. Gao et al. Chronic diseases spectrum and multimorbidity in elderly inpatients based on a 12-year epidemiological survey in china. *BMC Public Health*, 24(1):509, 2024.

[41] E. Shacter and S.A. Weitzman. Chronic inflammation and cancer. *Oncology (Williston Park, NY)*, 16(2):217–226, 229; discussion 230, 2002.

[42] M. Ezzati et al. Selected major risk factors and global and regional burden of disease. *The Lancet*, 360(9343):1347–1360, 2002.

[43] G. Colditz et al. Harvard report on cancer prevention. volume 1. causes of human cancer. *Cancer Causes and Control*, 7(Suppl 1):1–59, 1996.

[44] S. Gurunathan, M.-H. Kang, M. Qasim, and J.-H. Kim. Nanoparticle-mediated combination therapy: two-in-one approach for cancer. *International Journal of Molecular Sciences*, 19(10):3264, 2018.

[45] C. Stein and G. Colditz. Modifiable risk factors for cancer. *British Journal of Cancer*, 90(2):299–303, 2004.

[46] K. Masood et al. Trends and analysis of cancer incidence for common male and female cancers in the population of punjab province of pakistan during 1984 to 2014. *Asian Pacific Journal of Cancer Prevention*, 16(13):5297–5304, 2015.

[47] N. Azamjah, Y. Soltan-Zadeh, and F. Zayeri. Global trend of breast cancer mortality rate: a 25-year study. *Asian Pacific Journal of Cancer Prevention*, 20(7):2015, 2019.

[48] M. Arnold et al. Current and future burden of breast cancer: Global statistics for 2020 and 2040. *The Breast*, 66:15–23, 2022.

[49] F. Bray et al. Global cancer statistics 2018: Globocan estimates of incidence and mortality worldwide for 36 cancers in 185 countries. *CA: a Cancer Journal for Clinicians*, 68(6):394–424, 2018.

[50] L.A. Brinton, M.E. Sherman, J.D. Carreon, and W.F. Anderson. Recent trends in breast cancer among younger women in the united states. *JNCI: Journal of the National Cancer Institute*, 100(22):1643–1648, 2008.

[51] B.G. Haffty et al. Locoregional relapse and distant metastasis in conservatively managed triple negative early-stage breast cancer. *Journal of Clinical Oncology*, 24(36):5652–5657, 2006.

[52] M. Elbaiomy et al. Clinical impact of breast cancer stem cells in metastatic breast cancer patients. *Journal of Oncology*, 2020, 2020.

[53] J. Ursini-Siegel and P.M. Siegel. The influence of the pre-metastatic niche on breast cancer metastasis. *Cancer Letters*, 380(1):281–288, 2016.

[54] B. Weigelt, F.C. Geyer, and J.S. Reis-Filho. Histological types of breast cancer: how special are they? *Molecular Oncology*, 4(3):192–208, 2010.

[55] G. Cserni, E. Chmielik, B. Cserni, and T. Tot. The new tnm based staging of breast cancer. *Virchows Archiv*, 472:697–703, 2018.

[56] K. Armstrong, A. Eisen, and B. Weber. Assessing the risk of breast cancer. *New England Journal of Medicine*, 342(8):564–571, 2000.

[57] J. Majidpoor and K. Mortezaee. Steps in metastasis: an updated review. *Medical Oncology*, 38(1):3, 2021.

[58] D.R. Welch and D.R. Hurst. Defining the hallmarks of metastasis. *Cancer Research*, 79(12):3011–3027, 2019.

[59] M.Y. Kim. *Breast cancer metastasis*, pages 183–204. Springer, 2021.

[60] D. Yao, C. Dai, and S. Peng. Mechanism of the mesenchymal?epithelial transition and its relationship with metastatic tumor formation. *Molecular Cancer Research*, 9(12):1608–1620, 2011.

[61] G.S. Offeddu et al. The cancer glycocalyx mediates intravascular adhesion and extravasation during metastatic dissemination. *Communications Biology*, 4(1):255, 2021.

[62] G. Doglioni, S. Parik, and S.-M. Fendt. Interactions in the (pre) metastatic niche support metastasis formation. *Frontiers in Oncology*, 9:219, 2019.

[63] V. Gensbittel et al. Mechanical adaptability of tumor cells in metastasis. *Developmental Cell*, 56(2):164–179, 2021.

[64] A.J.A. Yousef. Male breast cancer: epidemiology and risk factors. In *Seminars in Oncology*. Elsevier, 2017.

[65] P. Thakur et al. Breast cancer risk factor evaluation in a western himalayan state: A case?control study and comparison with the western world. *South Asian Journal of Cancer*, 6(03):106–109, 2017.

[66] K. Mahouri, M. Dehghani Zahedani, and S. Zare. Breast cancer risk factors in south of islamic republic of iran: a case-control study. *EMHJ - Eastern Mediterranean Health Journal*, 13(6):1265–1273, 2007.

[67] D. Kashyap et al. Global increase in breast cancer incidence: risk factors and preventive measures. *BioMed Research International*, 2022, 2022.

[68] S.A. Meo et al. Association of abo and rh blood groups with breast cancer. *Saudi Journal of Biological Sciences*, 24(7):1609–1613, 2017.

[69] J.C. Prior. Women?s reproductive system as balanced estradiol and progesterone actions?a revolutionary, paradigm-shifting concept in women?s health. *Drug Discovery Today: Disease Models*, 32:31–40, 2020.

[70] M.-H. Wu et al. Hormonal and body-size factors in relation to breast cancer risk: a prospective study of 11,889 women in a low-incidence area. *Annals of Epidemiology*, 16(3):223–229, 2006.

[71] S.M. Lima et al. Trends in parity and breast cancer incidence in us women younger than 40 years from 1935 to 2015. *JAMA Network Open*, 3(3): e200929, 2020.

[72] F. Clavel-Chapelon et al. Reproductive factors and breast cancer risk: Effect of age at diagnosis. *Annals of Epidemiology*, 5(4):315–320, 1995.

[73] A. Bhadoria, U. Kapil, N. Sareen, and P. Singh. Reproductive factors and breast cancer: A case?control study in tertiary care hospital of north india. *Indian Journal of Cancer*, 50(4):316–321, 2013.

[74] E.F. Beaber et al. Recent oral contraceptive use by formulation and breast cancer risk among women 20 to 49 years of age. *Cancer Research*, 74(15): 4078–4089, 2014.

[75] P.A. Marchbanks et al. Oral contraceptives and the risk of breast cancer. *New England Journal of Medicine*, 346(26):2025–2032, 2002.

[76] R. Taheripanah et al. Breast cancer and ovulation induction treatments. *Clinical Breast Cancer*, 18(5):395–399, 2018.

[77] V. Beral et al. Collaborative group on hormonal factors in breast cancer breast cancer and hormone replacement therapy: Collaborative reanalysis of data from 51 epidemiological studies of 52,705 women with breast cancer and 108,411 women without breast cancer. *Lancet*, 350:1047–1059, 1997.

[78] M.M. Basree et al. Abrupt involution induces inflammation, estrogenic signaling, and hyperplasia linking lack of breastfeeding with increased risk of breast cancer. *Breast Cancer Research*, 21:1–18, 2019.

[79] C. Bodelon et al. Mammary collagen architecture and its association with mammographic density and lesion severity among women undergoing image-guided breast biopsy. *Breast Cancer Research*, 23:1–14, 2021.

[80] C. Byrne et al. Mammographic density change with estrogen and progestin therapy and breast cancer risk. *JNCI: Journal of the National Cancer Institute*, 109(9):djx001, 2017.

[81] M. Roman et al. Cumulative risk of breast cancer screening outcomes according to the presence of previous benign breast disease and family history of breast cancer: supporting personalised screening. *British Journal of Cancer*, 116(11):1480–1485, 2017.

[82] P.H. Lahmann et al. Body size and breast cancer risk: findings from the european prospective investigation into cancer and nutrition (epic). *International Journal of Cancer*, 111(5):762–771, 2004.

[83] M. Chen et al. Body mass index and breast cancer: analysis of a nation-wide population-based prospective cohort study on 1,393,985 taiwanese women. *International Journal of Obesity*, 40(3):524–530, 2016.

[84] E. Miller et al. Connecting the dots between breast cancer, obesity and alcohol consumption in middle-aged women: ecological and case control studies. *BMC Public Health*, 18:1–14, 2018.

[85] F. Xue et al. Cigarette smoking and the incidence of breast cancer. *Archives of Internal Medicine*, 171(2):125–133, 2011.

[86] A. McTiernan et al. Recreational physical activity and the risk of breast cancer in postmenopausal women: the women's health initiative cohort study. *Jama*, 290(10):1331–1336, 2003.

[87] I. Tabassum, H. Mahmood, and M. Faheem. Type 2 diabetes mellitus as a risk factor for female breast cancer in the population of northern pakistan. *Asian Pacific Journal of Cancer Prevention*, 17(7):3255–3258, 2016.

[88] S.C. Larsson, C.S. Mantzoros, and A. Wolk. Diabetes mellitus and risk of breast cancer: a meta-analysis. *International Journal of Cancer*, 121(4): 856–862, 2007.

[89] E.M. John et al. Medical radiation exposure and breast cancer risk: findings from the breast cancer family registry. *International Journal of Cancer*, 121 (2):386–394, 2007.

[90] E.H. Houssein, M.M. Emam, A.A. Ali, and P.N. Suganthan. Deep and machine learning techniques for medical imaging-based breast cancer: A comprehensive review. *Expert Systems with Applications*, 167:114161, 2021.

[91] S.S. Nazari and P. Mukherjee. An overview of mammographic density and its association with breast cancer. *Breast Cancer*, 25:259–267, 2018.

[92] S.W. Duffy et al. Mammography screening reduces rates of advanced and fatal breast cancers: Results in 549,091 women. *Cancer*, 126(13):2971–2979, 2020.

[93] E. Warner et al. Systematic review: using magnetic resonance imaging to screen women at high risk for breast cancer. *Annals of Internal Medicine*, 148(9):671–679, 2008.

[94] K.M. Kelly, J. Dean, W.S. Comulada, and S.J. Lee. Breast cancer detection using automated whole breast ultrasound and mammography in radiographically dense breasts. *European Radiology*, 20:734–742, 2010.

[95] W.F. Anderson, H.A. Katki, and P.S. Rosenberg. Incidence of breast cancer in the united states: current and future trends. *Journal of the National Cancer Institute*, 103(18):1397–1402, 2011.

[96] G.W. Sledge et al. Past, present, and future challenges in breast cancer treatment. *Journal of Clinical Oncology*, 32(19):1979, 2014.

[97] A.N. Shah and M. Cristofanilli. The growing role of cdk4/6 inhibitors in treating hormone receptor-positive advanced breast cancer. *Current Treatment Options in Oncology*, 18:1–16, 2017.

[98] R.S. Finn et al. Palbociclib and letrozole in advanced breast cancer. *New England Journal of Medicine*, 375(20):1925–1936, 2016.

[99] R. Wuerstlein and N. Harbeck. Neoadjuvant therapy for her2-missing positive breast cancer. *Reviews on Recent Clinical Trials*, 12(2):81–92, 2017.

[100] R. Nahta and F.J. Esteva. Her2 therapy: molecular mechanisms of trastuzumab resistance. *Breast Cancer Research*, 8:1–8, 2006.

[101] C. Liedtke et al. Response to neoadjuvant therapy and long-term survival in patients with triple negative breast cancer. *Journal of Clinical Oncology*, 26(8):1275–1281, 2008.

[102] N. Berrada, S. Delaloge, and F. Andre. Treatment of triple-negative metastatic breast cancer: toward individualized targeted treatments or chemosensitization? *Annals of Oncology*, 21:vii30–vii35, 2010.

[103] C.W. Tong, M. Wu, W.C. Cho, and K.K. To. Recent advances in the treatment of breast cancer. *Frontiers in Oncology*, 8:227, 2018.

[104] A. Delprato and D.G. Lambright. Structural basis for rab gtpase activation by vps9 domain exchange factors. *Nature Structural and Molecular Biology*, 14(5):406–412, 2007.

[105] M.A. Antonyak, K.F. Wilson, and R.A. Cerione. R (h) oads to microvesicles. *Small GTPases*, 3(4):219–224, 2012.

[106] R. Mesa et al. Overexpression of rab22a hampers the transport between endosomes and the golgi apparatus. *Experimental Cell Research*, 304(2): 339–353, 2005.

[107] M. Kauppi et al. The small gtpase rab22 interacts with eea1 and controls endosomal membrane trafficking. *Journal of Cell Science*, 115(5):899–911, 2002.

[108] M.G. Waters and F.M. Hughson. Membrane tethering and fusion in the secretory and endocytic pathways. *Traffic*, 1(8):588–597, 2000.

[109] M. Ren et al. Hydrolysis of gtp on rab11 is required for the direct delivery of transferrin from the pericentriolar recycling compartment to the cell surface but not from sorting endosomes. *Proceedings of the National Academy of Sciences*, 95(11):6187–6192, 1998.

[110] D.L. Johnson, J. Wayt, J.M. Wilson, and J.G. Donaldson. Arf6 and rab22 mediate t cell conjugate formation by regulating clathrin-independent endosomal membrane trafficking. *Journal of Cell Science*, 130(14):2405–2415, 2017.

[111] H. He et al. Identification and characterization of nine novel human small gtpases showing variable expressions in liver cancer tissues. *Gene Expression The Journal of Liver Research*, 10(5-6):231–242, 2002.

[112] I. Okamoto et al. Seven novel and stable translocations associated with oncogenic gene expression in malignant melanoma. *Neoplasia*, 7(4):303–311, 2005.

[113] F. Su et al. Rab22a overexpression promotes the tumor growth of melanoma. *Oncotarget*, 7(44):71744, 2016.

[114] B. Zhang et al. Microrna-204-5p inhibits gastric cancer cell proliferation by downregulating usp47 and rab22a. *Medical Oncology*, 32:1–8, 2015.

[115] J. Wang et al. Rab22a promotes the proliferation, migration, and invasion of lung adenocarcinoma via up-regulating pi3k/akt/mtor signaling pathway. *Experimental Cell Research*, 416(2):113179, 2022.

[116] H. Li, L. Prever, E. Hirsch, and F. Gulluni. Targeting pi3k/akt/mtor signaling pathway in breast cancer. *Cancers*, 13(14):3517, 2021.

[117] R. Sinha, G.J. Kim, S. Nie, and D.M. Shin. Nanotechnology in cancer therapeutics: bioconjugated nanoparticles for drug delivery. *Molecular Cancer Therapeutics*, 5(8):1909–1917, 2006.

[118] K.D. Miller et al. Cancer treatment and survivorship statistics, 2016. *CA: A Cancer Journal for Clinicians*, 66(4):271–289, 2016.

[119] M.F. Attia et al. An overview of active and passive targeting strategies to improve the nanocarriers efficiency to tumour sites. *Journal of Pharmacy and Pharmacology*, 71(8):1185–1198, 2019.

[120] J.-J. Wang, K.-F. Lei, and F. Han. Tumor microenvironment: recent advances in various cancer treatments. *European Review for Medical and Pharmacological Sciences*, 22(12), 2018.

[121] D. Basak, S. Arrighi, Y. Darwiche, and S. Deb. Comparison of anticancer drug toxicities: paradigm shift in adverse effect profile. *Life*, 12(1):48, 2021.

[122] A. Hussain et al. The potential role of dietary plant ingredients against mammary cancer: a comprehensive review. *Critical Reviews in Food Science and Nutrition*, 62(10):2580–2605, 2022.

[123] M.J. Hossain, A. Al Mamun, and M.S.S. Khan. Traditional ethnobotanical practice in indigenous communities of australia, asia, and south asia, and modern medicinal prospects. *TBA*.

[124] B.M. Twaij and M.N. Hasan. Bioactive secondary metabolites from plant sources: types, synthesis, and their therapeutic uses. *International Journal of Plant Biology*, 13(1):4–14, 2022.

[125] V.G. Zuin, M.L. Segatto, and L.Z. Ramin. Plants as resources for organic molecules: Facing the green and sustainable future today. *Current Opinion in Green and Sustainable Chemistry*, 9:1–7, 2018.

[126] Y.A. El-Amier and I.A.A. Aisha. Phytochemical constituents of common growing fagonia species (zygophyllaceae) in egyptian deserts and its biological activities. *Plant Archives*, 19(2), 2019.

[127] B.A. Beier. A revision of the desert shrub fagonia (zygophyllaceae). *Systematics and Biodiversity*, 3(3):221–263, 2005.

[128] R. Farheen, I. Mahmood, and R. Parveen. Review on medicinal and bioactive role of genus fagonia. *FUUAST Journal of Biology*, 7(1):33–36, 2017.

[129] R. Faarheen et al. Triterpenoids and triterpenoid saponins from the aerial parts of fagonia indica burm. *Phytochemistry Letters*, 13:256–261, 2015.

[130] M. Lam, A.R. Carmichael, and H.R. Griffiths. An aqueous extract of fagonia cretica induces dna damage, cell cycle arrest and apoptosis in breast cancer cells via foxo3a and p53 expression. *PloS One*, 7(6):e40152, 2012.

[131] I.A. Walbi et al. A preliminary cytotoxicity study of fagonia arabica against breast (mcf-7), oral (kb-3-1), and lung cancer (a-549) cell lines: A study supported by molecular marker analysis using dual staining dyes. *Separations*, 10(2):110, 2023.

[132] L.F. Ibrahim et al. A new kaempferol triglycoside from fagonia taeckholmiana: cytotoxic activity of its extracts. *Carbohydrate Research*, 343(1):155–158, 2008.

[133] A. Almilaibary, E.A. Abdallah, and M.F. El-Refaei. Fagonia indica attenuates chromium-induced nephrotoxicity via antioxidant and anti-inflammatory activities in mice. *Heliyon*, 8(8), 2022.

[134] I. Bagban et al. Hepatoprotective activity of the methanolic extract of fagonia indica burm in carbon tetra chloride induced hepatotoxicity in albino rats. *Asian Pacific Journal of Tropical Biomedicine*, 2(3):S1457–S1460, 2012.

[135] Tahir Razi M. et al. Antihaemorrhagic potentials of fagonia cretica against naja naja karachiensis (black pakistan cobra) venom. *Natural Product Research*, 25(20):1902–1907, 2011.

[136] M. Tafrihi et al. The wonderful activities of the genus mentha: Not only antioxidant properties. *Molecules*, 26(4):1118, 2021.

[137] F. Anwar et al. Mentha: A genus rich in vital nutra-pharmaceuticals—a review. *Phytotherapy Research*, 33(10):2548–2570, 2019.

[138] F. Brahmi, M. Khodir, C. Mohamed, and D. Pierre. Chemical composition and biological activities of mentha species. *Aromatic and Medicinal Plants-Back to Nature*, 10:47–79, 2017.

[139] A. Eftekhari et al. Phytochemical and nutra-pharmaceutical attributes of mentha spp.: A comprehensive review. *Arabian Journal of Chemistry*, 14 (5):103106, 2021.

[140] S.S.K. Al-Taie and N.F.M. Al Kenane. Study biochemistry of mentha longifolia (l.) huds.: a review. *Herbs and Spices*, page 27, 2020.

[141] M.H. Farzaei et al. Pharmacological activity of mentha longifolia and its phytoconstituents. *Journal of Traditional Chinese Medicine*, 37(5):710–720, 2017.

[142] Z. Mirza and S. Karim. Nanoparticles-based drug delivery and gene therapy for breast cancer: Recent advancements and future challenges. In *Seminars in Cancer Biology*. Elsevier, 2021.

[143] D. Swami, M. Anitha, M.C.S. Rao, and A. Sharangi. Medicinal plants: perspectives and retrospectives. pages 1–28, 2022.

[144] P. Singh and A.K. Pandey. Prospective of essential oils of the genus mentha as biopesticides: A review. *Frontiers in Plant Science*, 9:409763, 2018.

[145] M. Soleimani, A. Arzani, V. Arzani, and T.H. Roberts. Phenolic compounds and antimicrobial properties of mint and thyme. *Journal of Herbal Medicine*, 36:100604, 2022.

[146] M.T. Yassin, A.A. Mostafa, and A.A. Al-Askar. Anticandidal and anticarcinogenic activities of mentha longifolia (wild mint) extracts in vitro. *Journal of King Saud University-Science*, 32(3):2046–2052, 2020.

[147] I. Shaheen, A. Khalil, R. Shaheen, and M.B. Tahir. A review on nanomaterials: Types, synthesis, characterization techniques, properties and applications. *Innovation in Science and Technology*, 2(1):56–62, 2023.

[148] A.B. Asha and R. Narain. Nanomaterials properties. In *Polymer Science and Nanotechnology*, pages 343–359. Elsevier, 2020.

[149] R.D. Prasad et al. A review on aspects of nanotechnology in food science and animal nutrition. *ES Food and Agroforestry*, 8:12–46, 2022.

[150] N. Abid et al. Synthesis of nanomaterials using various top-down and bottom-up approaches, influencing factors, advantages, and disadvantages: A review. *Advances in Colloid and Interface Science*, 300:102597, 2022.

[151] S. Ramanathan et al. Nanoparticle synthetic methods: strength and limitations. In S.C.B. Gopinath and F. Gang, editors, *Nanoparticles in Analytical and Medical Devices*, pages 31–43. Elsevier, 2021.

[152] I. Ijaz et al. Detail review on chemical, physical and green synthesis, classification, characterizations and applications of nanoparticles. *Green Chemistry Letters and Reviews*, 13(3):223–245, 2020.

[153] Y. Sun et al. Metal–organic framework nanocarriers for drug delivery in biomedical applications. *Nano-Micro Letters*, 12:1–29, 2020.

[154] A. Ahmad et al. Extracellular biosynthesis of silver nanoparticles using the fungus fusarium oxysporum. *Colloids and Surfaces B: Biointerfaces*, 28(4): 313–318, 2003.

[155] S. Iravani et al. Synthesis of silver nanoparticles: chemical, physical and biological methods. *Research in Pharmaceutical Sciences*, 9(6):385–406, 2014.

[156] C.D. De Souza et al. Review of the methodologies used in the synthesis of gold nanoparticles by chemical reduction. *Journal of Alloys and Compounds*, 798:714–740, 2019.

[157] S. Asgari et al. Microemulsions as nanoreactors for synthesis of biopolymer nanoparticles. *Trends in Food Science and Technology*, 86:118–130, 2019.

[158] G. Asab et al. Synthesis of silica-coated fe3o4 nanoparticles by microemulsion method: characterization and evaluation of antimicrobial activity. *International Journal of Biomaterials*, 2020, 2020.

[159] N. Devi et al. A review of the microwave-assisted synthesis of carbon nanomaterials, metal oxides/hydroxides and their composites for energy storage applications. *Nanoscale*, 13(27):11679–11711, 2021.

[160] K.N. Thakkar et al. Biological synthesis of metallic nanoparticles. *Nanomedicine: Nanotechnology, Biology and Medicine*, 6(2):257–262, 2010.

[161] K. Moghaddam. An introduction to microbial metal nanoparticle preparation method. *Journal of Young Investigators*, 19(1), 2010.

[162] A. Saxena et al. Biological synthesis of silver nanoparticles by using onion (allium cepa) extract and their antibacterial activity. *Digest Journal of Nanomaterials and Biostructures*, 5(2):427–432, 2010.

[163] A. Prakash et al. Bacteria mediated extracellular synthesis of metallic nanoparticles. *International Research Journal of Biotechnology*, 1(5):071–079, 2010.

[164] S. Waghmare et al. Biosynthesis and characterization of manganese and zinc nanoparticles. *Universal Journal of Environmental Research and Technology*, 1(1), 2011.

[165] M. Sanjivkumar et al. Biosynthesis and characterization of zinc oxide nanoparticles from an estuarine-associated actinobacterium streptomyces spp. and its biotherapeutic applications. *Archives of Microbiology*, 204(1): 17, 2022.

[166] P. Mukherjee et al. Extracellular synthesis of gold nanoparticles by the fungus fusarium oxysporum. *ChemBioChem*, 3(5):461–463, 2002.

[167] M. Rai et al. Fusarium as a novel fungus for the synthesis of nanoparticles: mechanism and applications. *Journal of Fungi*, 7(2):139, 2021.

[168] F. Khan et al. Prospects of algae-based green synthesis of nanoparticles for environmental applications. *Chemosphere*, 293:133571, 2022.

[169] A. Mukherjee et al. A review of green synthesis of metal nanoparticles using algae. *Frontiers in Microbiology*, 12:693899, 2021.

[170] S. Jadoun et al. Green synthesis of nanoparticles using plant extracts: A review. *Environmental Chemistry Letters*, 19(1):355–374, 2021.

[171] M.B. da Costa Rocha et al. Recent advances (2016-2020) in green synthesis of metal oxide nanoparticles: An overview. *Research, Society and Development*, 10(16):e399101623406–e399101623406, 2021.

[172] J.A. DiMasi, H.G. Grabowski, and R.W. Hansen. Innovation in the pharmaceutical industry: new estimates of rand costs. *Journal of Health Economics*, 47:20–33, 2016.

[173] D. Vohora and G. Singh. *Pharmaceutical Medicine and Translational Clinical Research*. Academic Press, 2017.

[174] F. Zhong et al. Artificial intelligence in drug design. *Science China Life Sciences*, 61:1191–1204, 2018.

[175] T. Hou and X. Xu. Recent development and application of virtual screening in drug discovery: an overview. *Current Pharmaceutical Design*, 10(9):1011–1033, 2004.

[176] W. Yu and A.D. MacKerell. Computer-aided drug design methods. In *Antibiotics: Methods and Protocols*, pages 85–106. 2017.

[177] S.J.Y. Macalino, V. Gosu, S. Hong, and S. Choi. Role of computer-aided drug design in modern drug discovery. *Archives of Pharmacal Research*, 38: 1686–1701, 2015.

[178] P. Prajapat, S. Agarwal, and G. Talesara. Significance of computer aided drug design and 3d qsar in modern drug discovery. *J Med Org Chem*, 1(1): 1, 2017.

[179] W. Duch, K. Swaminathan, and J. Meller. Artificial intelligence approaches for rational drug design and discovery. *Current Pharmaceutical Design*, 13 (14):1497–1508, 2007.

[180] M. Hassan Baig et al. Computer aided drug design: success and limitations. *Current Pharmaceutical Design*, 22(5):572–581, 2016.

[181] I.D. Kuntz et al. A geometric approach to macromolecule-ligand interactions. *Journal of Molecular Biology*, 161(2):269–288, 1982.

[182] D.J. Diller and K.M. Jr Merz. High throughput docking for library design and library prioritization. *Proteins: Structure, Function, and Bioinformatics*, 43(2):113–124, 2001.

[183] M. Karplus and J.A. McCammon. Molecular dynamics simulations of biomolecules. *Nature Structural Biology*, 9(9):646–652, 2002.

[184] S. Shahid et al. Cuo-go-ag; green synthesis with fagonia arabica and biomedical potential is a bioinspired nano theranostics composite. *Frontiers in Materials*, 9:875148, 2022.

[185] W. Ahmed et al. Trail mediated apoptosis ruling and anticancer trigger by fine-tuned nano spheres of fagonia cretica methanolic extracts as novel cancer regime. *Scientific Reports*, 13(1):671, 2023.

[186] Z. Hussain et al. Synthesis and characterization of silver nanoparticles mediated by the mentha piperita leaves extract and exploration of its antimicrobial activities. *Journal of the Chilean Chemical Society*, 68(2):5865–5870, 2023.

[187] W.J. Aziz and H.A. Jassim. Green chemistry for the preparation of silver nanoparticles using mint leaf leaves extracts and evaluation of their antimicrobial potential. *World News of Natural Sciences*, 18(2):163–170, 2018.

[188] S. Sharma, K. Kumar, S. Chauhan, and M. Chauhan. Synthesis and characterization of zno nanoparticles using mint plant leaves.

[189] H. Arshad, M.A. Sami, S. Sadaf, and U. Hassan. Salvadora persica mediated synthesis of silver nanoparticles and their antimicrobial efficacy. *Scientific Reports*, 11(1):5996, 2021.

[190] S. Mourdikoudis, R.M. Pallares, and N.T. Thanh. Characterization techniques for nanoparticles: comparison and complementarity upon studying nanoparticle properties. *Nanoscale*, 10(27):12871–12934, 2018.

[191] V. Manikandan et al. Green synthesis of silver oxide nanoparticles and its antibacterial activity against dental pathogens. *3 Biotech*, 7:1–9, 2017.

[192] X.-F. Zhang, Z.-G. Liu, W. Shen, and S. Gurunathan. Silver nanoparticles: synthesis, characterization, properties, applications, and therapeutic approaches. *International Journal of Molecular Sciences*, 17(9):1534, 2016.

[193] O. Wetzel et al. Metal–ligand interface and internal structure of ultrasmall silver nanoparticles (2 nm). *The Journal of Physical Chemistry B*, 125(21): 5645–5659, 2021.

[194] A. Gupta, A.R. Koirala, B. Gupta, and N. Parajuli. Improved method for separation of silver nanoparticles synthesized using the nyctanthes arbortristis shrub. *Acta Chemica Malaysia*, 3(1):35–42, 2019.

[195] N. Ahmad et al. Antimicrobial efficacy of mentha piperata-derived biogenic zinc oxide nanoparticles against uti-resistant pathogens. *Scientific Reports*, 13(1):14972, 2023.

[196] P. Hayat et al. Myogenesis and analysis of antimicrobial potential of silver nanoparticles (agnps) against pathogenic bacteria. *Molecules*, 28(2):637, 2023.

[197] A. Moshfegh et al. Phytochemical analysis, antioxidant, anticancer and antibacterial properties of the caspian sea red macroalgae, laurencia caspica. *Iranian Journal of Science and Technology, Transactions A: Science*, 43:49–56, 2019.

[198] A.E. Fadiji and O.O. Babalola. Metagenomics methods for the study of plant-associated microbial communities: a review. *Journal of Microbiological Methods*, 170:105860, 2020.

[199] S.E. Fard, F. Tafvizi, and M.B. Torbati. Silver nanoparticles biosynthesised using centella asiatica leaf extract: apoptosis induction in mcf-7 breast cancer cell line. *IET Nanobiotechnology*, 12(7):994–1002, 2018.

[200] H. Saadi et al. Development of an elisa detecting tumor protein 53-induced nuclear protein 1 in serum of prostate cancer patients. *Results in Immunology*, 3:51–56, 2013.

[201] A. Bouaouich and F. Bouguerche. Hplc chromatographic analysis antioxidant activity of seeds some varieties of prickly pear (opuntia ficus-indica l.) from the sidi-fredj souk ahras algeria. *Algerian Journal of Biosciences*, 3(1): 038–046, 2022.

[202] Z. Liu et al. Application of molecular docking for the degradation of organic pollutants in the environmental remediation: A review. *Chemosphere*, 203: 139–150, 2018.

[203] A.N. Singh, M.M. Baruah, and N. Sharma. Structure based docking studies towards exploring potential anti-androgen activity of selected phytochemicals against prostate cancer. *Scientific Reports*, 7(1):1955, 2017.

[204] G. Madhavi Sastry et al. Protein and ligand preparation: parameters, protocols, and influence on virtual screening enrichments. *Journal of Computer-Aided Molecular Design*, 27:221–234, 2013.

[205] H.S. Chan, S. Filipek, and S. Yuan. The principles of ligand specificity on beta-2-adrenergic receptor. *Scientific Reports*, 6(1):34736, 2016.

[206] M. Blum et al. The interpro protein families and domains database: 20 years on. *Nucleic Acids Research*, 49(D1):D344–D354, 2021.

[207] R.E. Rigsby and A.B. Parker. Using the pymol application to reinforce visual understanding of protein structure. *Biochemistry and Molecular Biology Education*, 44(5):433–437, 2016.

[208] O. Trott and A.J. Olson. Autodock vina: improving the speed and accuracy of docking with a new scoring function, efficient optimization, and multithreading. *Journal of Computational Chemistry*, 31(2):455–461, 2010.

[209] A.C. Wallace, R.A. Laskowski, and J.M. Thornton. Ligplot: a program to generate schematic diagrams of protein-ligand interactions. *Protein Engineering, Design and Selection*, 8(2):127–134, 1995.

[210] N. Singh, C. Sudandiradoss, and J. Abraham. Screening of furanone in cucurbita melo and evaluation of its bioactive potential using in silico studies. *Interdisciplinary Sciences: Computational Life Sciences*, 8:395–402, 2016.

[211] P. Bhardwaj et al. Exploration of binding mechanism of triclosan towards cancer markers using molecular docking and molecular dynamics. *Chemosphere*, 293:133550, 2022.

[212] M.J. Abraham et al. Gromacs: High performance molecular simulations through multi-level parallelism from laptops to supercomputers. *SoftwareX*, 1:19–25, 2015.

[213] H.J. Berendsen, J.P. Postma, W.F. van Gunsteren, and J. Hermans. Interaction models for water in relation to protein hydration. In *Intermolecular Forces: Proceedings of the Fourteenth Jerusalem Symposium on Quantum Chemistry and Biochemistry Held in Jerusalem, Israel, April 13–16, 1981.* Springer, 1981.

[214] G. Bussi, D. Donadio, and M. Parrinello. Canonical sampling through velocity rescaling. *The Journal of Chemical Physics*, 126(1), 2007.

[215] M. Parrinello and A. Rahman. Polymorphic transitions in single crystals: A new molecular dynamics method. *Journal of Applied Physics*, 52(12): 7182–7190, 1981.

[216] U. Essmann et al. A smooth particle mesh ewald method. *The Journal of Chemical Physics*, 103(19):8577–8593, 1995.

[217] B. Hess, H. Bekker, H.J. Berendsen, and J.G. Fraaije. Lincs: A linear constraint solver for molecular simulations. *Journal of Computational Chemistry*, 18(12):1463–1472, 1997.

[218] A. Daina, O. Michielin, and V. Zoete. Swissadme: a free web tool to evaluate pharmacokinetics, drug-likeness and medicinal chemistry friendliness of small molecules. *Scientific Reports*, 7(1):42717, 2017.

[219] S. Tran, P.-J. DeGiovanni, B. Piel, and P. Rai. Cancer nanomedicine: a review of recent success in drug delivery. *Clinical and Translational Medicine*, 6:1–21, 2017.

[220] A. Gaur, A. Midha, and A.L. Bhatia. Significance of nanotechnology in medical sciences. *Asian Journal of Pharmaceutics (AJP)*, 2(2), 2008.

[221] R.M. Navalakhe and T.D. Nandedkar. Application of nanotechnology in biomedicine. 2007.

[222] M. Alhujaily et al. Recent advances in plant-mediated zinc oxide nanoparticles with their significant biomedical properties. *Bioengineering*, 9(10):541, 2022.

[223] T. Iqbal et al. Plant-mediated green synthesis of zinc oxide nanoparticles for novel application to enhance the shelf life of tomatoes. *Applied Nanoscience*, pages 1–13, 2022.

[224] R.G. Saratale et al. A comprehensive review on green nanomaterials using biological systems: Recent perception and their future applications. *Colloids and Surfaces B: Biointerfaces*, 170:20–35, 2018.

[225] Y.Y. Chan, Y.L. Pang, S. Lim, and W.C. Chong. Facile green synthesis of zno nanoparticles using natural-based materials: Properties, mechanism, surface modification and application. *Journal of Environmental Chemical Engineering*, 9(4):105417, 2021.

[226] S. Swain, P. Kumar Sahu, S. Beg, and S. Manohar Babu. Nanoparticles for cancer targeting: current and future directions. *Current Drug Delivery*, 13 (8):1290–1302, 2016.

[227] R. Hussain et al. Casting zinc oxide nanoparticles using fagonia blend microbial arrest. *Applied Biochemistry and Biotechnology*, 195(1):264–282, 2023.

[228] A. Abdelkhalek and A.A. Al Askar. Green synthesized zno nanoparticles mediated by mentha spicata extract induce plant systemic resistance against tobacco mosaic virus. *Applied Sciences*, 10(15):5054, 2020.

[229]

[230] B.H. Kiani et al. Comparative evaluation of biomedical and phytochemical applications of zinc nanoparticles by using fagonia cretica extracts. *Scientific Reports*, 12(1):10024, 2022.

[231] S.T. Karam and A.F. Abdulrahman. Green synthesis and characterization of zno nanoparticles by using thyme plant leaf extract. *Photonics*, 2022.

[232] B.H. Shnawa et al. Scolicidal activity of biosynthesized zinc oxide nanoparticles by mentha longifolia l. leaves against echinococcus granulosus protoscolices. *Emergent Materials*, 5(3):683–693, 2022.

[233] M. Afzal et al. Photocatalytic degradation of organic dyes and biological potentials of biogenic zinc oxide nanoparticles synthesized using the polar extract of cyperus scariosus r. br.(cyperaceae). *Green Processing and Synthesis*, 13(1):20240038, 2024.

[234] R. Mariam et al. Fagonia stabilized gold nanoparticles as antimicrobial agents. *Materials Research Express*, 8(8):085011, 2021.

[235] M. Adil et al. Evaluation of the antibacterial potential of silver nanoparticles synthesized through the interaction of antibiotic and aqueous callus extract of fagonia indica. *AMB Express*, 9:1–12, 2019.

[236] M.A. Tahir and M. Abbasi. Ftir spectroscopic analysis of mentha spicata l.(garden mint). *Asian Journal of Chemical Sciences*, 1(4):1–5, 2020.

[237] X.L. Loh, Z.X. Ooi, Y.P. Teoh, and S.H. Shuit. Synthesis and characterization of zinc oxide nanoparticles using peppermint tea (mentha piperita) dregs extract and their photocatalytic performance. *Environmental Progress and Sustainable Energy*, 42(6):e14202, 2023.

[238] V. Singh et al. Oxidized guar gum–zno hybrid nanostructures: synthesis, characterization and antibacterial activity. *Applied Nanoscience*, 8:1149–1160, 2018.

[239] S. Faisal et al. Fagonia cretica-mediated synthesis of manganese oxide (mno2) nanomaterials their characterization and evaluation of their biocatalytic and enzyme inhibition potential for maintaining flavor and texture in apples. *Catalysts*, 12(5):558, 2022.

[240] A. López-Soto, S. Gonzalez, M.J. Smyth, and L. Galluzzi. Control of metastasis by nk cells. *Cancer Cell*, 32(2):135–154, 2017.

[241] T. Lancet. Globocan 2018: counting the toll of cancer. page 985, 2018.

[242] Y.T. Lee, Y.J. Tan, and C.E. Oon. Molecular targeted therapy: Treating cancer with specificity. *European Journal of Pharmacology*, 834:188–196, 2018.

[243] Z. Cheng, M. Li, R. Dey, and Y. Chen. Nanomaterials for cancer therapy: current progress and perspectives. *Journal of Hematology and Oncology*, 14: 1–27, 2021.

[244] H.R. Kelidari et al. Anticancer effect of solid-lipid nanoparticles containing mentha longifolia and mentha pulegium essential oils: in vitro study on human melanoma and breast cancer cell lines. *Biointerface Research in Applied Chemistry*, 12(2):2128–2137, 2022.

[245] H. Umar, M. Aliyu, and D. Ozsahin. Iron oxide nanoparticles synthesized using mentha piperita extract and evaluation of its antibacterial and antimigratory potential on highly metastatic human breast cells. *NanoWorld J*, 9 (4):144–151, 2023.

[246] M.-H. Moosavy et al. Green synthesis, characterization, and biological evaluation of gold and silver nanoparticles using mentha spicata essential oil. *Scientific Reports*, 13(1):7230, 2023.

[247] S. Khalid et al. In vitro antimutagenic, cytotoxic and anticancer potential of fagonia indica phytochemicals. *Pakistan Journal of Pharmaceutical Sciences*, 34, 2021.

[248] I. Ullah et al. Green-synthesized silver nanoparticles induced apoptotic cell death in mcf-7 breast cancer cells by generating reactive oxygen species and activating caspase 3 and 9 enzyme activities. *Oxidative Medicine and Cellular Longevity*, 2020(1):1215395, 2020.

[249] R.L. Siegel, K.D. Miller, and A. Jemal. Cancer statistics, 2018. *CA: A Cancer Journal for Clinicians*, 68(1):7–30, 2018.

[250] C. Wang, X.-X. Xie, W.-J. Li, and D.-Q. Jiang. Lncrna dleu1/microrna-300/rab22a axis regulates migration and invasion of breast cancer cells. *European Review for Medical and Pharmacological Sciences*, 23(23), 2019.

[251] N.A. Papanikolaou, M. Kakavoulia, C. Ladias, and A.G. Papavassiliou. The ras-related protein rab22a interacts with hypoxia-inducible factor 1-alpha (hif-1α) in mda-mb-231 breast cancer cells in hypoxia. *Molecular Biology Reports*, 51(1):564, 2024.

[252] F. Wen et al. Characterization of prognostic value and immunological roles of rab22a in hepatocellular carcinoma. *Frontiers in Immunology*, 14:1086342, 2023.

[253] L.S. Mayorga and I. Cebrian. Rab22a: A novel regulator of immune functions. *Molecular Immunology*, 113:87–92, 2019.

[254] M. Nouri Hajbaba et al. The function of chitosan/agarose biopolymer on fe2o3 nanoparticles and evaluation of their effects on mcf-7 breast cancer cell line and expression of bcl2 and bax genes. *Biotechnology Progress*, 39 (1):e3305, 2023.

[255] L. Patrón-Romero et al. Mitochondrial dysfunction induced by zinc oxide nanoparticles. *Crystals*, 12(8):1089, 2022.

[256] C. Rodriguez-Furlan et al. Interaction between vps35 and rabg3f is necessary as a checkpoint to control fusion of late compartments with the vacuole. *Proceedings of the National Academy of Sciences*, 116(42):21291–21301, 2019.

[257] A. Boroumand Moghaddam et al. Eco-friendly formulated zinc oxide nanoparticles: induction of cell cycle arrest and apoptosis in the mcf-7 cancer cell line. *Genes*, 8(10):281, 2017.

[258] L. Wang et al. Zinc oxide nanoparticles induce murine photoreceptor cell death via mitochondria-related signaling pathway. *Artificial Cells, Nanomedicine, and Biotechnology*, 46(sup1):1102–1113, 2018.

[259] N. Susnow, L. Zeng, D. Margineantu, and D.M. Hockenbery. Bcl-2 family proteins as regulators of oxidative stress. In *Seminars in Cancer Biology*. Elsevier, 2009.

[260] A. Bandyopadhyay et al. Cytotoxic effect of green synthesized silver nanoparticles in mcf7 and mda-mb-231 human breast cancer cells in vitro. *The Nucleus*, 63:191–202, 2020.

[261] A. Alamami et al. The species of genus fagonia in libya: A comprehensive review. *Journal of Pharmacognosy and Phytochemistry*, 11(5):28–37, 2022.

[262] K. Ali and H. Khan. Fagonia indica; a review on chemical constituents, traditional uses and pharmacological activities. *Current Pharmaceutical Design*, 27(22):2648–2660, 2021.

[263] T. Tabassum et al. Fagonia cretica: identification of compounds in bioactive gradient high performance liquid chromatography fractions against multidrug resistant human gut pathogens. 2022.

[264] I. Kanwal et al. Fagonia arabica linn, a miraculous medicinal plant with diminutive scientific data but hefty potential. *RADS Journal of Pharmacy and Pharmaceutical Sciences*, 9(3):185–189, 2021.

[265] S. Naz and S. Manzoor. Phenolic profiling and antimicrobial studies of fagonia crefica native to pakistan. *Journal Advances of Nutrition Science and Technology*, 1:19–32, 2021.

[266] A.U. Khayam et al. Quinovic acid purified from medicinal plant fagonia indica mediates anticancer effects via death receptor 5. *Molecular and Cellular Biochemistry*, 474:159–169, 2020.

[267] S. Kamran et al. Metabolic profiling and investigation of the modulatory effect of fagonia cretica l. aerial parts on hepatic cyp3a4 and ugt2b7 enzymes in streptozotocin—induced diabetic model. *Antioxidants*, 12(1):119, 2023.

[268] N.Z. Mamadalieva, H. Hussain, and J. Xiao. Recent advances in genus mentha: Phytochemistry, antimicrobial effects, and food applications. *Food Frontiers*, 1(4):435–458, 2020.

[269] S. Faisal et al. Exploring the antibacterial, antidiabetic, and anticancer potential of mentha arvensis extract through in-silico and in-vitro analysis. *BMC Complementary Medicine and Therapies*, 23(1):267, 2023.

[270] M. Tourabi et al. Efficacy of various extracting solvents on phytochemical composition, and biological properties of mentha longifolia l. leaf extracts. *Scientific Reports*, 13(1):18028, 2023.

[271] R.O. Bakr et al. The metabolomic analysis of five mentha species: cytotoxicity, anti-helicobacter assessment, and the development of polymeric micelles for enhancing the anti-helicobacter activity. *RSC Advances*, 11(13): 7318–7330, 2021.

[272] H.O. Elansary et al. Polyphenol profile and antimicrobial and cytotoxic activities of natural mentha× piperita and mentha longifolia populations in northern saudi arabia. *Processes*, 8(4):479, 2020.

[273] N. Bouali et al. Phytochemical profiling, antioxidant, and antifungal activities of ethyl acetate and chloroformic extracts from three mentha species. *Pharmacognosy Magazine*, 20(1):137–145, 2024.

[274] A. Mumtaz et al. Mpd3: a useful medicinal plants database for drug designing. *Natural Product Research*, 31(11):1228–1236, 2017.

[275] V.T. Sabe et al. Current trends in computer aided drug design and a highlight of drugs discovered via computational techniques: A review. *European Journal of Medicinal Chemistry*, 224:113705, 2021.

[276] K. Dzobo. The role of natural products as sources of therapeutic agents for innovative drug discovery. *Comprehensive Pharmacology*, page 408, 2022.

[277] C. Zardecki et al. Pdb-101: Educational resources supporting molecular explorations through biology and medicine. *Protein Science*, 31(1):129–140, 2022.

[278] R. Santhoshkumar and A. Yusuf. In silico structural modeling and analysis of physicochemical properties of curcumin synthase (curs1, curs2, and curs3) proteins of curcuma longa. *Journal of Genetic Engineering and Biotechnology*, 18(1):24, 2020.

[279] V. Widjaja et al. Identification of uncharacterized plasmodium falciparum proteins via in-silico analysis. *BIOEDUSCIENCE J Pendidik Biol Dan Sains*, 6:198–210, 2022.

[280] L. Aravind, L.M. Iyer, D.D. Leipe, and E.V. Koonin. A novel family of p-loop ntpases with an unusual phyletic distribution and transmembrane segments inserted within the ntpase domain. *Genome Biology*, 5:1–10, 2004.

[281] L.P. Kagami et al. Geo-measures: A pymol plugin for protein structure ensembles analysis. *Computational Biology and Chemistry*, 87:107322, 2020.

[282] K. Raval and T. Ganatra. Basics, types and applications of molecular docking: A review. *IP International Journal of Comprehensive and Advanced Pharmacology*, 7(1):12–16, 2022.

[283] Y. Liu et al. Cb-dock: A web server for cavity detection-guided protein–ligand blind docking. *Acta Pharmacologica Sinica*, 41(1):138–144, 2020.

[284] A.M. da Fonseca et al. Screening of potential inhibitors targeting the main protease structure of sars-cov-2 via molecular docking, and approach with molecular dynamics, rmsd, rmsf, h-bond, sasa and mmgbsa. *Molecular Biotechnology*, pages 1–15, 2023.

[285] S.A. Ahmed et al. Inhibitive property of catechin and chlorogenic acid against human pancreatic lipase: molecular docking and molecular dynamics simulation investigations. *Advanced Journal of Chemistry-Section A*, 5: 226, 2022.

[286] A.K. Singh et al. Evaluation of antidiabetic activity of dietary phenolic compound chlorogenic acid in streptozotocin induced diabetic rats: Molecular docking, molecular dynamics, in silico toxicity, in vitro and in vivo studies. *Computers in Biology and Medicine*, 134:104462, 2021.

[287] R. Sehrawat et al. In silico design of novel bioactive molecules to treat breast cancer with chlorogenic acid derivatives: a computational and sar approach. *Frontiers in Pharmacology*, 14:1266833, 2023.